THE EFFECT OF CURVATURE ON BOUNDARY LAYER TRANSITION

Thesis by

Alexander Crane Charters Jr.

In Partial Fulfillment of the Requirements for the Degree of Doctor of Philosophy

California Institute of Technology

Pasadena, California

1938

ACKNOWLEDGMENT

The author wishes to acknowledge his sincere appreciation for the generous advice and encouragement given by Drs. von Karman and Millikan during the carrying out of this research project. He also wishes to thank Mr. P. Kyropoulos and Mr. A. H. Hughey for their assistance in making the observations, and the other members of the department for their generous help and many excellent suggestions.

Alexander Crane Charters Jr.

TABLE OF CONTENTS

ABSTRACT

Discrepancies in the boundary layer profiles of NACA T.N. 613, * and recent work done at Cambridge University, England, on the effect of inclination on transition required the reinvestigation of the effect of curvature on boundary layer transition using a more fundamentally sound experimental technique than previously. This technique consisted in comparing velocity profiles taken at different speeds at each measuring station with the universal Blasius laminar profile; a further indication of transition was obtained by measuring the local shear coefficient with a small total head tube pressed against the surface. Agreement between the two methods was complete in all but one case. The effect of inclination was investigated by rotating the working section of the tunnel as a whole around a fixed pivot. Unfavorable inclination produced a decrease in transition Reynolds number on either side of the sheet but a neutral region was found

* National Advisory Committee for Aeronautics Technical Note.

to exist in which inclination had no effect on the transition and in which the effect of curvature alone acted. The effect of curvature could be expressed as a function of the single variable, $\frac{1000\,\delta_m}{r_c}$. As to the exact nature of the $(R_{\delta_m})_T$ vs $\frac{1000\,\delta_m}{r_c}$ curve, little as yet can be said since a sufficient range of $\frac{1000\,\delta_m}{r_c}$ has not been investigated as yet. The results of T.N. 613 were thus validated qualtatively but the values of transition given there were found to be too large.

LIST OF FIGURES

Figure	Profile	Station	Side	α	
16	Shear	7	Convex	6.2	Stable
17	Boundary Layer	"	"	"	"
18	"	"	"	3.2	Unstable
19	Shear	4	"	4.8	"
20	Boundary Layer	"	"	"	"
21	Shear	"	"	3.2	"
22	Boundary Layer	"	"	"	"
23	Shear	"	"	1.6	"
24	Boundary Layer	"	"	"	"

	Description
25	Effect of Inclination on Transition: "Jones' Effect".

	Profile	Station	Side	α
26 & 27	Boundary Layer	2	Concave	0
28 & 29	"	3	"	"
30	Shear	4	Convex	"
31	Boundary Layer	"	"	"
32	Shear	5	"	"
33	Boundary Layer	"	"	"
34	Shear	6	"	"
35	Boundary Layer	"	"	"
36	Shear	7	"	"
37	Boundary Layer	"	"	"
38	Shear	8	"	"
39	Boundary Layer	"	"	"

Figure		Station	Side	α
40	Momentum Defect	2	Concave	0
41	"	3	"	"
42	"	4	Convex	"
43	"	5	"	"
44	"	6	"	"
45	"	7	"	"
46	"	8	"	"

Description

47 Momentum Thickness of Boundary Layer vs R_x for all stations.

48 Total Shear Coefficient vs R_x for all stations.

49 Momentum Defect, $e\int_0^\infty u(\bar{u}-u)\,dy$, vs R_x for all stations.

50 $(R_x)_T$ vs x/r_c

51 Effect of Curvature on Transition: $(R_{\delta_m})_T$ vs $\frac{1000\,\delta_m}{r_c}$

NOTATION

(in the order used)

Symbol	Description
x	Distance along central sheet from its leading edge.
r_c	Radius of curvature of central sheet.
u	Local Velocity in boundary layer.
U	Velocity of Free Stream at Edge of Boundary Layer.
$f(-)$	Function of (-).
y	Distance of Point in Question from Surface of Sheet.
R_x	Reynolds number of Free Stream based on x. $R_x = \frac{Ux}{\nu}$
ν	Coefficient of Kinematic Viscosity = μ/ρ
δ	Real Boundary Layer Thickness.
η	Blasius Non-dimential Distance from sheet $\eta = y/x\sqrt{R_x}$
$(R_x)_T$	R_x at which Transition Occurs.
p_s	Static Pressure of Air Flow at any given point.
Q	Dynamic Pressure of Free Stream = $\frac{1}{2}\rho U^2$
ρ	Density of Air.
u'	Additional Fluctuating Component of Velocity in x direction.

Symbol	Description
$\sqrt{\left(\frac{u'}{U}\right)^2}$	Root Mean Square of u'/U averaged over an Interval of Time.
Δy	Additional Distance necessary to add to y to correct for Effective Center of "Total-Static Tube". (see pages 10 and 11).
y_e	Effective Distance at which Total-Static Tube measures the velocity when in contact with the surface of Sheet.
u_e	Velocity measured at y_e .
τ_o	Local Shear Acting at Surface of Sheet.
μ	Coefficient of Viscosity.
q_e	Dynamic Head measured at y_e .
c_f	Local Shear Coefficient = $\frac{\tau_o}{\frac{1}{2}\rho U^2}$
α	Angle of Incidence of Tangent to Leading Edge of Central Sheet with the Wind Direction.
δ_m	Momentum Thickness of Boundary Layer = $\int_o^\infty \frac{u}{U}\left(1-\frac{u}{U}\right) dy$
$f = u/U$	Function occurring in Blasius Integral.
$\eta' = y/\delta$	Non-dimensional y distance based on δ .
$\alpha' = \int_o^\infty f(1-f)\, d\eta' =$	Constant for Laminar Flow.
M	Momentum Defect of Boundary Layer at Point in Question.
F	Total Shear Force acting on Surface of Sheet from Leading Edge to x.

Symbol	Description
C_f	Total Shear Coefficient = $\frac{F}{\frac{1}{2}\rho \overline{u}^2 x}$
R_{δ_m}	Reynolds Number of Free Stream based on δ_m $R_{\delta_m} = \frac{\overline{u}\,\delta_m}{\nu}$
$(R_{\delta_m})_T$	Value of R_{δ_m} at Point where Transition Occurs.

INTRODUCTION

In the scholastic year of 1936-37, a new wind tunnel was constructed at GALCIT * under a NACA ** grant by Drs. M. and F. Clauser and the author for the particular purpose of investigating the effect of curvature on the transition point between laminar and turbulent flow on a smooth, plane surface. At the end of the year, Drs. M. and F. Clauser carried out the preliminary investigation on this problem; the merits of the tunnel, their methods of research, and their results and conclusions are discussed in reference #1. Their work had two fundamental conclusions: (1) that curvature has a large effect on the transition point, and (2) that this effect can be represented by a linear function of x/r_c. Unfortunately a certain discrepancy appeared in their experimental results that combined with some recent English investigations on the transition phenomena to cast a serious shadow of doubt on the validity of the Clauser's two fundamental conclusions. The

* Guggenheim Laboratory of Aeronautics at the California Institute of Technology

** National Advisory Committee for Aeronautics

purpose of the present investigation, carried out by the author under the supervision of Drs. Millikan and von Karman, is to reinvestigate the effect of curvature on the transition phenomena under the same experimental conditions as the previous investigation but using a fundamentally more sound experimental technique coupled with a redesign of certain parts of the tunnel's working section enabling the author to repeat the series of measurements carried out by the English which are pertinent to the present problem and thus to evaluate the magnitude of their influence. This work was done during the past scholastic year of 1937-38.

The discrepancy that appeared in the Clauser's work is contained in the failure of their velocity profiles to indicate the transition region. As is known, the non-dimensional velocity profile in the laminar region is a universal function of the non-dimensional distance from the wall: the equation may be expressed in the usual Blasius form,

$$\frac{u}{U} = f\left(\frac{y}{x}\sqrt{R_x}\right) = f\left(\frac{y}{\delta}\right)$$

and is valid provided the pressure gradient in the

axial direction is zero or so small as to be negligible (δ/c is of the order of magnitude of 0.01 and hence the influence of curvature on the velocity profile may be neglected, as Prandtl has pointed out in reference #5.) According to this criterion the Clauser profiles do not indicate any clearly defined laminar regime. An investigation of the pressure gradient in the channel subsequent to their work disclosed that this gradient, based on the dynamic pressure of the free stream, was far from ideal, varying in an arbitrary fashion between limits of ±10% from one measuring station to the next. This may in itself account for the discrepancy. Also, their basing the velocity profile on δ instead of the Blasius non-dimensional distance, $y/x\sqrt{R_x}$, is an unfortunate choice, since the present investigation showed that the actual boundary layer thickness is a very difficult quantity to determine with any degree of consistancy to an accuracy better than 10% since u approaches U asymptotically at the edge of the boundary layer. Furthermore, turbulence as criterion of transition is not as yet firmly established. Dryden's recent work at the Bureau of Standards has indicated that the laminar and turbulent regimes of the boundary layer are not

distinguishable on the basis of the magnitude of turbulence when the free stream itself has a reasonable amount of turbulence. The free stream in the present case has a magnitude of turbulence of close to $\frac{1}{3}\%$; whether this can be called a "reasonable amount" is not known, but in any case the turbulence method of determining transition must be viewed at the present with considerable scepticism.

Work done this past year in England at Cambridge University under the direction of Prof. Melvill Jones showed that the transition point of the flow along a flat plate depends very critically on the inclination of the plate to the air flow's direction. During Prof. Jones visit at the laboratory this past year he left here experimental curves showing the effect of inclination on the transition point of a smooth, flat plate with in one case a rounded and in the other case a sharpened leading edge (the latter corresponds to the case here). Since the author is unaware of any publication containing these results at the present time, he will take the liberty of reproducing the experimental curve for the sharp edged sheet. (Figure #1) Jones' results

show that an unfavorable inclination of the sheet will greatly reduce the Reynold's number of transition. Hence if the sheet during the Clauser's investigation were so aligned to preserve a high value of $(R_x)_T$ on the convex side but cause a greatly reduced $(R_x)_T$ on the concave side, the effect that they attributed to curvature might be due simply to the sheets' inclination. (Figure #2) An inspection of their alignment showed such a condition to be quite possible.

Before going further, the author wishes to say that, despite these sources of possible error, the present investigation validated in the main the Clauser's fundamental conclusions, although their absolute values of transition Reynolds number could not be checked. Hence, this report serves not to discredit, but to support the Clauser' investigation qualitatively and correct it quantitatively.

DEVELOPMENT OF NEW EXPERIMENTAL EQUIPMENT

In order to investigate the problem more comprehensively and to secure more accurate measurements, several new pieces of equipment were built and part of the working section and motor unit of the tunnel were reconstructed.

The problem of vibration in such a centrally suspended steel sheet as exists in the tunnels' working section is very difficult to completely eliminate. The motor-propeller unit had previously been attached rigidly to the rest of the tunnel and at high speeds was causing a very undesirable vibration in the sheet. This vibration was eliminated almost entirely by separating the motor-propeller unit structurally from the rest of the tunnel and connecting the two by a flexible ring of rubberized cloth. The unit was mounted on an improved spring mounting, which, in combination with the flexible coupling, allowed the motor-propeller unit to vibrate by itself without distrubing the remainder of the tunnel. The sheet deflects slightly under a natural pressure drop

across it, but observation showed that if any vibration exists, its amplitude must be less than 0.001 cm.

In making velocity surveys it is necessary to traverse the boundary layer in the y direction, perpendicular to the tangent plane of the sheet. The total distance traversed is of the order of a centimeter or less. Hence, in order to make accurate observations on the boundary layer it is very necessary to be able to set and maintain the measuring instrument in position to a tolerence of less than 0.001 cm. The walls of the tunnel are neither sufficiently rigid nor suitable for attaching the measuring instruments to them. So a standard was built consisting of a 6 inch Shelby tube fastened rigidly with its axis vertical to a triangular base of 3 foot sides which rests on the concrete floor outside the tunnel. In the top of the tube is a rotatible head carrying an arm 2 feet in length on the end which is fastened a small movable carriage holding the measuring instrument (hot-wire or pitot tube) and actuated by two micrometer heads placed in tandem, one being used to establish a zero position and the other being

used for traversing the boundary layer. The micrometer heads are graduated in thousandths of centimeters. The zero position was established by an electrical contact method which it is felt is accurate to 0.002 cm or less. The standard can be moved about on the floor of the research room, the arm can be rotated about a vertical axis and adjusted vertically and horizontally, and the carriage itself can be swiveled about a vertical axis. Hence the measuring instrument can be placed in any position relative to the central sheet that is desired. In making velocity surveys with the total-static tube (to be discussed shortly) the carriage was set in such a position that the head of the tube was accurately aligned parallel to a tangent plane to the central sheet opposite the measuring station that was being used at the time. This was done by a double contact electrical instrument especially built for this purpose.

The ideal instrument for making velocity profiles in the boundary layer is the hot-wire anemometer as used by van der Hegge Zijnen, Dryden, and many other investigators. It causes

very little disturbance of the flow, being very small, and in the preliminary investigations carried out by the author, it was able to be constructed so that its calibration held to an accuracy of well within ½%. However, its technique is involved and lengthy and from considerations of speed and the necessary tolerances of accuracy, a pitot-static method of measuring the velocity in the boundary layer was decided upon. In order to obtain the dynamic pressure at any point it is necessary to measure both the total and static pressures at that point. The total pressure measurement has no difficulties. However, there is considerable uncertainty in measuring the static pressure due to the effect of curvature and the effect of the boundary layer. A preliminary survey of the static pressure across the boundary layer was carried out with a small static tube (figure #3). This yielded surprisingly favorable results. As far as the boundary layer is concerned the static pressure is appearantly quite unaware of its existance. The static tubes employed were built from 18 guage steel hypodermic needle and were consequently quite small (the length of the head) being only 1.125 inches. Building a single tube of

such small size, similar to the standard Prandtl pitot-static tube, for measuring both the total and static pressures with a simgle tube is not practical. Hence a tube was constructed consisting of two 18 guage hypodermics, each bent to the shape of a "L" and soldered into parallel shafts of brass tubing separated laterally about one centimeter by spacers. The one hypodermic had its end drilled out and flattened, leaving a slot 0.005 cm wide and 0.100 cm in width; this measured the total pressure and is very similar to the type of total head tube used by Jones, and earlier by Stanton (reference 3). The other hypodermic had a rounded brass plug fitted into its end and a double series of holes drilled in its side 8 diameters back from its nose and 16 diameters out from its stem. This tube measured the static pressure and is similar to the type recommended by the NACA (reference 4). The lengths of the heads of the two are 1.125 inches each, and the plane of the heads lies parallel to the sheet at the point of measurement, the tubes being separated a distance sufficient to avoid interference effects. The total head tube is bent

slightly inward to give good clean contact with the sheet. Such a tube should record the dynamic pressure to an accuracy of one percent. For lack of a better name, this tube has been called a "total-static tube".

The laboratory is well equipped with many excellent micromanometers, accurate to 0.001 cm. These were used to record the dynamic pressures measured by the total-static tube. One thousandth of a centimeter vertical displacement is well below the desired accuracy required for most air flow measurements of the present type. However, for certain measurements very close to the sheet, the dynamic pressure was of the order of magnitude of one thousandth of a centimeter of alcohol and hence it was necessary to extend the accuracy of measurement to one ten-thousandth of a cm. The customary method of doing this is with a modified Chattock guage. However, in the present case it was found sufficiently accurate to fasten a microscope rigidly to the carriage of the manometer and to observe the image of the fluid's meniscus in the sight tube with a four-power objective. The

eyepiece of the microscope contained a moveable cross-hair combined with a graduated scale having 1000 divisions. A very sharp image of the meniscus could be obtained and the cross-hair placed tangent to it very accurately. The inclination of the sight tube was set so that a movement of the meniscus across the entire field of the microscope amounted to about 0.030 cm vertical displacement; this gave about the right range, minimized fluctuations, and enabled the observer to measure to within one ten-thousandth of a centimeter vertical head of the fluid. The position of the cross-hair on the eyepiece scale was calibrated against the angular rotation of the accurately machined manometer lead screw, which calibration proved to be very satisfactorily linear and relatively constant (figure #4). The most obstinant bug in this type of instrument is the change of zero level with temperature. By passing the illumination of the sight tube through a long water cell and calibrating immediately before each run this trouble was largely eliminated.

In order to change the angle of attack of the

sheet with the wind direction to investigate the so-called "Jones Effect", the structual support of the working section was modified so as to make the entire working section moveable about a fixed pivot. The working section was separated structurally from the pressure reservoir. Beneath the working section's triangular base, which is normally jacked up six inches off the floor by adjustment screws, was placed a subsidiary base fastened rigidly to the cement floor; the two were separated by two sets of cold rolled, steel bars, each fastened to its respective base, and the contacting faces well greased to permit sliding. A pivot pin was placed through one set, the pin being placed on a line parallel to the principal tunnel axis 3/8" upstream from leading edge of the sheet and 3/8" downstream from the end of the converging section; two push-pull screws were fastened to the other set, which moved the base of the working section relative to the fixed subsidiary base and hence rotated the whole working section about the pivot as a center. The exit section was mounted on casters and fastened rigidly to the working section so that it moved with it. The 3/4" gap between the working section and the converging section was bridged by strips of

three inch wide Scotch tape, the tape being reset on each change of angle. A pointer attached to the moveable working section sliding across a scale attached to the fixed subsidiary base recorded the angular movement of the former. Hence by rotating the working section containing the sheet as a whole, any angle of inclination of the sheet to the wind direction could be obtained within a range of 20 degrees. This was found quite satisfactory to investigate completely the Jones effect.

Photographs of the new instruments are included at the end of this thesis.

EXPERIMENTAL PROCEEDURE AND RESULTS

After the instruments and changes in the tunnel described in the previous section were completed and certain preliminary measurements on transition were made (these will not be discussed here since they are not pertinent to final results), an investigation with smoke was carried out in order to determine whether a sufficient range of angularity was available to cause actual separation of flow from the leading edge on both the concave and convex sides. If such a range is available, the Jones effect must surely lie within this range. The smoke was generated by burning a mixture of sawdust and kerosene in a tube with the forced draft of a vacuum cleaner blower, and was injected into the air stream at the midpoint of the tunnel crossection about eight inches upstream from the leading edge of the central sheet. The smoke was brightly illuminated by an electric arc placed on the pressure reservoir's floor and viewed with a telescope fixed on the top of the working section just in front of the sheet's leading edge. The flow lines could be clearly distinguished, but no change in their general character could be observed through-

out a central range of angular inclination of the sheet. However, at one extreme or the other, when separation occurred at the leading edge, this phenomena of flow separation could be seen with great clarity and sharpness. As soon as it occurs a wedge of sharp, very dark shadow appears between the illuminated flow lines and the side of the sheet on which separation is taking place, the head of the wedge being at the leading edge, of course. Due to the difficulty of securing sufficient illumination no photographs were taken, however. The range of angular inclination between separation on the concave side, on the one hand, and the convex side, on the other, was found to be about 14°, and the positions at which separation would occur were established. In the rest of the measurements, a central position between these limits of separation was made an arbitrary zero, to which all angles are refered. Subsequent measurements validated the choice of this position as a neutral one in which the Jones effect does not influence the transition point and at which the only effect is that of curvature.

With the angular inclination of the sheet

set at the neutral zero position described above, the static pressure gradient was reduced to a minimum value by varying the width of the channel along its length. The measurement of static pressure was made with small static pressure tubes, carefully aligned so that their heads were precisely tangent to the surface of the sheet and set uniformly 0.6 cm out from the surface at their different stations. The pressure heads were recorded by one of the standard laboratory manometers. The variation of the non-dimensional static pressure, p_s/Q, downstream from one measuring station to the next for both sides of the working section is given in figure #6. The variation in p_s/Q is in most cases less than ½% between stations, the maximum never greater than 2%, and the over-all variation less than 1%. As the laminar velocity profiles later demonstrated, this was a satisfactory hydraulic approximation to a flow of zero pressure gradient. The variation of p_s/Q with speed proved to be negligible in the range of speeds covered during these experiments.

The magnitude of the turbulence in the free stream of the channel was measured at the leading

edge of the sheet in the center of the convex side of the channel with some very modern hot-wire equipment built during the past year at GALCIT. This checked the Clauser's value at $\sqrt{\left(\frac{u'}{U}\right)^2} = 0.52\%$ and is felt to be an accurate measurement. The quantity, $\sqrt{\left(\frac{u'}{U}\right)^2}$, was found to be independent of speed throughout the range used.

With the pressure gradient reduced to a minimum, measurements on the transition phenomena were started. The tunnel is not suitable for traversing the boundary layer in the x direction, as in the case of Jones' experiments; hence the boundary layer was traversed in a "U" direction, figuratively speaking. The position of the total-static tube was established at one of the measuring stations, and measurements were made at different velocities throughout the speed range of the tunnel. Hence, for each station the speed at which transition occurs was determined. This is the most arduous method, as the results will show, but from structural consideration the most practical in the present case.

The technique of determining the speed at which transition occurs at any given station was twofold.

First, a series of velocity profiles was obtained by traversing the boundary layer in a y direction with the total-static tube. The results were plotted in the non-dimensional form:

$$\frac{u}{U} = f\left(\frac{y}{x}\sqrt{R_x}\right)$$

and compared with the theoretical Blasius curve for laminar flow. There was one experimental parameter which had to be determined before the profiles could be computed, this being the effective y distance at which the slot of the total head tube acts. The zero position on the micrometer head was set with the total head tube just touching the sheet. The slot is still a distance from the wall, however, and the effective distance at which the tube indicates the total pressure of the flow was found to be somewhat greater than the half width of the tube's end, the geometrical distance at which one would expect it to act. In the laminar region, the velocity profile, plotted against a y distance based on the geometry of the tube instead of its effective center, has in most cases precisely the same shape as the Blasius profile but lies slightly displaced from it to right or left. Since

the curve must go through the origin it seemed justified to add a small amount, Δ y, to the y distance of the tube's geometrical center, thus determining an effective center which would shift the velocity profile to right or left, as the case demanded, so that it would satisfy the relation u = o at the wall. When this is done, the laminar profile falls very beautifully along the theoretical Blasius curve (figure #7). This displacement of the geometrical center to an outward effective position may be due to the disturbance in flow caused by the tube's presence or to the slot being inclined at some slight angle to a plane parallel to the sheet or to both. It varies from station to station but remains a constant at any particular station. A few of the laminar profiles are seen to be a little fatter than the Blasius curve beyond $\frac{u}{U}$ = 0.500. This may be due to the slight remaining pressure gradient or to a reduction in the effective distance of the tube's center as it passes further and further out of the boundary layer. In any case, this discrepancy is quite small. This verification of the theoretical Blasius curve in the laminar regime provided a very fundamentally sound method of determining the transition point. As long as the

flow is laminar, all profiles lie along the Blasius curve. As soon as transition sets in the profile departs from the Blasius curve, being above it for small values of η ($= y/x\sqrt{R_x}$) crossing it at some moderate value of η , and lying below it for large values of η .

This departure becomes the more pronounced the further the speed is from the end of the laminar regime. Eventually, of course, the profile, would become a fully developed turbulent profile, but in the range of speeds available, the course from pure laminar to fully developed turbulent flow at any one station could not be completed. The departure from the laminar curve in most cases stands out quite sharply and enables one to determine the beginning of transition within an accuracy of $R = 50{,}000$. The value of the Reynolds number at which the boundary layer profile first starts to break away from the Blasius laminar curve will be called the "transition point".

The time required to make a satisfactory, complete set of velocity profiles over the tunnel's speed range at each measuring station would have

proven quite considerable, so a shorter method of determining or at least indicating transition was desired. It is to be noted that in Jones' experiments one of his sharpest indications was a quick rise in the total pressure recorded by a tube in contact with the wing's surface. The physical significance of this is quite clear: the work of many investigators has shown that in any type of boundary layer flow there is a thin region quite close to the surface in which the flow is laminar in character in that the profile is linear, $u = \text{constant} \cdot y$. In the case of a tube having a slotted end in contact with the surface, the slot will measure the dynamic pressure of the air flow at some small effective distance from the wall, y_e, considering for the moment that $p_s = 0$.

$$u_e = \frac{\partial u}{\partial y} \text{CONSTANT} \cdot y_e$$

But this constant can be determined from the laws of laminar flow, in that

$$\tau_o = \mu \frac{\partial u}{\partial y}$$

Hence

$$\tau_o = \mu \frac{u_e}{y_e} \qquad \text{OR} \qquad u_e = \frac{\tau_o}{\mu} \cdot y_e$$

That the local shear force under-goes a violent increase in the transition region is well known; hence the violent increase in u_e. In the present case, since $\bar{u}$ rather than x was varied to determine the transition point, coefficients, rather than relative quantities were evaluated. The total-static tube was set so that the total-head tube just touched the sheet. Being bent slightly inward the total-head tube in contact with the wall meant that the static tube cleared the wall by about a millimeter. Since the static tube is aligned accurately parallel to the sheet, and since measurements showed the static pressure to be unaffected by the presence of the boundary layer, it should record the static pressure close to the wall with reasonable accuracy. The gradient of static-pressure between the point at which the static tube records it and the effective center of the total-head tube is surely negligible. Consequently, it seems reasonable to assume that the total-static tube measures the dynamic pressure of

the air flow at some small effective distance from the wall, y_e, determined by the shape of the total-head tube and its interference on the flow characteristics. The local shear coefficient can be determined from this dynamic head, q_e, and the dynamic head of the air flow in the free stream just at the edge of the boundary layer, Q, by the following analysis:

$$\tau_o = \mu \frac{\partial u}{\partial y} = \mu \frac{u_e}{y_e} = c_f \tfrac{1}{2} \rho \bar{u}^2$$

$$\therefore c_f = \frac{2\nu}{y_e} \cdot \frac{u_e}{\bar{u}} \cdot \frac{1}{\bar{u}} = \frac{2x}{y_e} \frac{u_e/\bar{u}}{R_x}$$

$$\text{BUT} \quad \frac{u_e}{\bar{u}} = \sqrt{q_e/Q}$$

$$\therefore c_f = \frac{2x}{y_e} \frac{\sqrt{q_e/Q}}{R_x}$$

Great care was taken to measure Q just at the edge of the boundary layer, since the curvature of the stream lines in the potential flow requires a gradient of U in the y direction. R_x was determined from Q, x, the density of the manometer fluid, the air temperature, the barometric pressure, and the relative humidity by the usual method, using the values of ν deduced from Smithsonian meterological

tables.

y_e was evaluated by fitting one value of c_f to the theoretical Blasius curve at a speed at which the flow was established as laminar by a boundary layer profile. It was assumed to remain constant throughout the speed range. The results showed that this assumption is not strictly true, since the general inclination of the laminar portion of the c_f vs R_x curve was in most cases steeper than that indicated by the Blasius curve. Also y_e varied from station to station, increasing as x increased. Hence these measurements could not be regarded as giving the true value of the local shear coefficient. However, the course of the shear coefficient computed in this manner seemed to be similar to the course taken by the actual shear coefficient. In particular the minimum value of the experimental shear coefficient was shown by boundary layer profiles to correspond to the start of transition; as at this point one would expect the real shear coefficient to leave its downward trend along the laminar curve and start upwards toward the fully developed turbulent curve, the shear method of determining the transition point

seemed justified. As a matter of fact, the correspondence between transition indicated on the one hand by velocity profiles and on the other by shear measurements was so excellent at the first station at which the method of shear was tried, that more confidence was developed in the shear measurements than they really merit (figures #35 and #36). Their true purpose is to be an indicator of the transition point. After determining the transition point's approximate location by shear measurements this location was verified by boundary layer profiles at speeds just below and just above. Hence, a combination of the two techniques proved very successful in establishing the transition regime, and, since the velocity profile is an exceedingly fundamental characteristic of the type of flow, this method must surely be an accurate one. In all boundary layer profile graphs the theoretical Blasius laminar profile is drawn in with a heavy line. In all shear graphs both the theoretical Blasius curve for the local shear coefficient of pure laminar flow and the theoretical von Karman curve for the local shear coefficient of fully developed turbulent flow are drawn in with heavy lines. In only one case did the shear and velocity profiles conflict.

This was at station #4 on the convex side at $\alpha = 0°$ (figures #29 and #30) where the transition occurred near the maximum velocity of the tunnel. Since the motor is a little unstable at high speeds, the observations were carried out with great difficulty and hence may not be accurate. In all other cases, the two methods agree very well indeed. The shear method was developed after the surveys of transition on the concave side had been completed; on this side, then, only boundary layer measurements are available for determining transition. However, they are quite complete and are felt to be sufficient to determine the transition point by themselves.

Using the technique just described for determining the transition point, the work was divided into two parts; first, an investigation of the Jones effect was carried out on both sides of the sheet by determining the transition point at a single station over a range of angles of incidence. On either side angles tending to preserve a high value of $(R_x)_T$ will be called "STABLE"; angles tending to reduce the neutral value of $(R_x)_T$ will be called "UNSTABLE". On the concave side, measurements were carried out at both stations #2 and #3,

the measurements at station #3 consisting only of a single profile in the transition regime. The purpose of this profile was to establish that $(R_x)_T$ did not exceed its value at $\alpha = 0$ throughout the range of stable angles. The measurements at station #2 located the transition point accurately and showed that over a range of 6° STABLE to 3° UNSTABLE, the transition point is unaffected by inclination. At 6° UNSTABLE, however, $(R_x)_T$ decreases markedly. As a matter of fact, even at the lowest speed the profile is not definitely laminar, but since 6° UNSTABLE would never be used, no further investigations at this point were carried out. It is well to note that with only 1° more toward the unstable, separation at the leading edge occurs on this (concave) side. On the convex side, the measurements for the stable angles were carried out at station #7, since this station was ideal for both shear and velocity profile measurements. Measurements were made at $\alpha = 0°$, 3°, and 6° STABLE. They showed that in this range $(R_x)_T$ was independent of inclination. One measurement at station #7 was carried out for the unstable angle of 3° ; a marked decrease in $(R_x)_T$ occurred, so great in fact that it was not possible to make a

satisfactory shear determination. Boundary layer velocity profiles however, were taken at station #7; then the tube was moved to station #4, where the dynamic heads at the wall were high enough to record satisfactorily. It was at this point that the micro-micromanometer was constructed. Measurements were carried out at station #4 at the unstable angles of 4.5°, 3°, 1.5°, and the neutral position, $\alpha = 0^\circ$. This series of measurements confirmed the choice of $\alpha = 0^\circ$ as a truly neutral position. The measurements on transition for the Jones effect investigation are given in figures #8--24, and #26, 27, 28, 29, 30, 31, 36, and 37; the results of the investigation are given in figure #25, as a plot of $(R_x)_T$ vs α. It is to be noted that the stable angles for both sides of the sheet are plotted to the right of the axis, the unstable to the left. In reality, this is not the case, since a stable angle for one side is an unstable angle for the other.

After completing the investigation of the Jones effect, which established that $\alpha = 0^\circ$ was a neutral position in which transition depended on

curvature and the general properties of the flow but was independent of inclination, the section was set at $\alpha = 0^{\circ}$, and a series of measurements at each station downstream were undertaken to determine the variation of $(R_x)_T$ along the length of the sheet and from the convex to the concave side. On the concave side stations #2 and #3 were the only stations at which transition occurred within the speed range of the tunnel, stations #4, #5, etc. requiring speeds lower than the minimum, and station #1 requiring speeds higher than the maximum. On the convex side stations #1, #2, and #3 required speeds higher than the maximum for transition to occur. However, at the remaining stations on this side, transition lay within the speed range, and, hence, a complete set of observations for stations #4, #5, #6, #7, and #8 were carried out. Except for station #4, as has been previously mentioned, the results were very satisfactory. The experimental results of this investigation are given in figures #26--39.

Prandtl has pointed out that the effect of curvature can be conveniently expressed by δ/r_c, where δ is the boundary layer thickness, reference 5.

The Clauser's plotted their results against x/r_c ; this does not take into account the velocity, however, and δ/r_c was felt to be the more fundamental parameter. δ , the actual thickness of the boundary layer is an exceedingly difficult quantity to determine with any accuracy, as has been mentioned, so von Karman suggested using the momentum thickness, δ_m , rather than the actual boundary layer thickness. This parameter, δ_m, is defined by the equation

$$\rho \bar{u}^2 \delta_m = \rho \int_0^\infty u(\bar{u} - u)\, dy$$

$$\text{or} \quad \delta_m = \int_0^\infty \frac{u}{\bar{u}}\left(1 - \frac{u}{\bar{u}}\right) dy = \int_0^\infty \left(\frac{u}{\bar{u}} - \frac{q}{Q}\right) dy$$

It has the clear physical significance of being the depth of a layer of fluid of unit width in the free stream that has the same amount of momentum as the momentum defect in the boundary layer at the point in question. In the case of laminar flow with zero pressure gradient along a plane flat boundary where δ/r_c is either zero or vanishingly small, δ_m is directly proportional δ , being related by the equation

$$\delta_m = \delta \int_0^1 \frac{u}{\bar{u}}\left(1 - \frac{u}{\bar{u}}\right) \frac{dy}{\delta} = \delta \int_0^1 f(1-f)\, d\eta' = \delta \alpha'$$

where $\alpha' = \int_0^1 f(1-f)\, d\eta' =$ constant for laminar flow. δ_m is also related to the total shear coefficient

by the relation,

$$\frac{dM}{dt} = \rho \bar{U}^2 \delta_m = F = C_f \tfrac{1}{2} \rho \bar{U}^2 x$$

$$\therefore \quad \frac{\delta_m}{x} = \frac{C_f}{2}$$

$\frac{u}{\bar{U}}\left(1-\frac{u}{\bar{U}}\right)$ was computed from the velocity profiles for each station concerned, and δ_m was determined from these curves by graphical integration. The curves $\frac{u}{\bar{U}}\left(1-\frac{u}{\bar{U}}\right)$ are given in figures #40--46, δ_m vs R_x in figure #47, $\frac{2\delta_m}{x} = C_f$ vs R_x in figure #48, and the momentum defect $= \int_0^\infty u(\bar{U}-u)\,dy = 2\delta_m Q$ vs R_x in figure #49. The final results of this investigation of the effect of curvature are plotted in the form of a graph of $(R_{\delta m})_T$ vs $\frac{1000\,\delta m}{r_c}$ (figure #51). The values of $\frac{1000\,\delta m}{r_c}$ for the convex or stable side are plotted as positive abscissa, the values of $\frac{1000\delta m}{r_c}$ for the concave or unstable side as negative abscissa. Thus the effect of curvature on the transition point can be shown by a single curve. The greatness of the curvature effect is immediately appearant. The value of $(R_{\delta m})_T$ for a flat plate would lie at the axis, $\frac{1000\,\delta m}{r_c} = 0$, since in this case $r_c \rightarrow \infty$. A graph of $(R_x)_T$ vs x/r_c is also included, on which the Clauser curves are indicated (figure #50).

CONCLUSIONS

The conclusions coming from the results of the investigation of the effect of inclination on the transition point are:

(1) On the concave side there is a wide range of angles over which the transition point is unaffected by inclination. As one approaches close to the limiting inclination where separation at the leading edge occurs, however, the transition point occurs at a much smaller value of R_x, one half or less, and rapidly loses significance since after separation occurs the boundary layer flow belongs in a category outside the province of this paper (reference 8).

(2) On the convex side there is a range of stable angles over which the transition point is unaffected by inclination and a range of unstable angles where the transition point is greatly reduced by the unfavorable inclination of the sheet, but remains at a fairly constant value. These two ranges are joined by a transition region. How sharp the transition region is, that is over what range of angularity it occurs, cannot be answered

until more complete measurements are taken. However, judging from Jones' results the transition should take place very sharply.

(3) There is a range of angles in which inclination does not effect the transition on either concave or convex side. In this neutral region the only effect can be that of curvature.

The conclusions coming from the investigation of the effect of curvature (in the neutral region) are:

(1) Qualitatively, curvature has a very great effect on the Reynolds number of transition. $(R_x)_T$ on the concave (unstable) side are considerably less than for a flat plate ($r_c \rightarrow \infty$) under similar experimental conditions whereas $(R_x)_T$ on the convex (stable) side are onsiderably greater. The $(R_x)_T$ on the concave side are reduced by a factor of 2 relative to the $(R_x)_T$ on the convex side. This confirms the Clauser's conclusions and, as they mention, is to be expected from theoretical considerations (references 6 and 7).

(2) Quantitatively, the effect of curvature

can be represented by a single graph of $(R_{\delta m})_T$ vs $\frac{1000\,\delta m}{r_c}$. As to the exact form of this function, little as yet can be said. The present measurements covered only a very limited range of values and within this small range the accuracy of the measurements is not sufficient to determine more than the general trend of the curve. Thus the linear curve of the Clausers could neither be verified nor corrected; however, all of their absolute values of $(R_x)_T$ were found to be too large. What the cause of this discrepancy is the author is not prepared to say. It may lie in their use of turbulence as a criterion instead of velocity profiles. The trend so far seems to be that $(R_{\delta m})_T$ increases with increasing $\frac{1000\,\delta m}{r_c}$; however, nothing more can be said until future measurements extend the range of investigation.

LIST OF REFERENCES

1. Clauser, M. and Clauser, F: The Effect of curvature on the Transition from Laminar to Turbulent Boundary Layer: NACA T.N. 613.
2. Dryden, H. L: Air Flow in the Boundary Layer near a Plate: NACA T.R. 562.
3. Jones, B Melvill: Flight Experiments on the Boundary Layer: J. Ae. Sci: Vol. 5, #3, Jan. 1938.
4. Merriam, K. G. and Spaulding, E. R: Comparative Tests of Pitot-Static Tubes: NACA T. N. 546.
5. Durand: Aerodynamic Theory: Vol III.
6. Wattendorf, F. L: A study of the Effect of Curvature on Fully Developed Turbulent Flow: Proc. Roy. Soc. Lond: Series A No. 865 vol. 148 pp. 565-598 Feb. 1935.
7. von Karman, Th: Some Aspects of the Turbulence Problem: Paper presented at the Congress of Applied Mechanics: Cambridge, England; 1934.
8. von Doenhoff, A. E: A Preliminary Investigation of Boundary Layer Transition along a Flat Plate with Adverse Pressure Gradient: NACA T.N. 639.

FIG 1

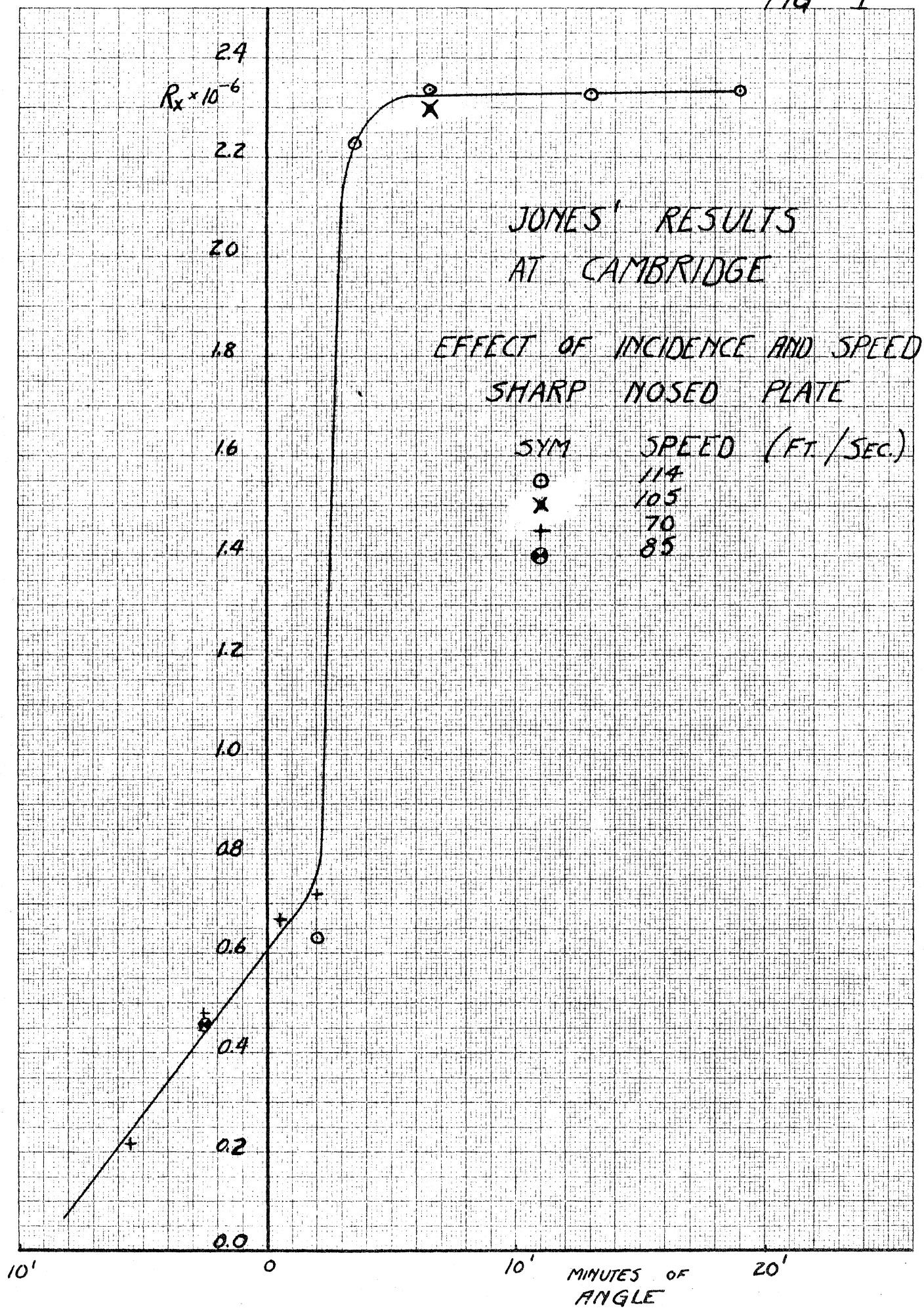

FIG 2

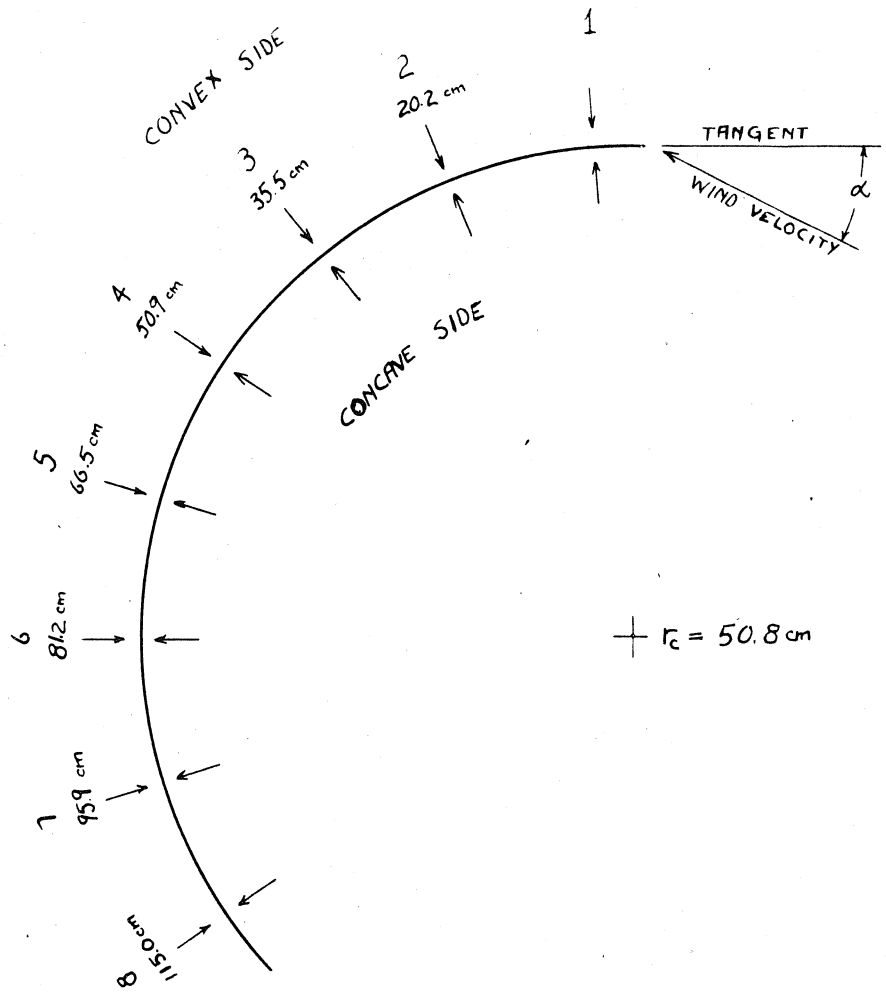

							TOLERANCES .010 OR ¼ UNLESS OTHERWISE NOTED
MATERIAL	FINISH	HEAT TREAT	DRAFTSMAN	CHECKED	APPROVED	ENGINEER	
GUGGENHEIM AERONAUTICAL LABORATORY CALIFORNIA INSTITUTE OF TECHNOLOGY			PROFILE OF CENTRAL SHEET : NACA TUNNEL				
			NAME				DRAWING NO.

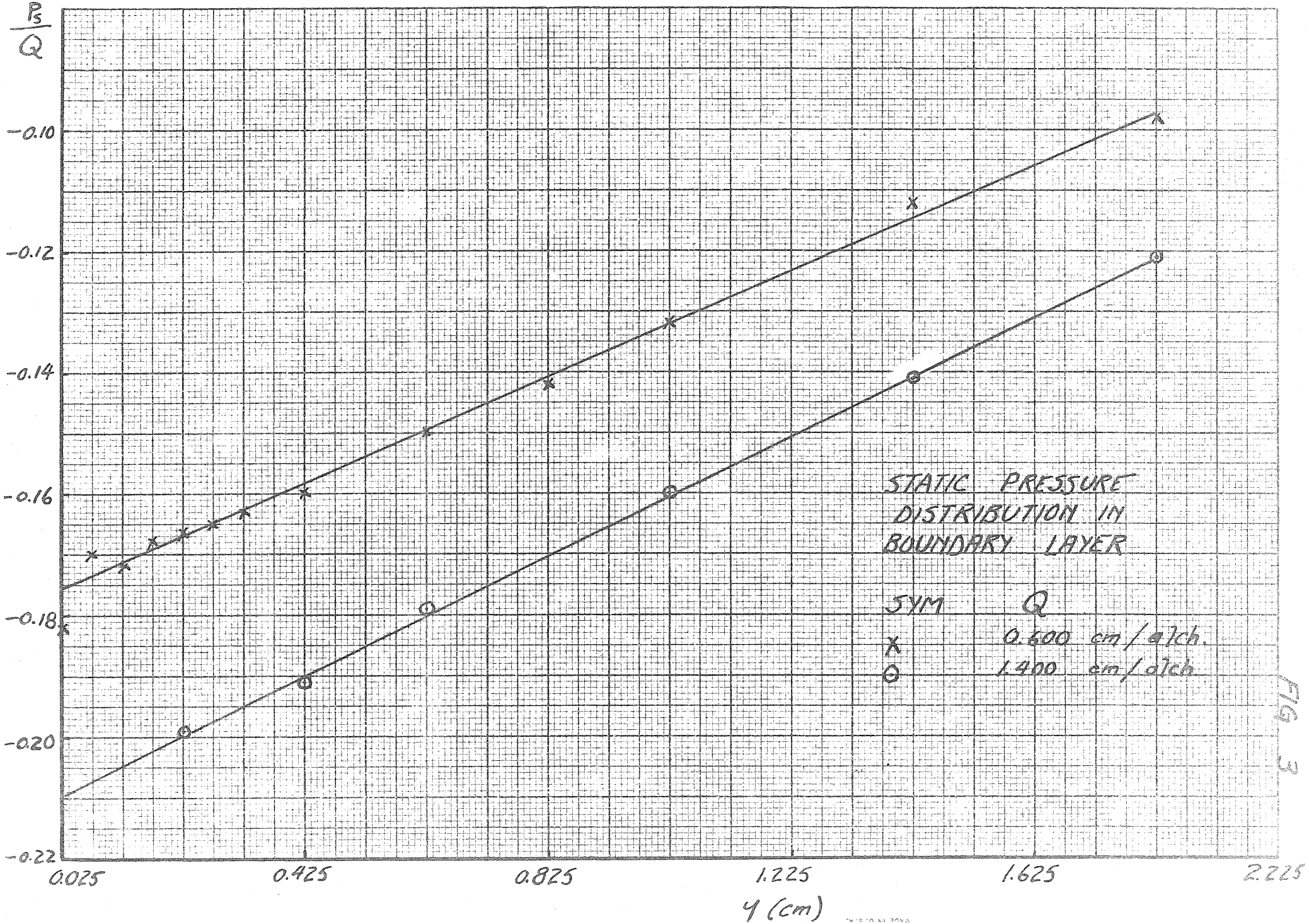
$\frac{P_s}{Q}$
-0.10
-0.12
-0.14
-0.16
-0.18
-0.20
-0.22
0.025
0.425
0.825
1.225
1.625
2.225
y (cm)
STATIC PRESSURE DISTRIBUTION IN BOUNDARY LAYER
SYM Q
X 0.600 cm/dich.
O 1.400 cm/dich

Fig 3

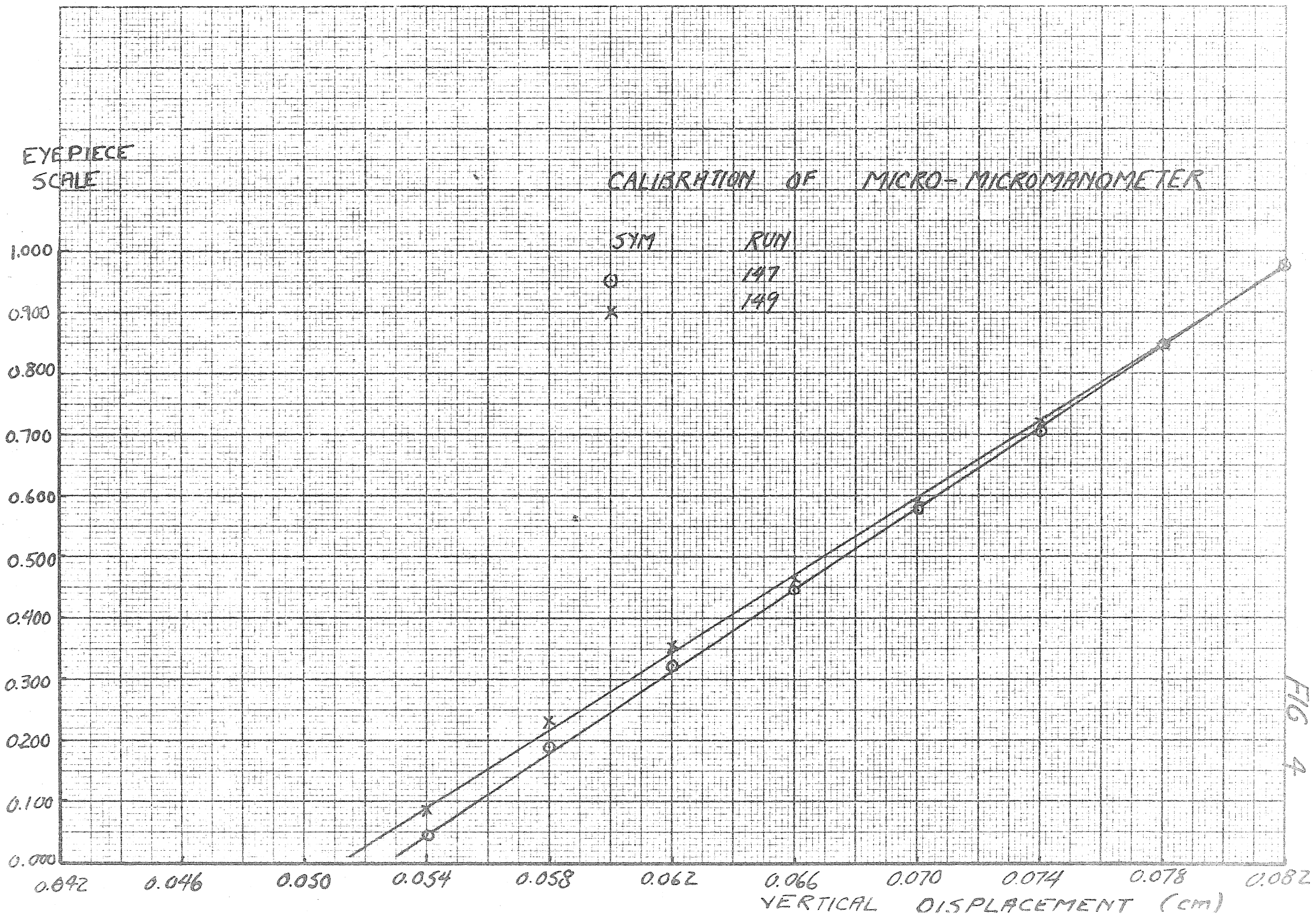

FIG 4

FIG 5

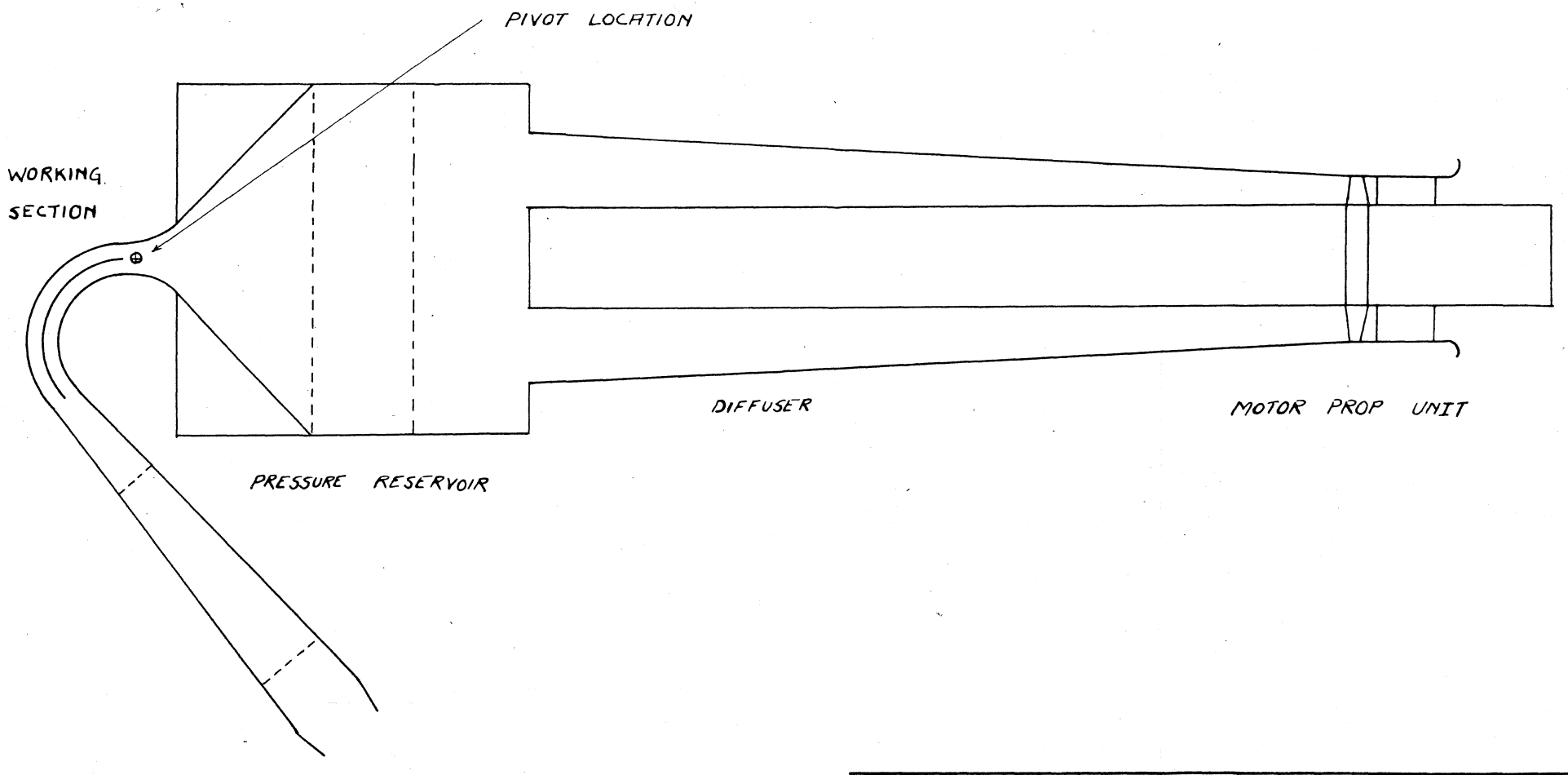

							TOLERANCES .010 OR UNLESS OTHERWISE NOTED
MATERIAL	FINISH	HEAT TREAT	DRAFTSMAN	CHECKED	APPROVED	ENGINEER	
GUGGENHEIM AERONAUTICAL LABORATORY CALIFORNIA INSTITUTE OF TECHNOLOGY			DIAGRAMATIC TOP-VIEW NACA TUNNEL				
			NAME				DRAWING NO

FIG 6

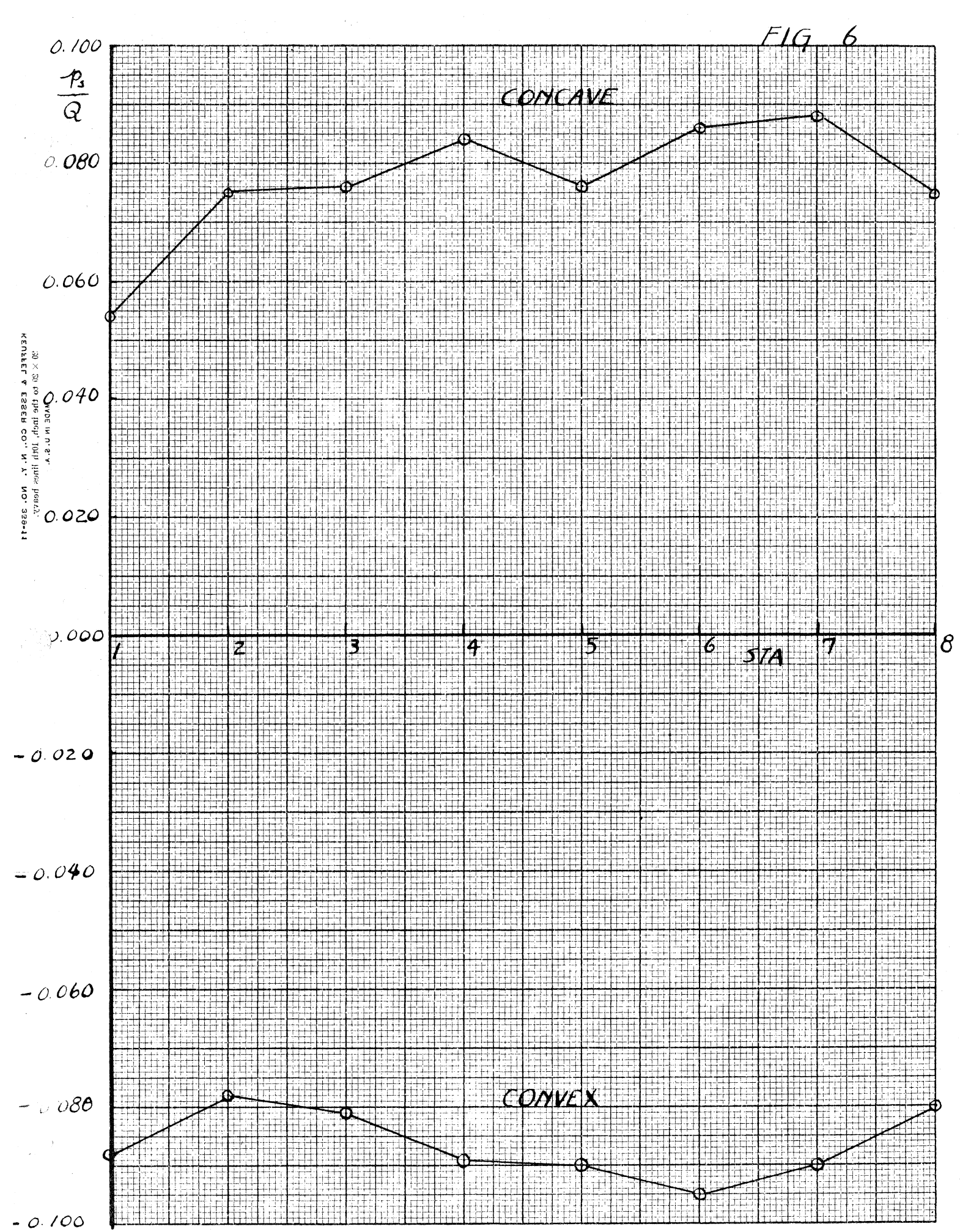

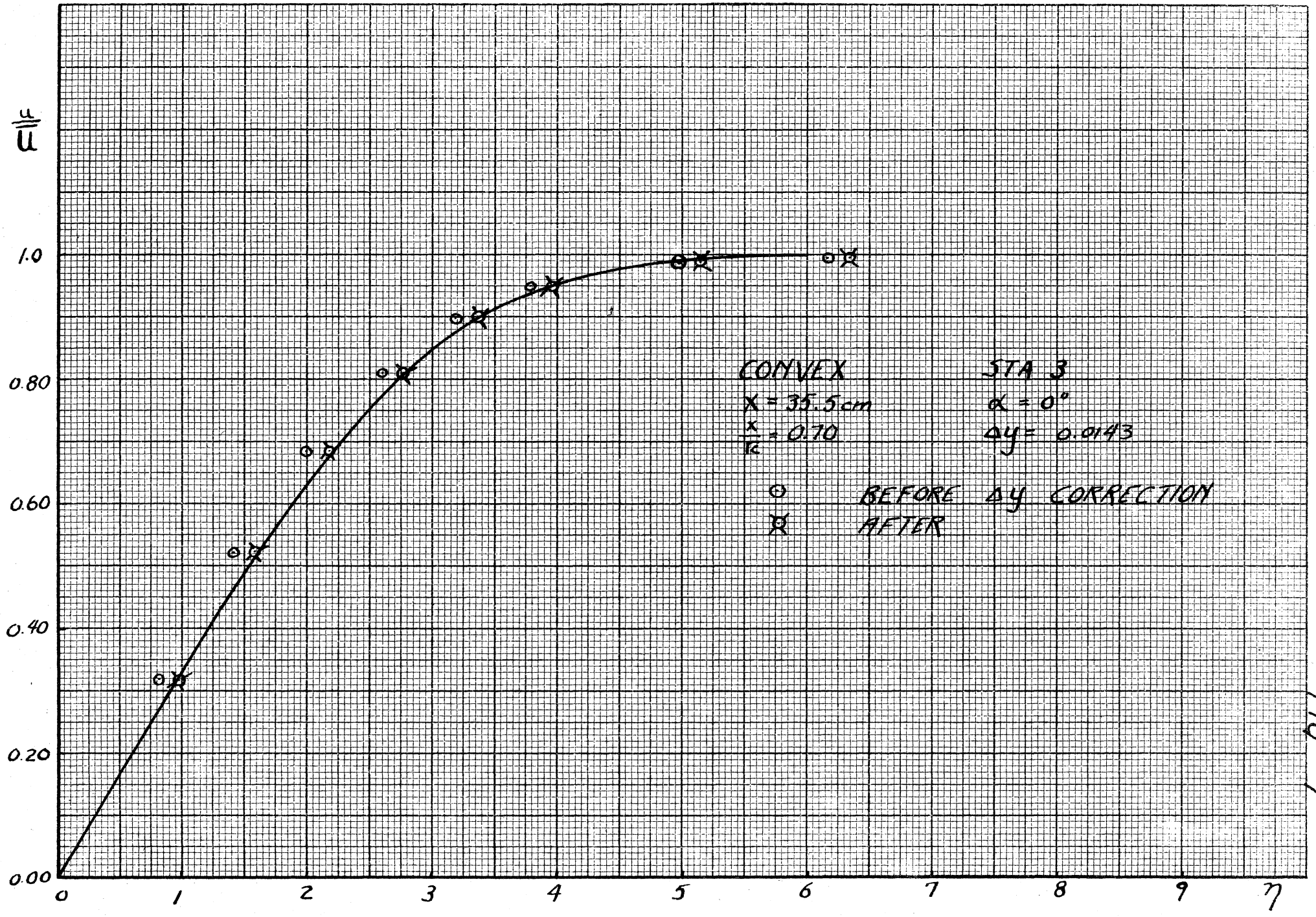

FIG 7

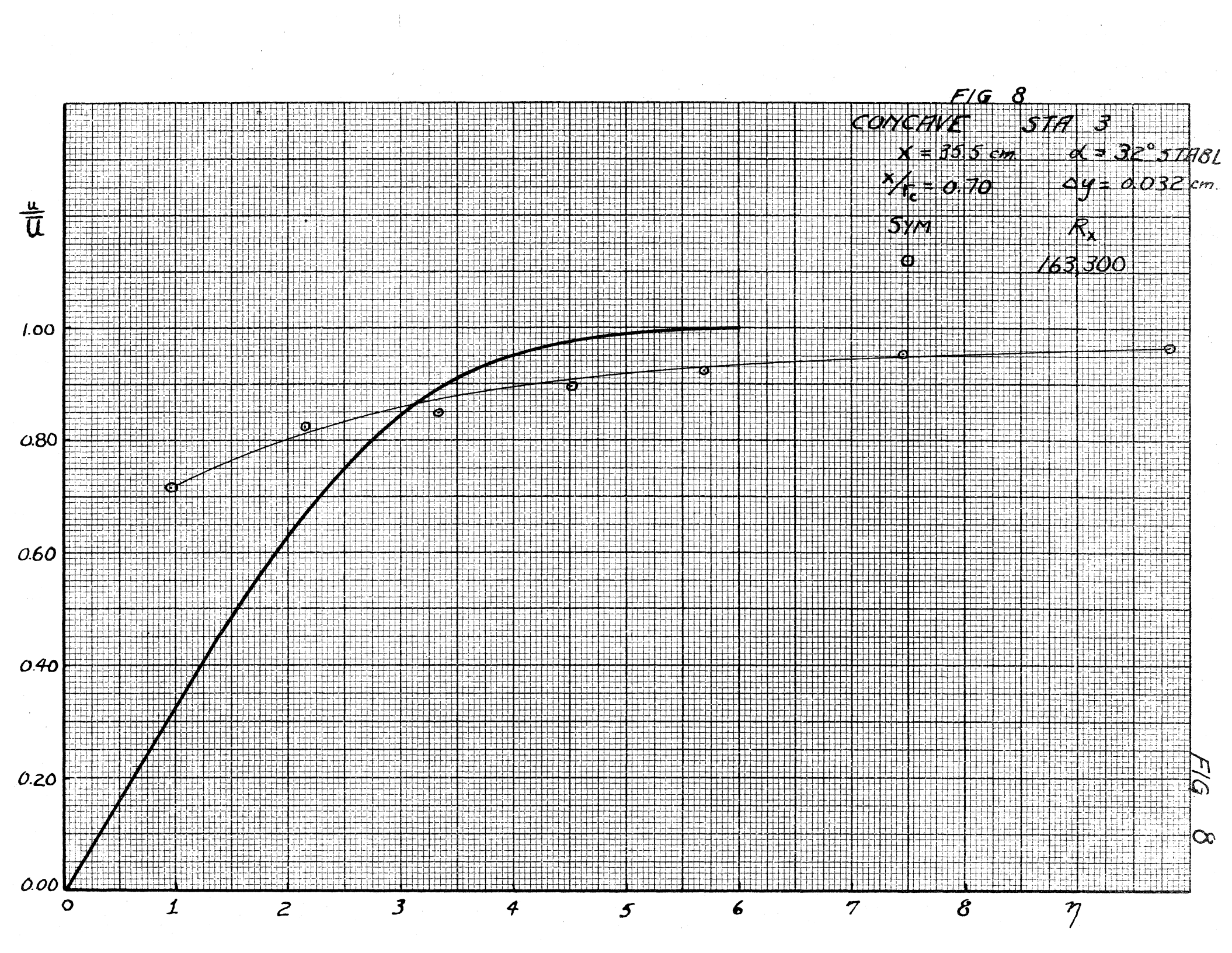
FIG 8
CONCAVE STA 3
x = 35.5 cm
x/c = 0.70
α = 32° STABL
Δy = 0.032 cm.
SYM
O
Rx
163,300
u/U
1.00
0.80
0.60
0.40
0.20
0.00
0
1
2
3
4
5
6
7
8
η
FIG 8

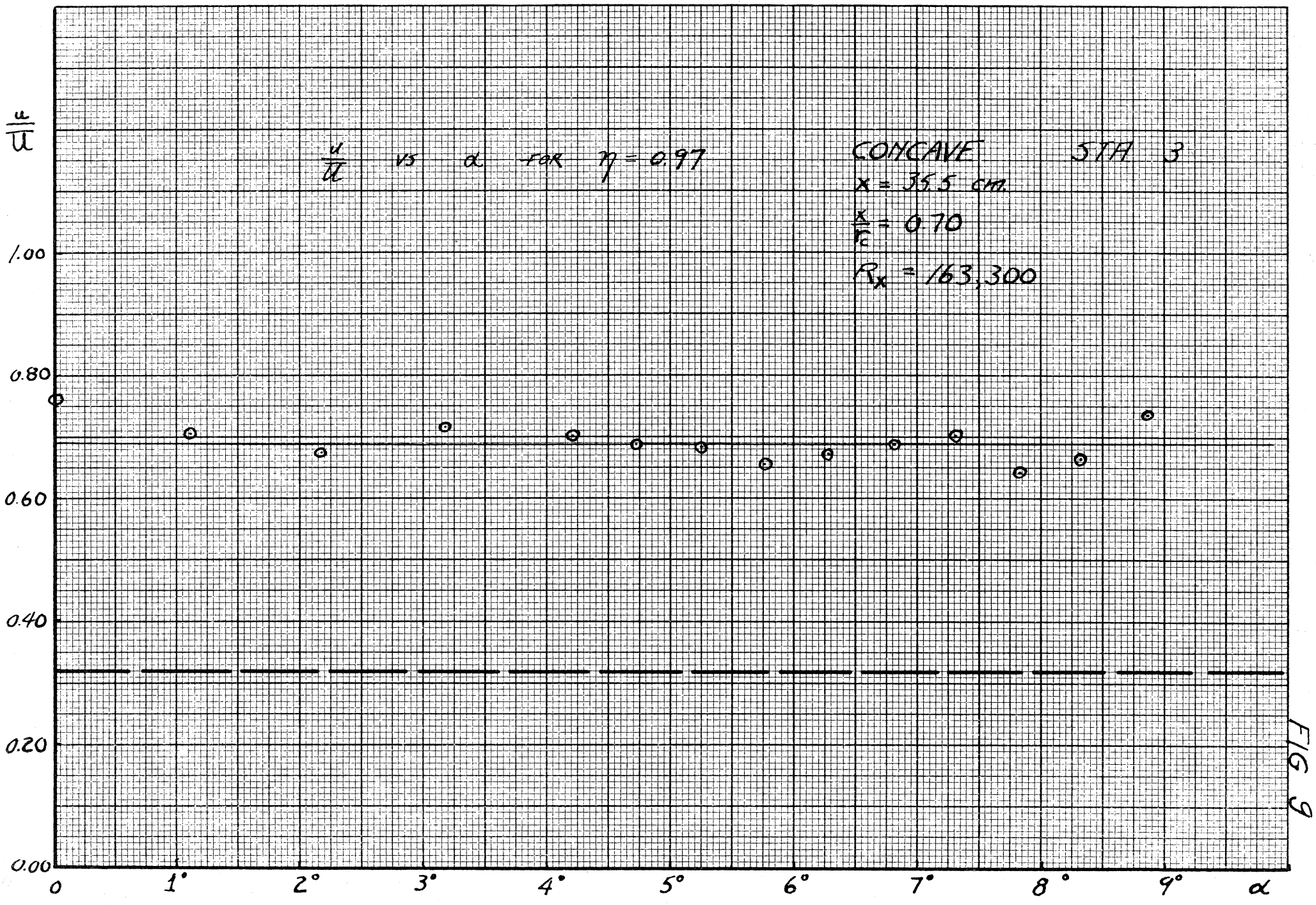
u/U
u/U vs α for η = 0.97
CONCAVE
STA 3
x = 35.5 cm.
x/c = 0.70
Rx = 163,300
1.00
0.80
0.60
0.40
0.20
0.00
0
1°
2°
3°
4°
5°
6°
7°
8°
9°
α

FIG 9

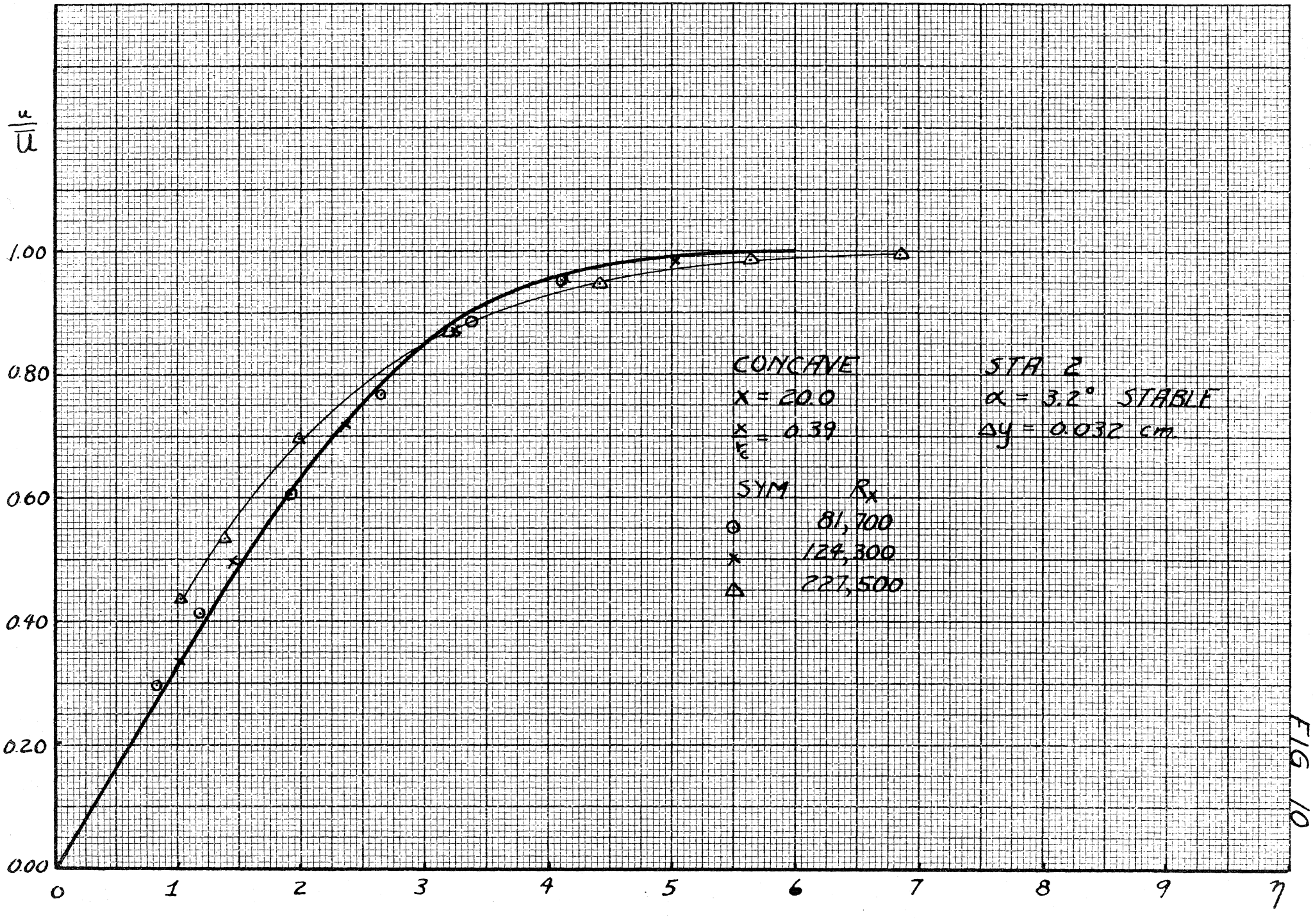
u/U
1.00
0.80
0.60
0.40
0.20
0.00
0
1
2
3
4
5
6
7
8
9
η
CONCAVE
x = 20.0
x/c = 0.39
SYM
Rx
81,700
124,300
227,500
STA 2
α = 3.2° STABLE
Δy = 0.032 cm

FIG 10

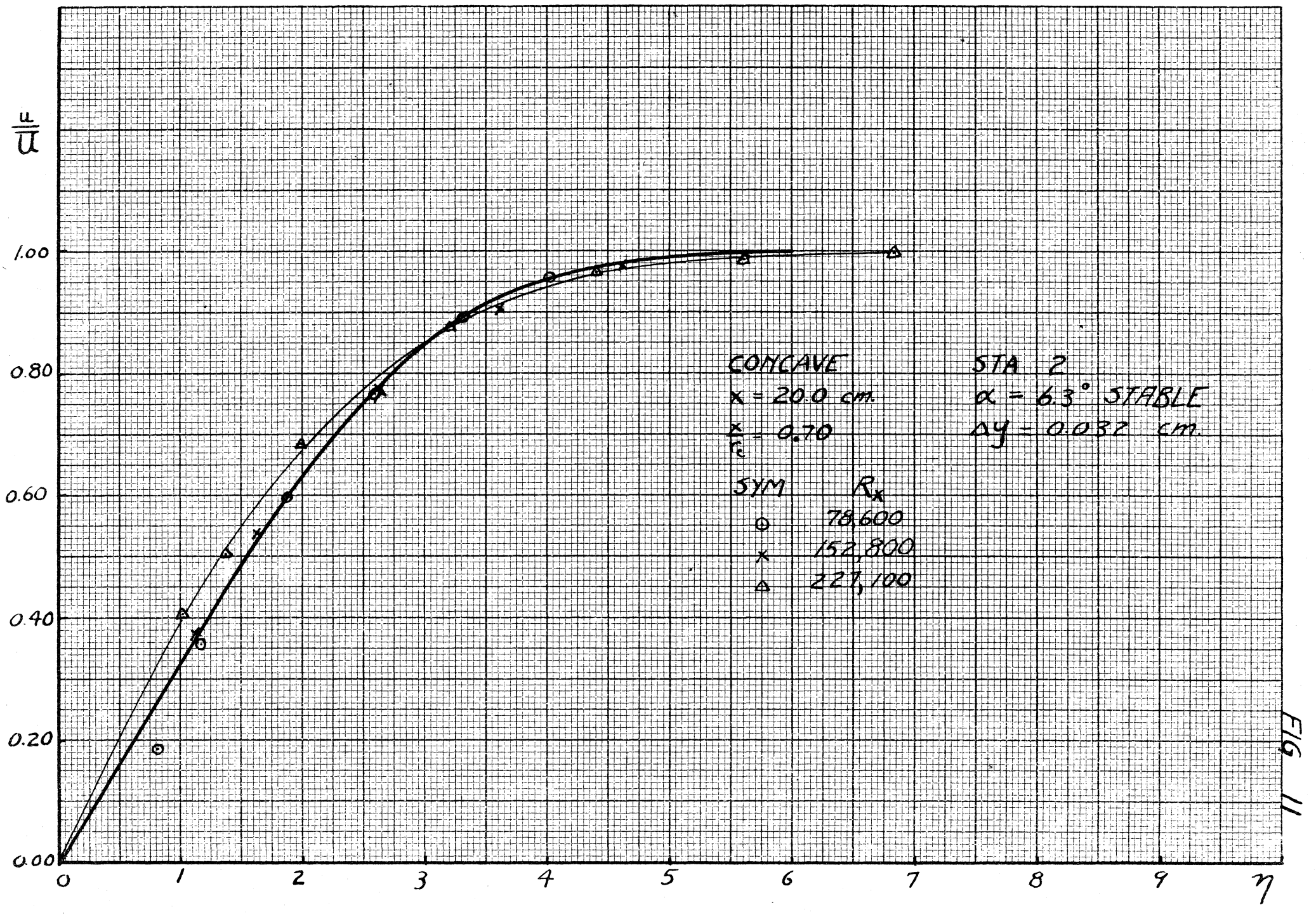
u/U
1.00
0.80
0.60
0.40
0.20
0.00
0
1
2
3
4
5
6
7
8
9
η
CONCAVE
x = 20.0 cm.
x/c = 0.70
SYM Rx
○ 78,600
× 152,800
△ 227,100
STA 2
α = 6.3° STABLE
Δy = 0.032 cm.

FIG 11

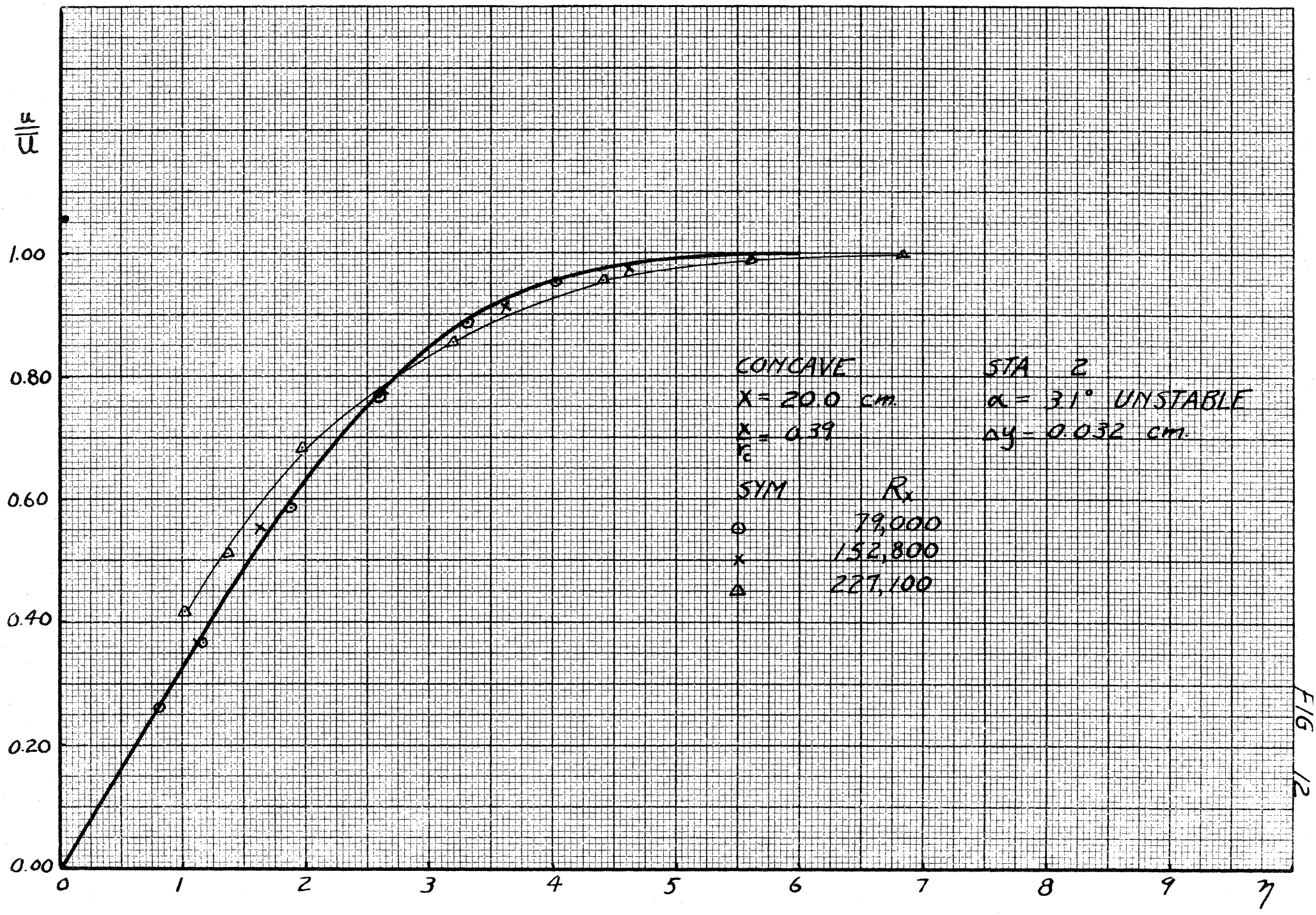
u/U
1.00
0.80
0.60
0.40
0.20
0.00
0
1
2
3
4
5
6
7
8
9
η
CONCAVE
X = 20.0 cm.
x/x_c = 0.39
SYM
R_x
79,000
152,800
227,100
STA 2
α = 31° UNSTABLE
Δy = 0.032 cm.

FIG 12

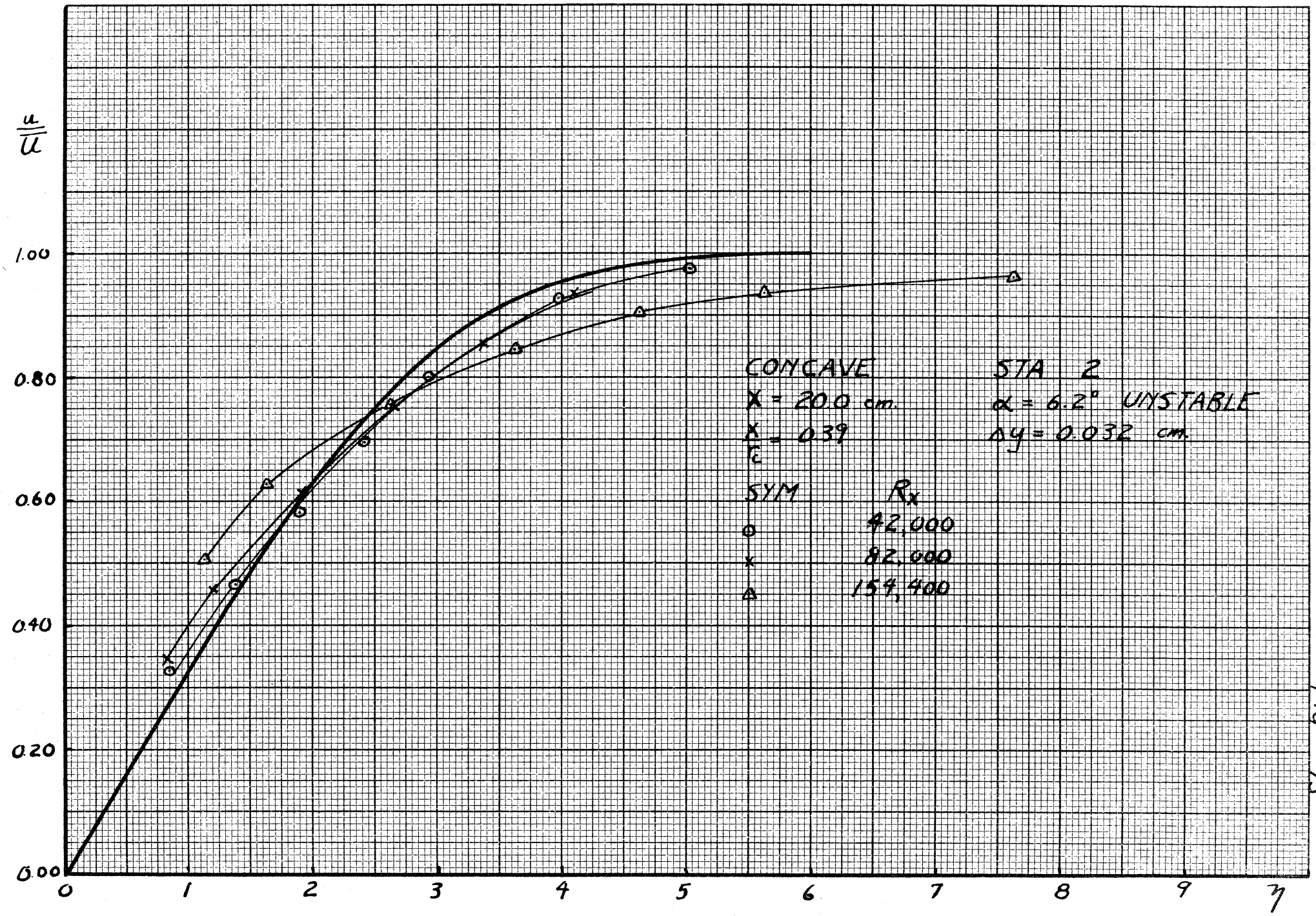
u/U
1.00
0.80
0.60
0.40
0.20
0.00
0
1
2
3
4
5
6
7
8
9
η
CONCAVE
X = 20.0 cm.
X/ℓc = 0.39
SYM
Rx
42,000
82,000
154,400
STA 2
α = 6.2° UNSTABLE
Δy = 0.032 cm.

FIG 13

FIG 14

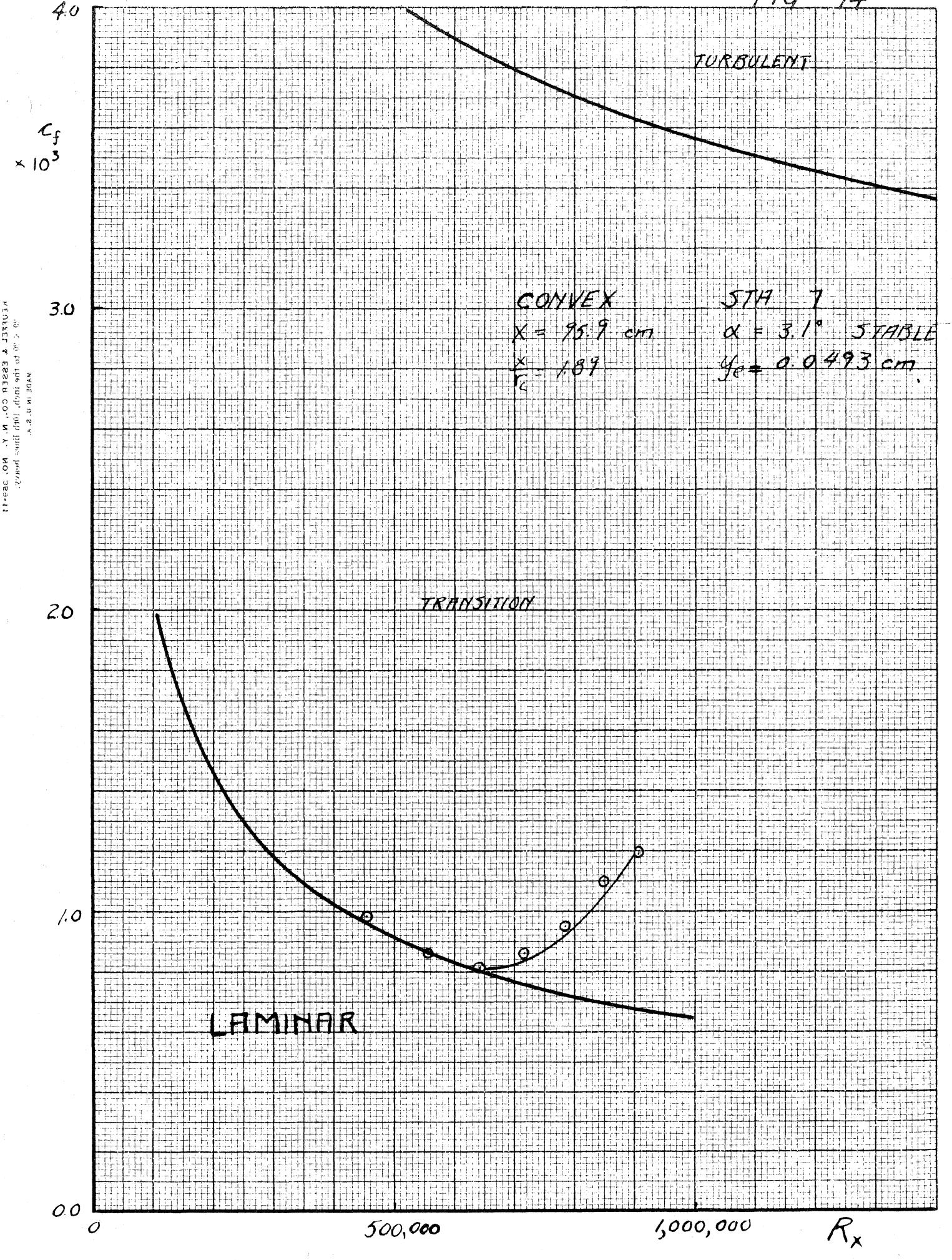
4.0
3.0
2.0
1.0
0.0
$c_f \times 10^3$
TURBULENT
CONVEX
X = 95.9 cm
$\frac{x}{r_c}$ = 1.89
STH 7
α = 3.1° STABLE
y_e = 0.0493 cm.
TRANSITION
LAMINAR
0
500,000
1,000,000
R_x

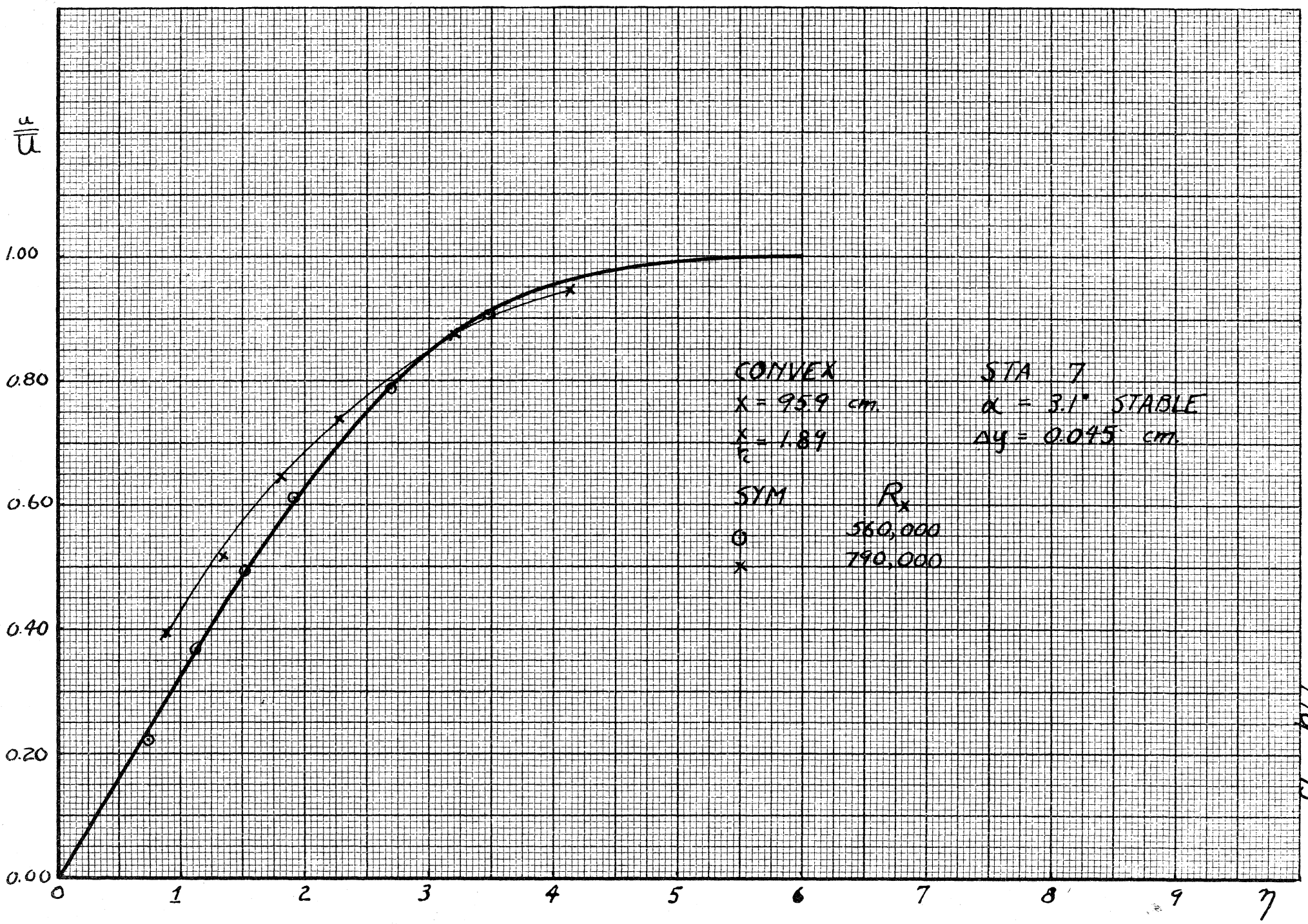
u/U
1.00
0.80
0.60
0.40
0.20
0.00
0
1
2
3
4
5
6
7
8
9
η
CONVEX
X = 95.9 cm.
X/Xc = 1.89
SYM
Rx
560,000
790,000
STA 7
α = 3.1° STABLE
Δy = 0.045 cm.

FIG 16

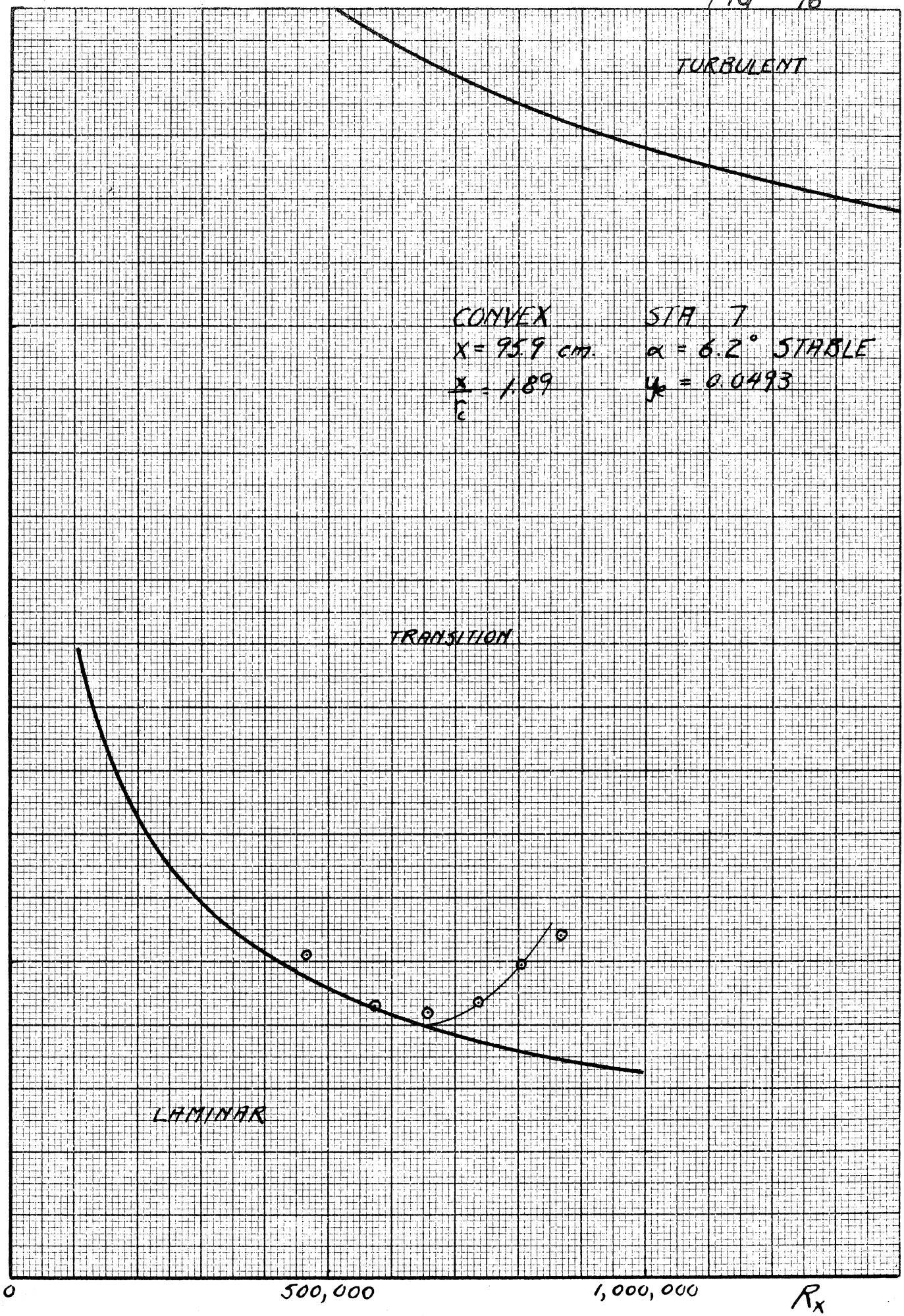
4.0
3.0
2.0
1.0
0.0
$C_f \times 10^3$
TURBULENT
CONVEX
X = 95.9 cm.
$\frac{x}{c} = 1.89$
STA 7
$\alpha = 6.2°$ STABLE
$y_k = 0.0493$
TRANSITION
LAMINAR
0
500,000
1,000,000
R_x

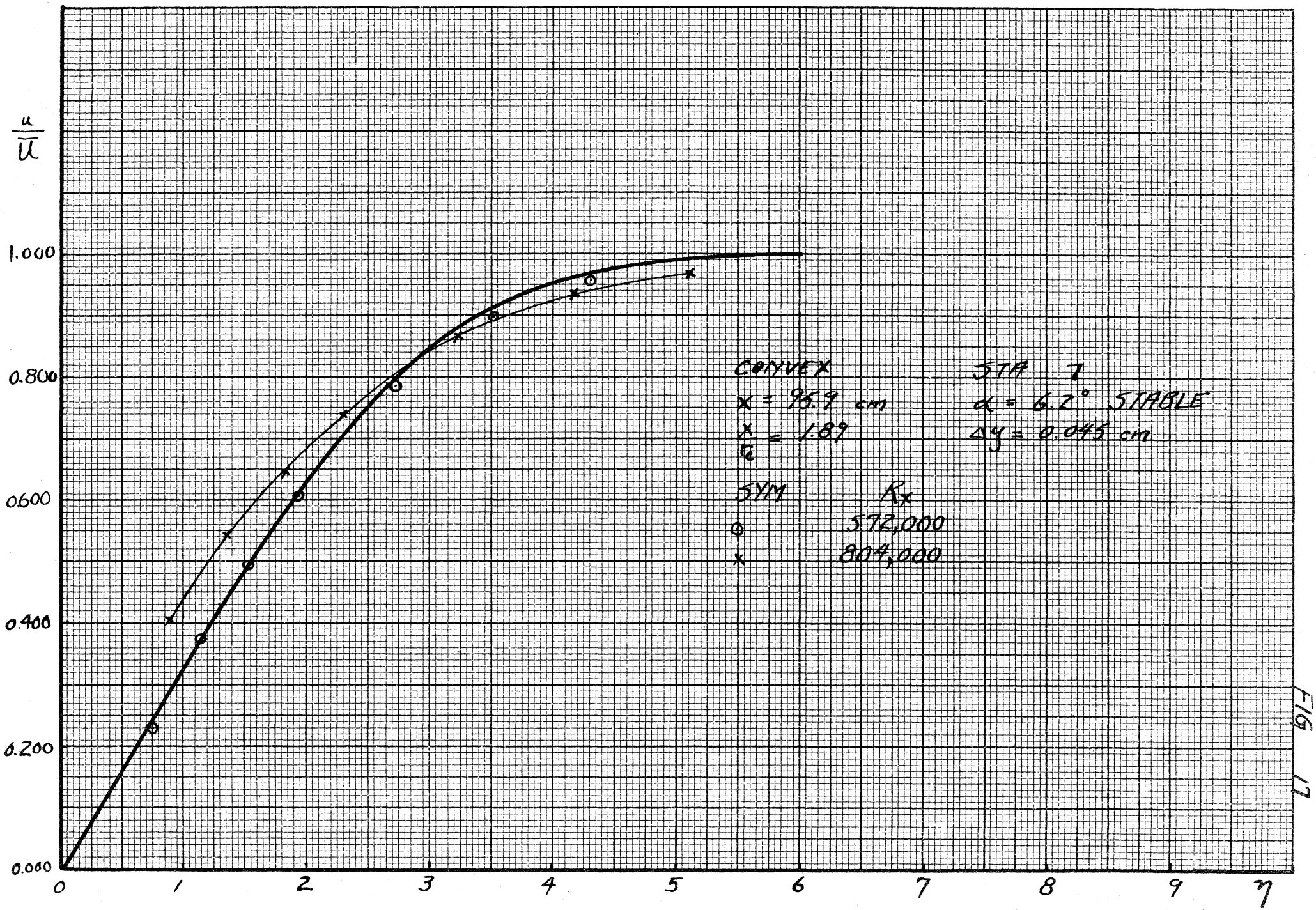
u/U
1.000
0.800
0600
0.400
0.200
0.000
0
1
2
3
4
5
6
7
8
9
η
CONVEX
x = 95.9 cm
x/c = 1.89
SYM
Rx
572,000
804,000
STA 1
α = 6.2° STABLE
Δy = 0.045 cm

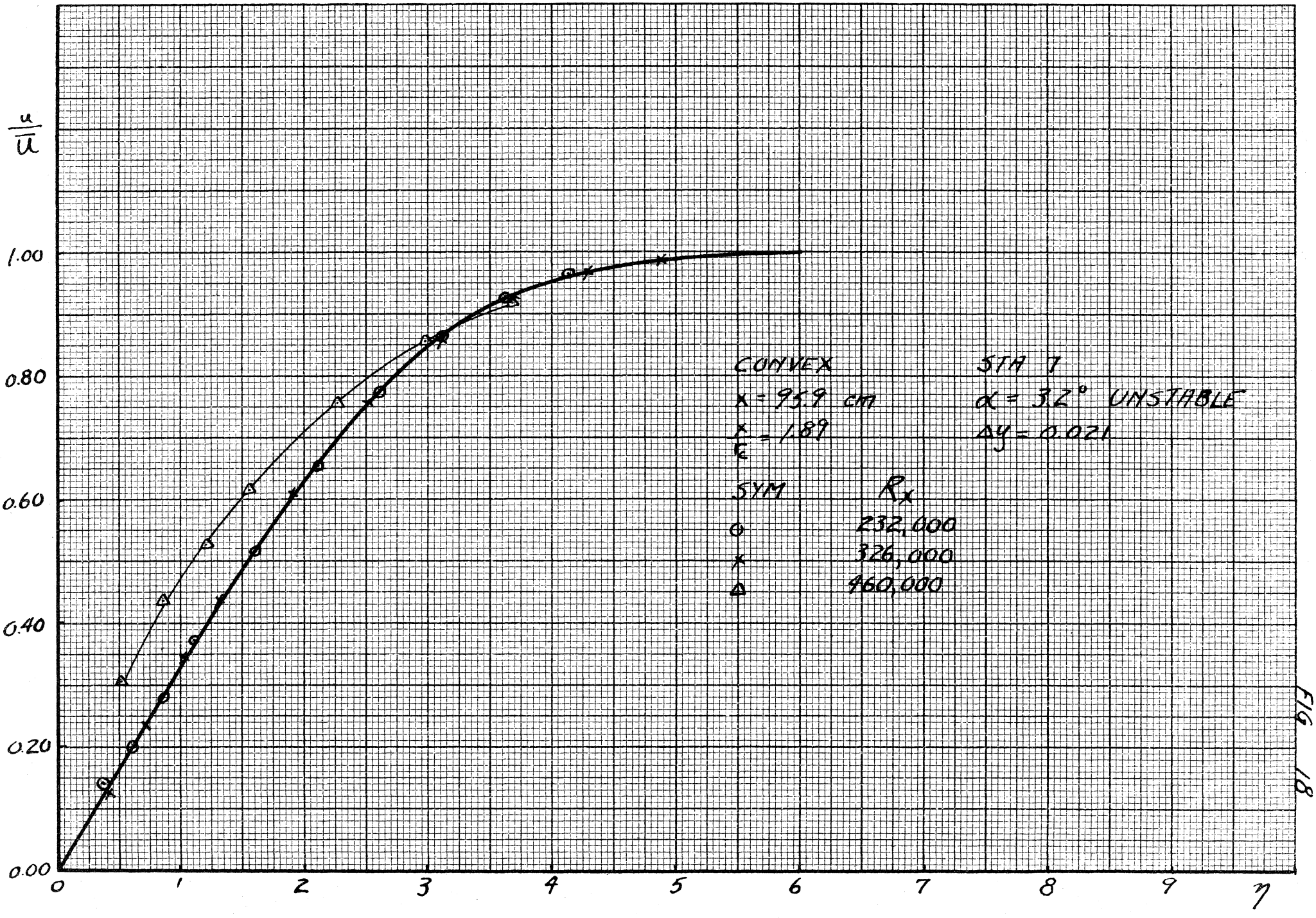
u/U
1.00
0.80
0.60
0.40
0.20
0.00
0
1
2
3
4
5
6
7
8
9
η
CONVEX
x = 95.9 cm
x/c = 1.89
SYM
Rx
232,000
326,000
460,000
STA 7
α = 3.2° UNSTABLE
Δy = 0.021

Fig 18

FIG 19

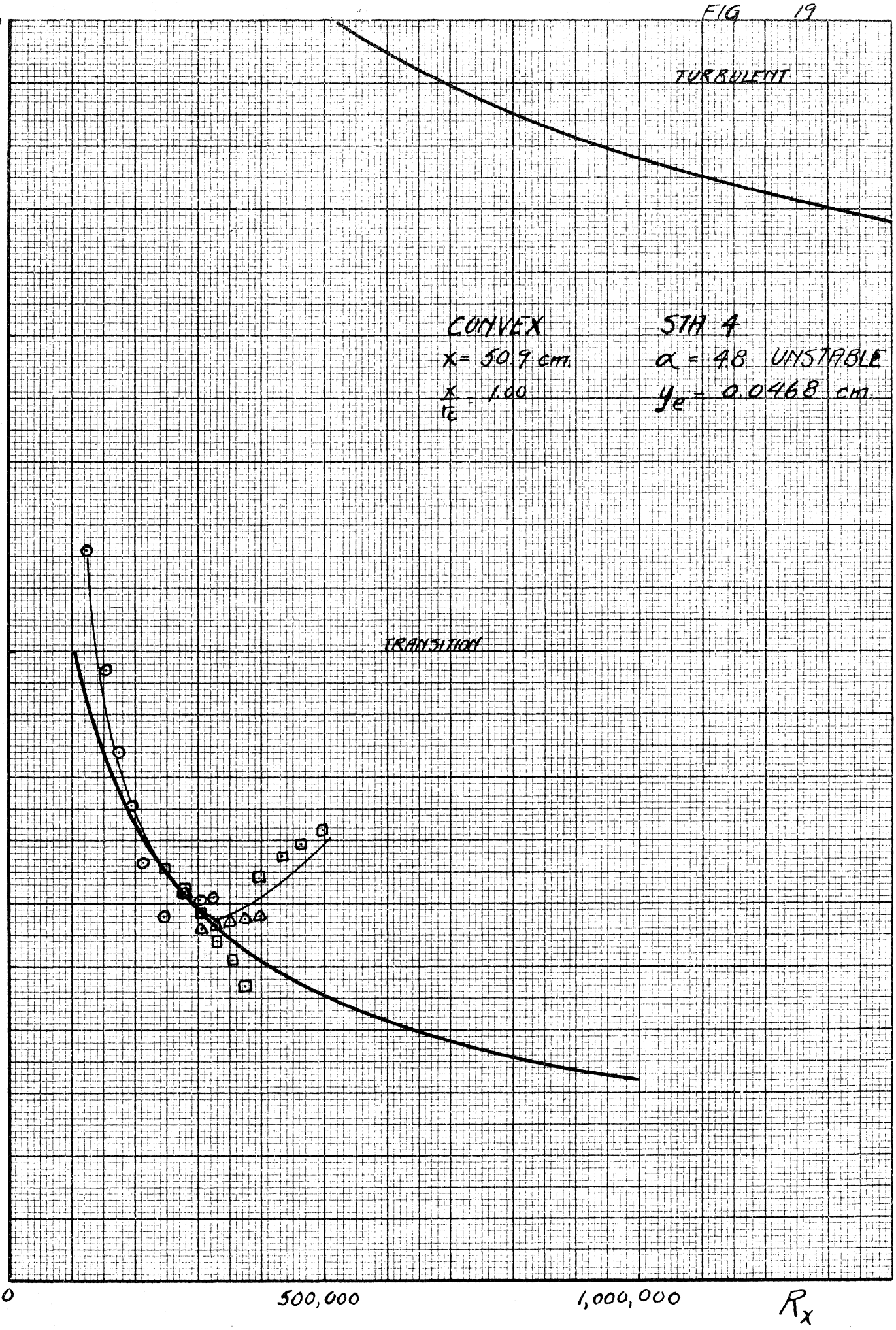
4.0
3.0
2.0
1.0
0.0
$c_f \times 10^3$
0
500,000
1,000,000
R_x
TURBULENT
TRANSITION
CONVEX
x = 50.9 cm.
$\frac{x}{r_c}$ = 1.00
STH 4
α = 4.8 UNSTABLE
y_e = 0.0468 cm.

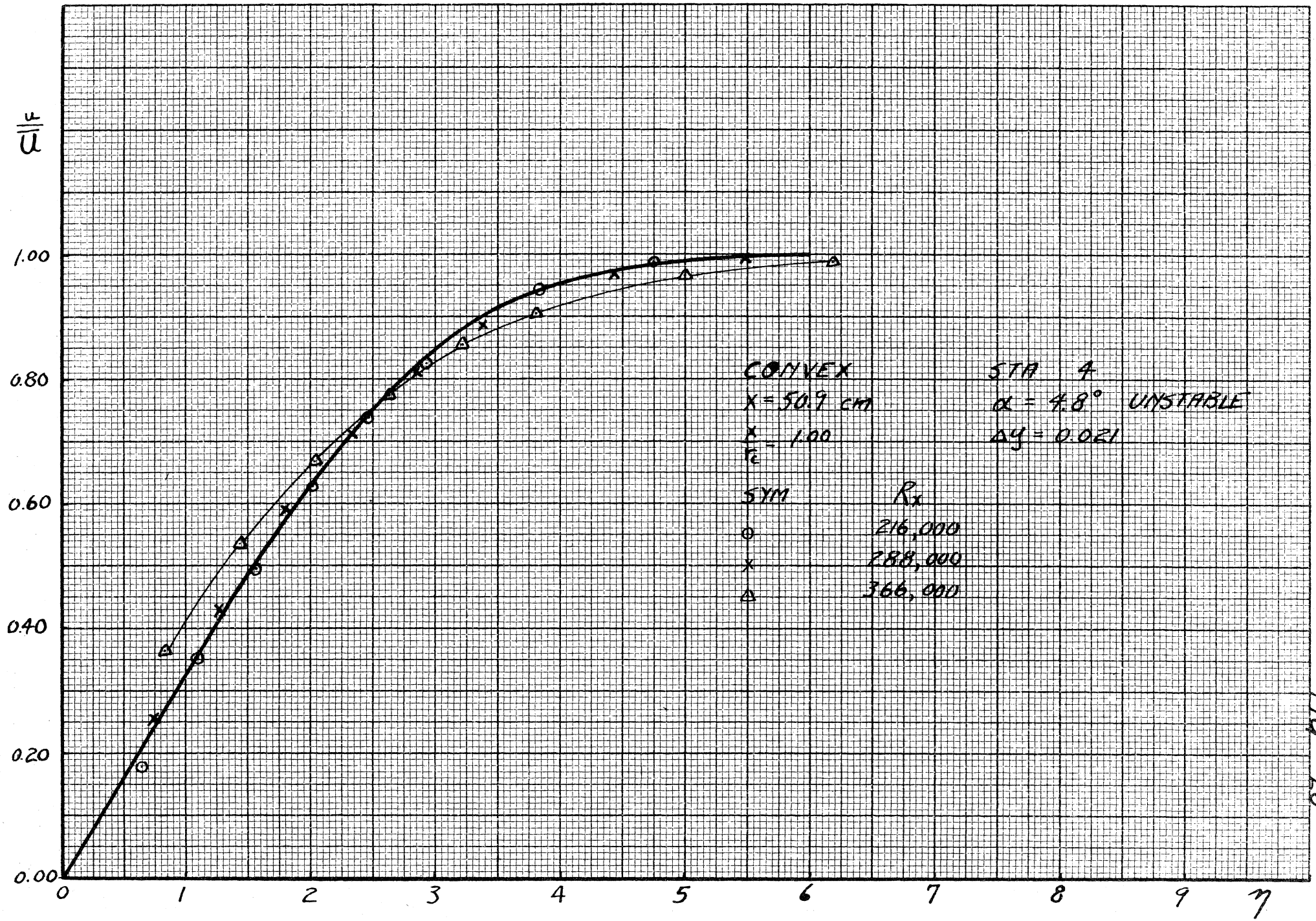
u/U
1.00
0.80
0.60
0.40
0.20
0.00
0
1
2
3
4
5
6
7
8
9
η
CONVEX
X = 50.9 cm
X/Rc = 1.00
SYM
Rx
216,000
288,000
366,000
STA 4
α = 4.8° UNSTABLE
Δy = 0.021

Fig 20

FIG 21

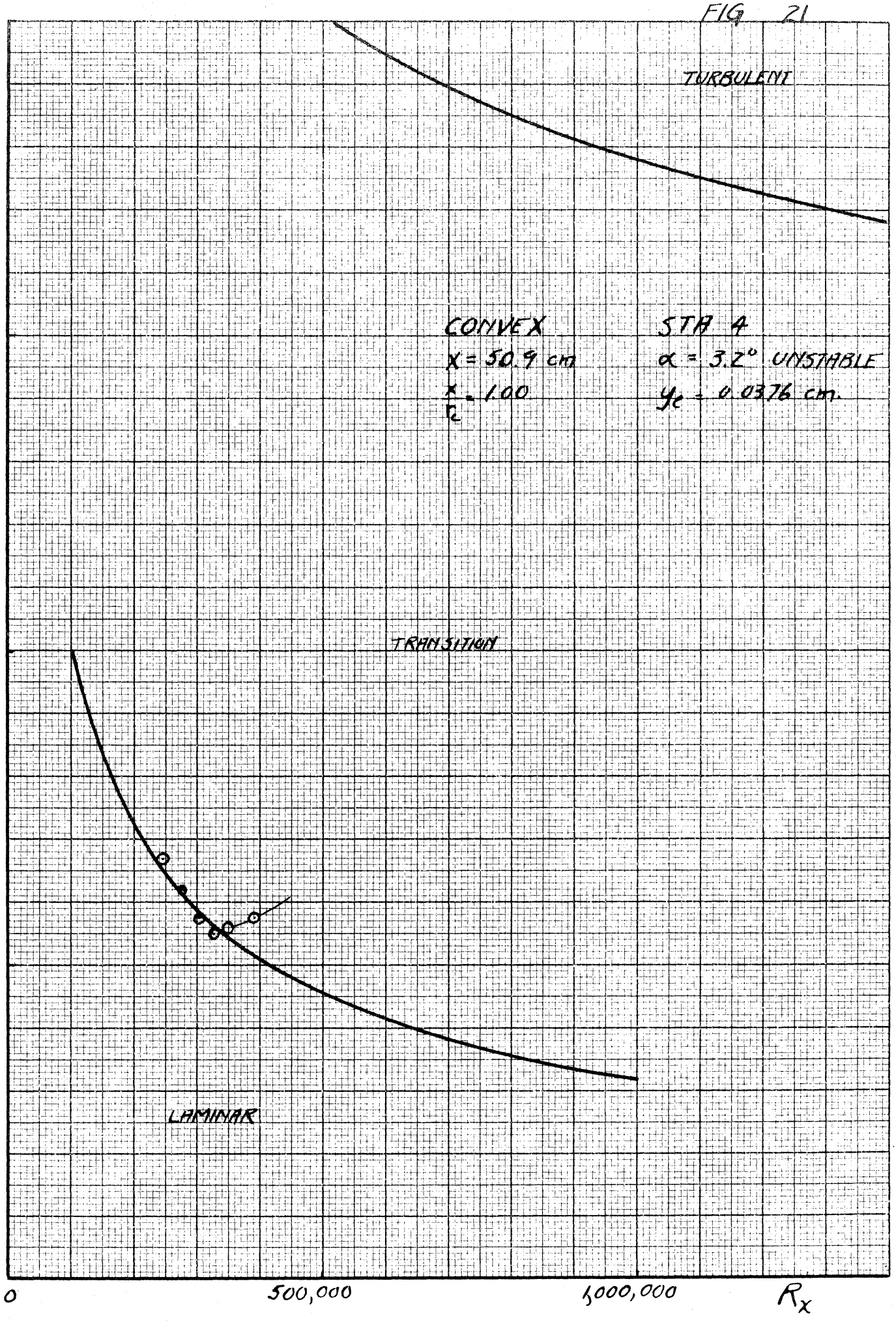
4.0
3.0
2.0
1.0
0.0
$C_f \times 10^3$
TURBULENT
CONVEX
$X = 50.9$ cm
$\frac{x}{r_L} = 1.00$
STA 4
$\alpha = 3.2°$ UNSTABLE
$y_c = 0.0376$ cm.
TRANSITION
LAMINAR
0
500,000
1,000,000
R_x

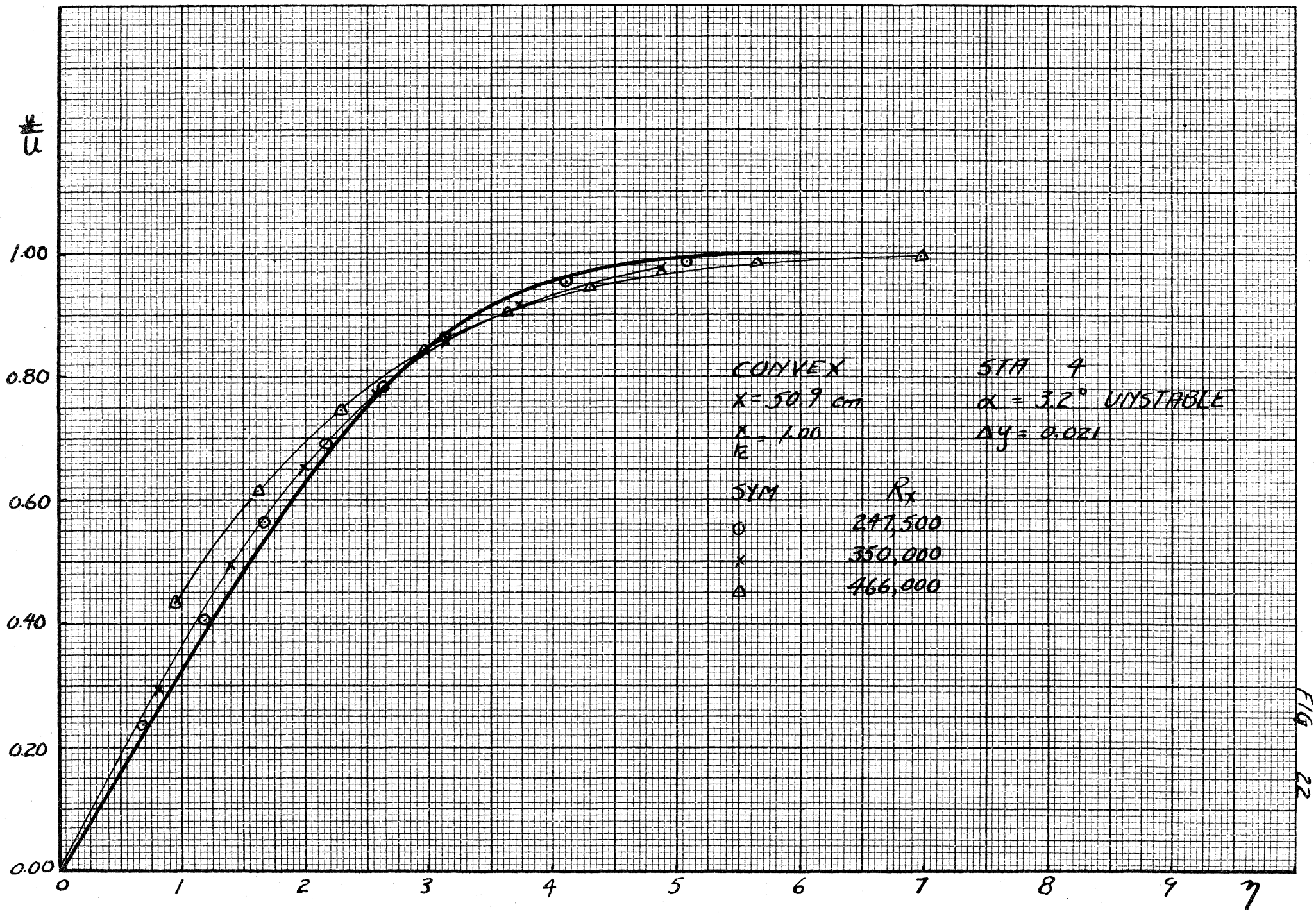
u/U
1.00
0.80
0.60
0.40
0.20
0.00
0
1
2
3
4
5
6
7
8
9
η
CONVEX
X = 50.9 cm
X/C = 1.00
SYM
Rx
247,500
350,000
466,000
STA 4
α = 3.2° UNSTABLE
Δy = 0.021

Fig 22

FIG 23

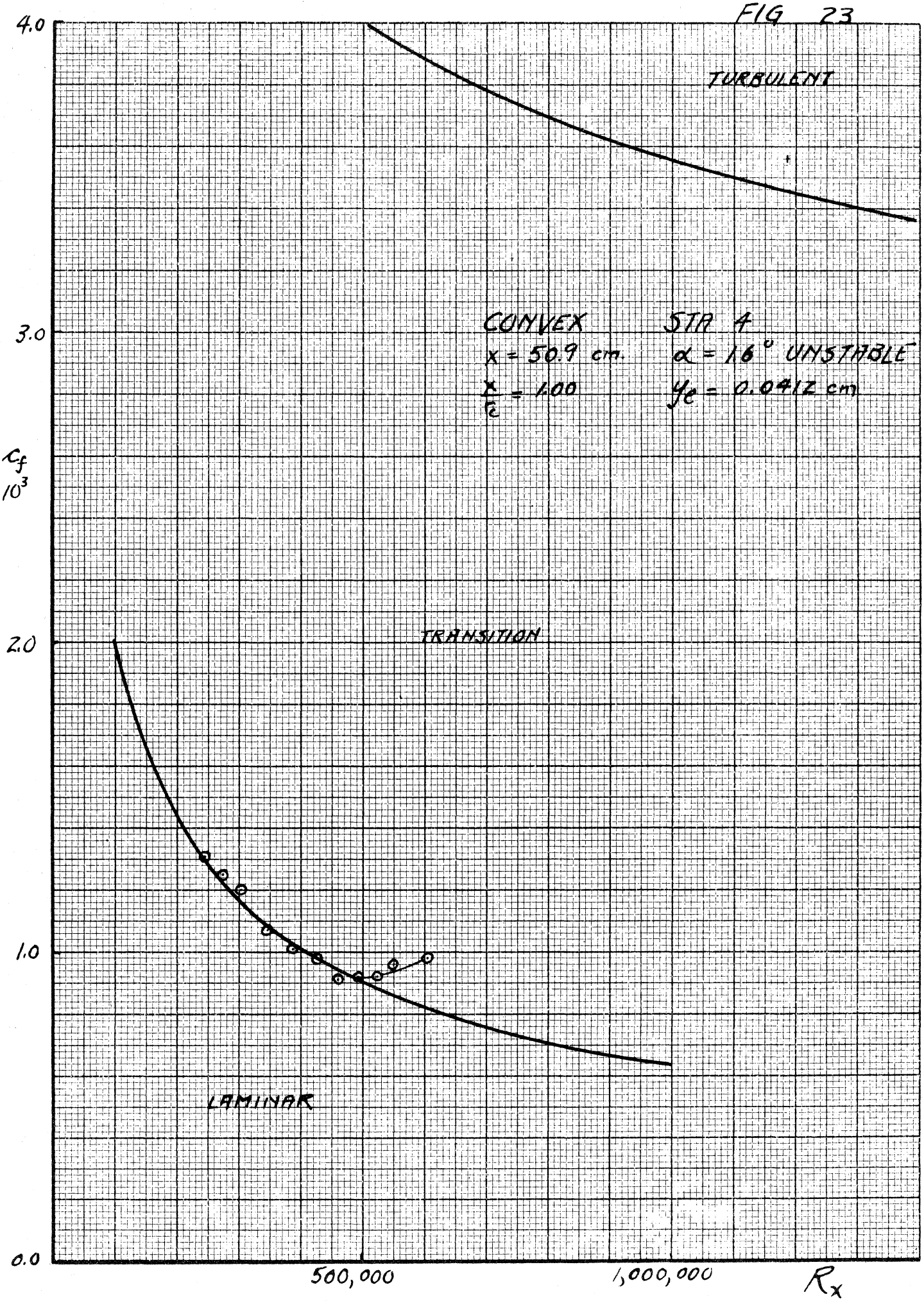

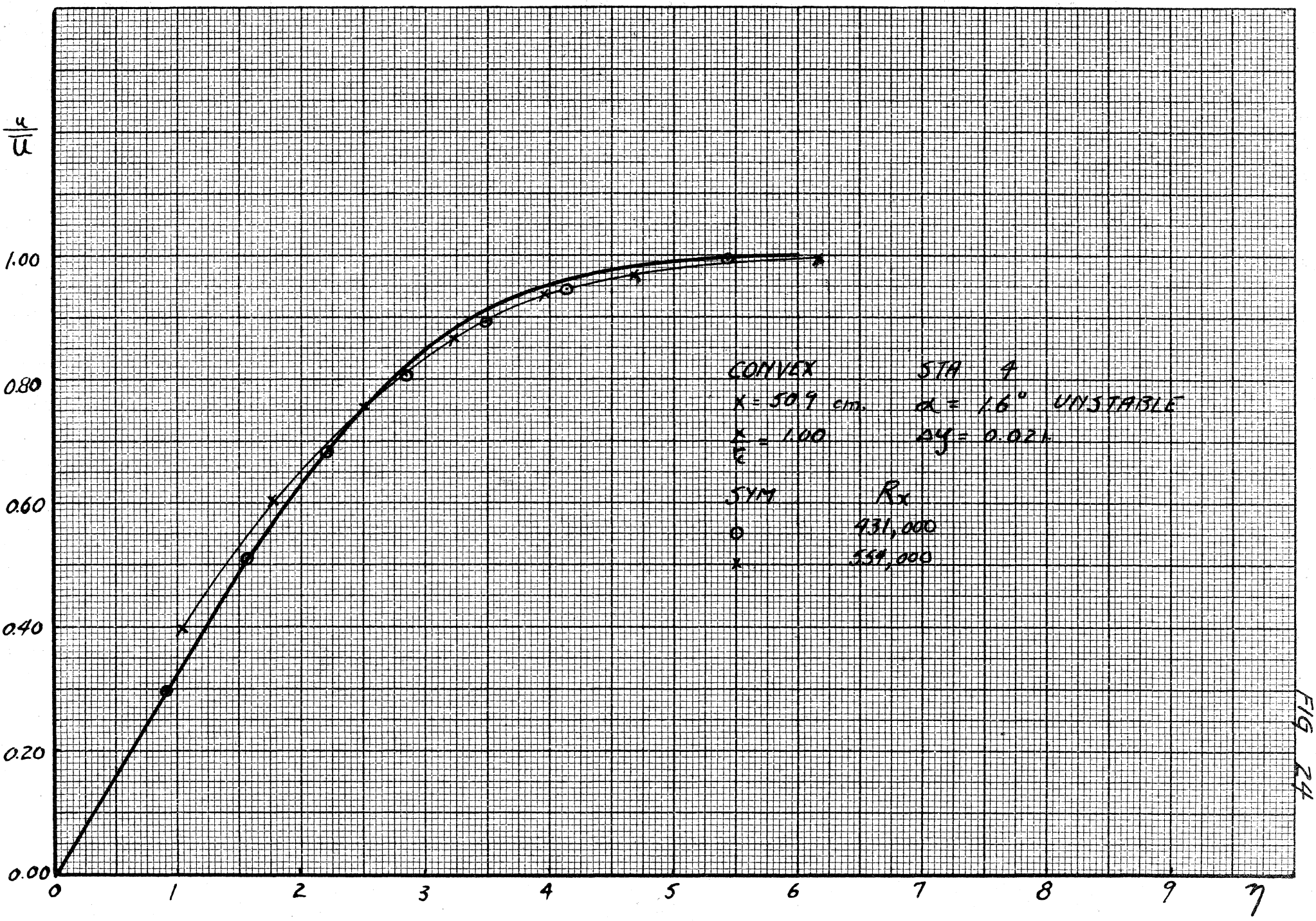
u/U
1.00
0.80
0.60
0.40
0.20
0.00
0
1
2
3
4
5
6
7
8
9
η
CONVEX
STA 4
x = 50.9 cm.
α = 1.6° UNSTABLE
x/c = 1.00
Δy = 0.021
SYM
Rx
○ 931,000
× 531,000

FIG 24

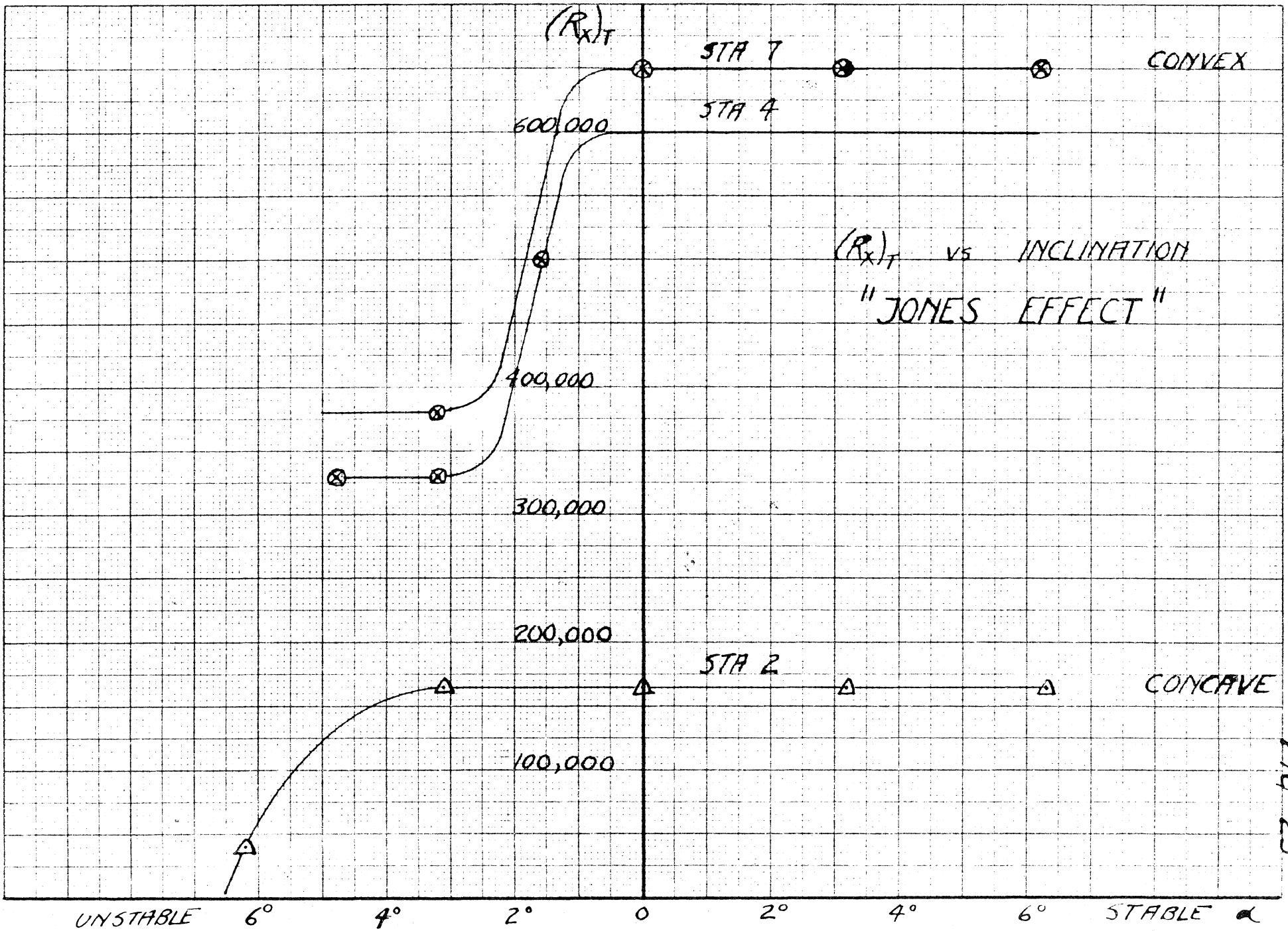
$(R_X)_T$
STA 7
CONVEX
STA 4
600,000
$(R_X)_T$ VS INCLINATION
"JONES EFFECT"
400,000
300,000
200,000
STA 2
CONCAVE
100,000
UNSTABLE
6°
4°
2°
0
2°
4°
6°
STABLE
α

FIG 25

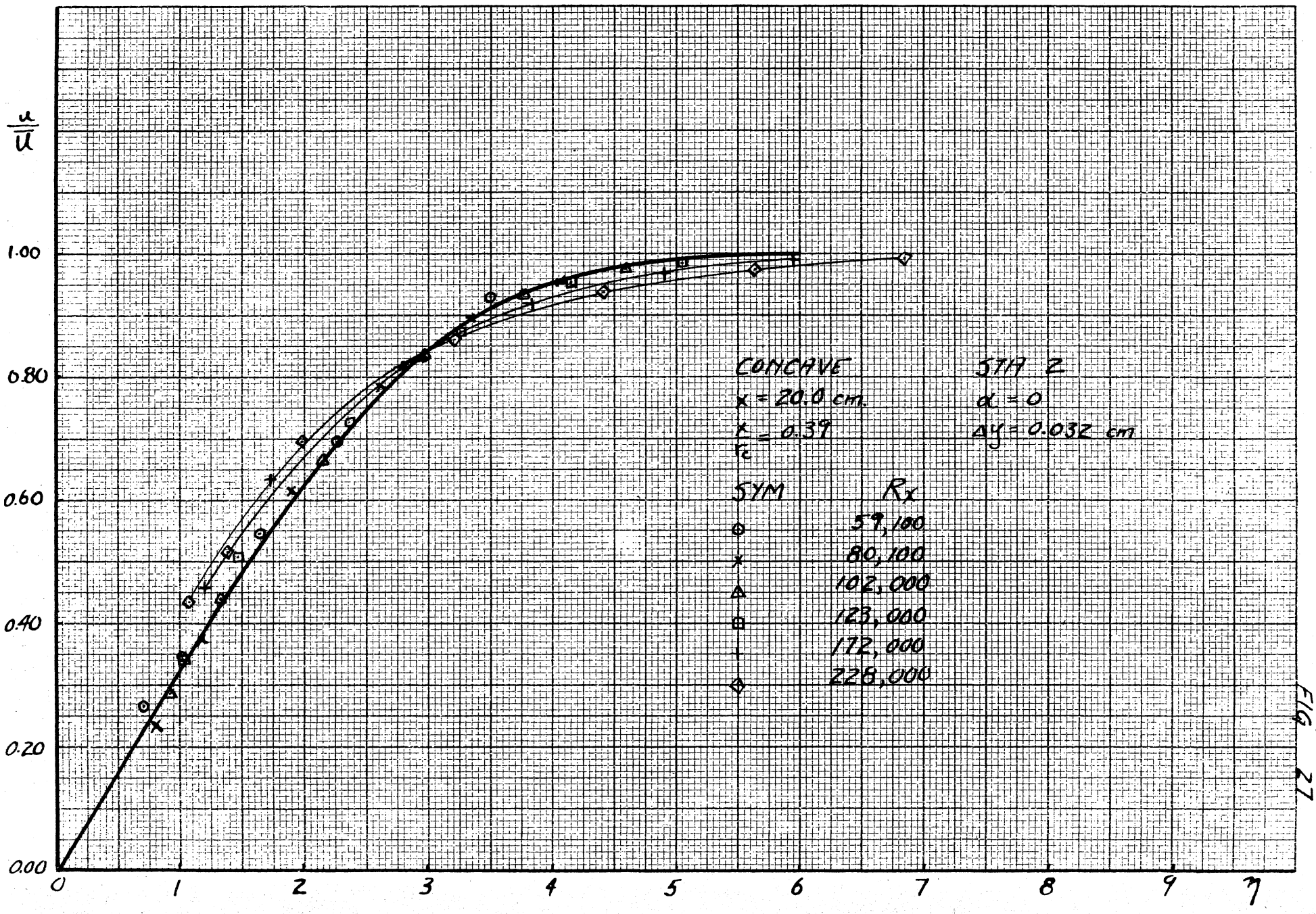
u/U
1.00
0.80
0.60
0.40
0.20
0.00
0
1
2
3
4
5
6
7
8
9
η
CONCAVE
x = 20.0 cm.
x/r_c = 0.39
SYM
Rx
59,100
80,100
102,000
123,000
172,000
226,000
STN 2
α = 0
Δy = 0.032 cm

FIG 26
FIG 27

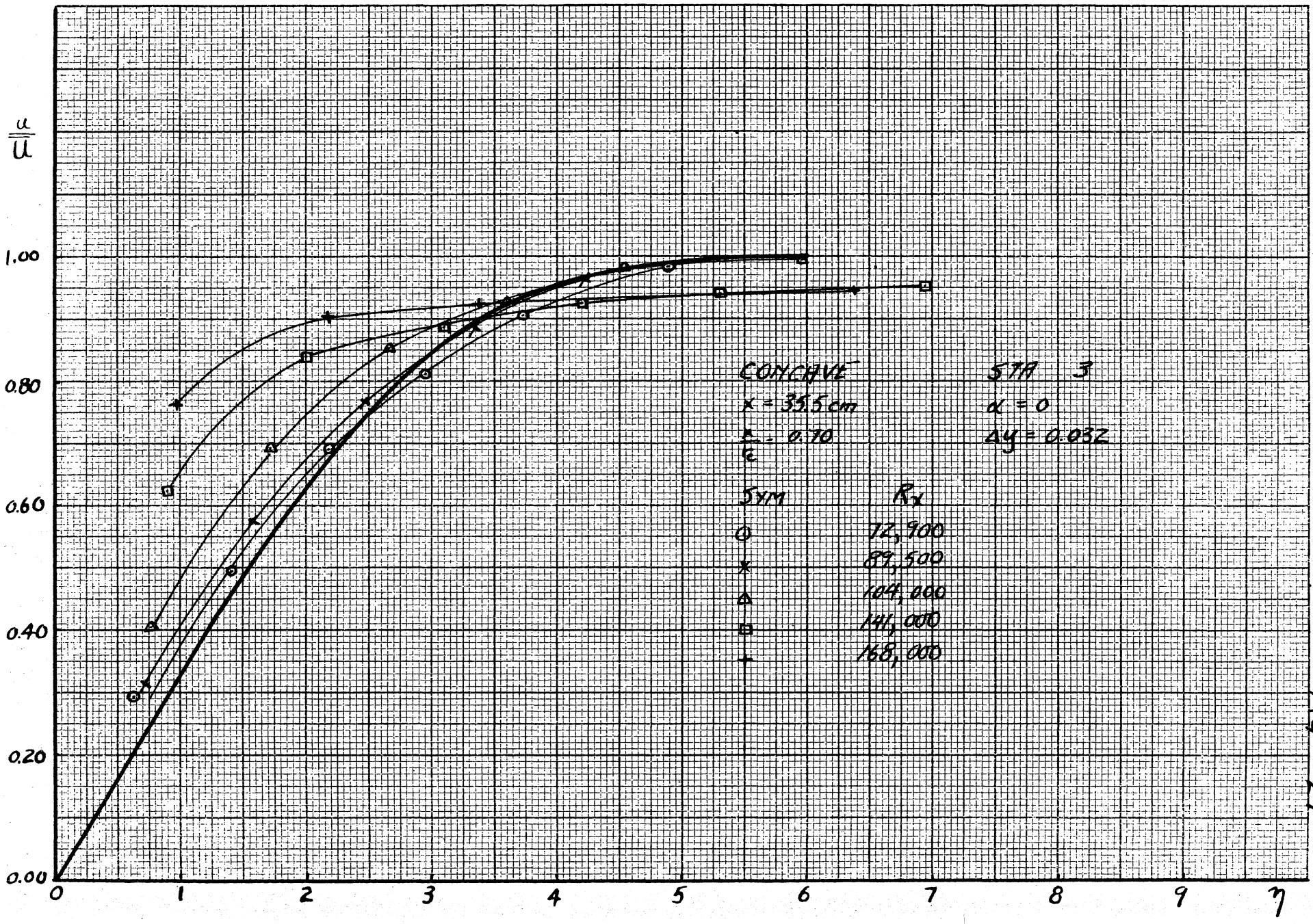
u/U
1.00
0.80
0.60
0.40
0.20
0.00
0
1
2
3
4
5
6
7
8
9
η
CONICAVE
x = 35.5 cm
x/c = 0.70
Sym
Rx
77,900
89,500
104,000
141,000
168,000
STA 3
α = 0
Δy = 0.032

FIG 28
FIG 29

FIG 30

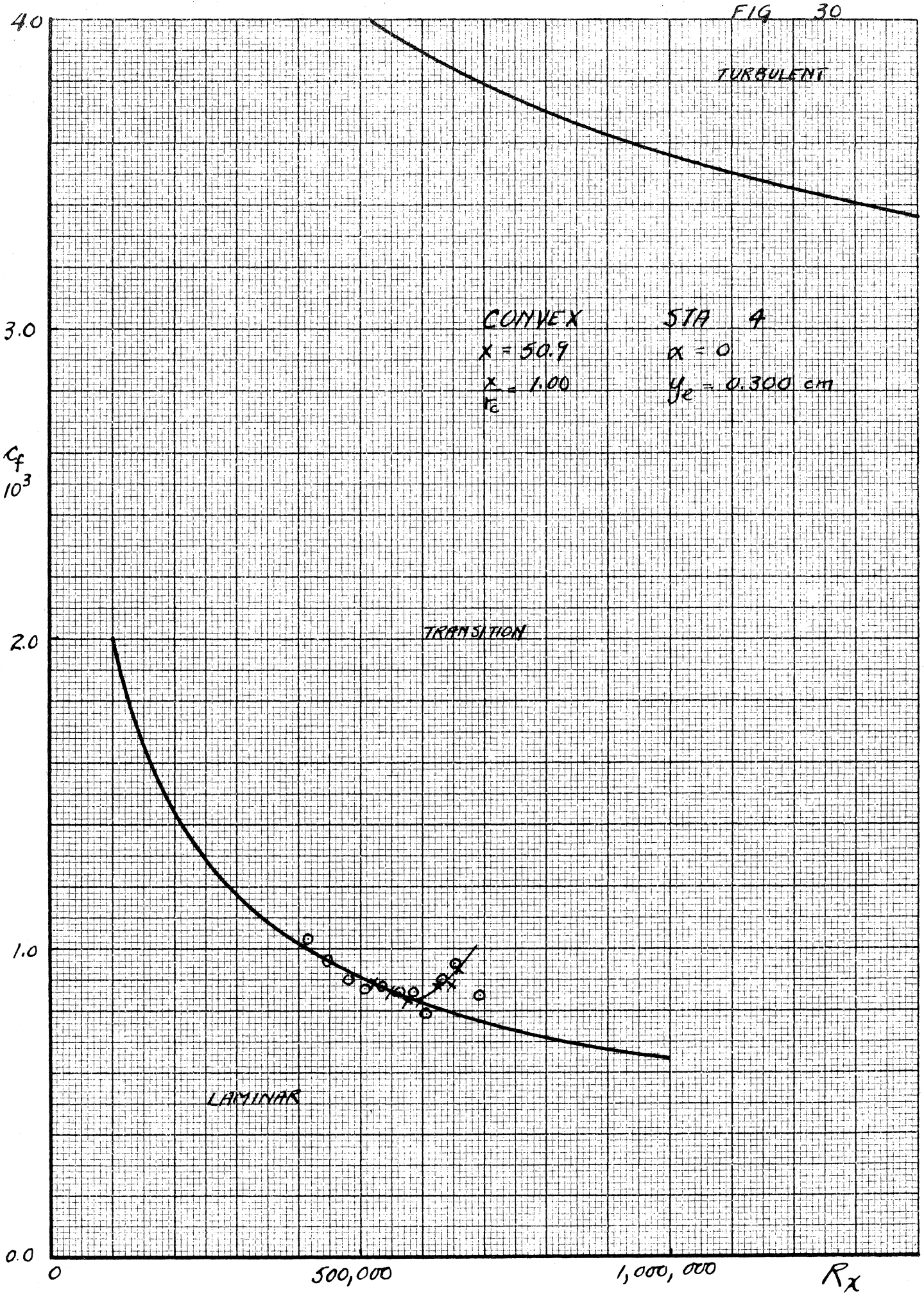
4.0
3.0
2.0
1.0
0.0
$C_f \times 10^3$
TURBULENT
CONVEX
STA 4
X = 50.9
α = 0
$\frac{x}{r_c}$ = 1.00
y_e = 0.300 cm
TRANSITION
LAMINAR
0
500,000
1,000,000
R_x

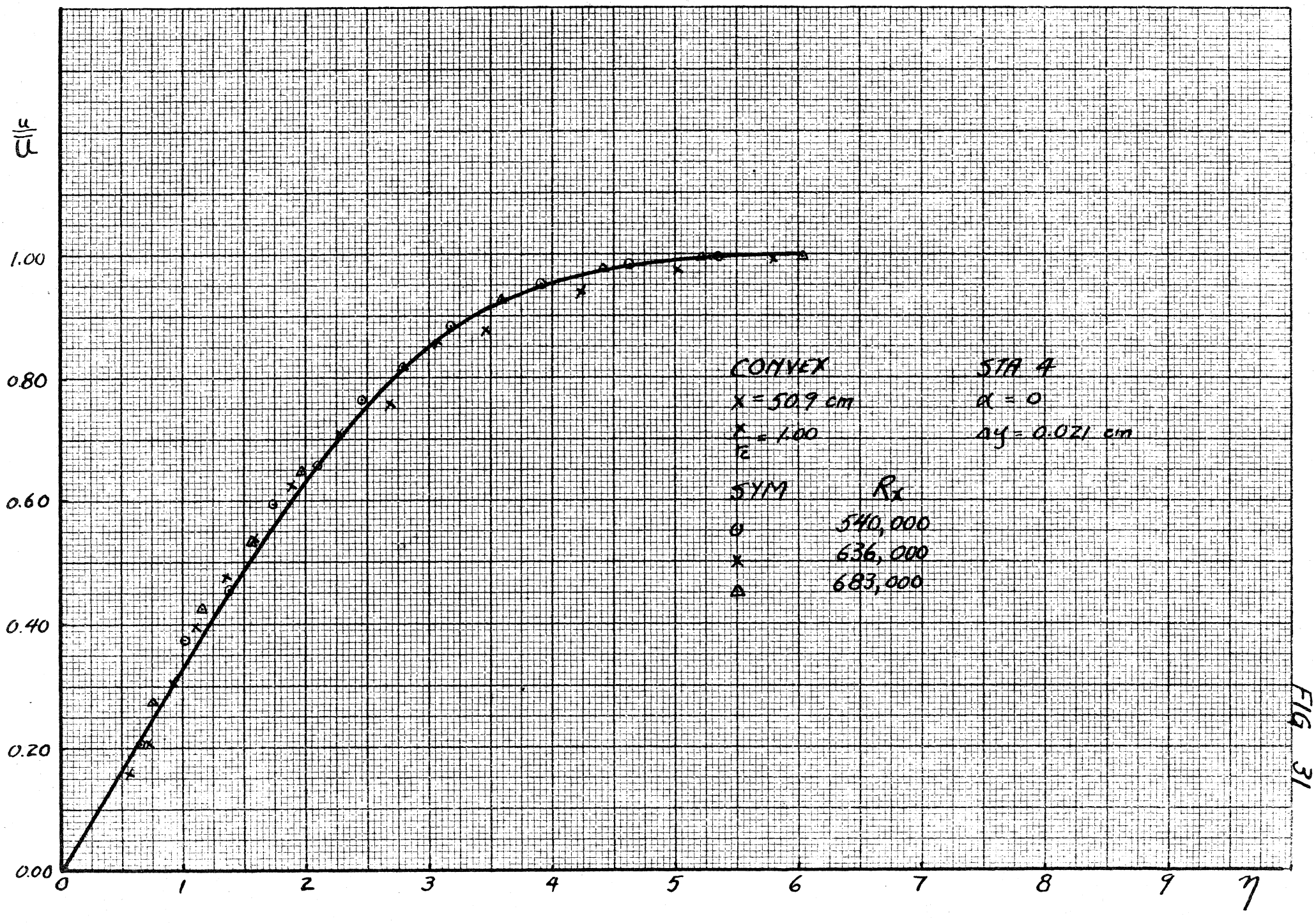
u/U
1.00
0.80
0.60
0.40
0.20
0.00
0
1
2
3
4
5
6
7
8
9
η
CONVEX
x = 50.9 cm
x/c = 1.00
SYM
Rx
540,000
636,000
683,000
STA 4
α = 0
Δy = 0.021 cm

FIG 31

FIG 32

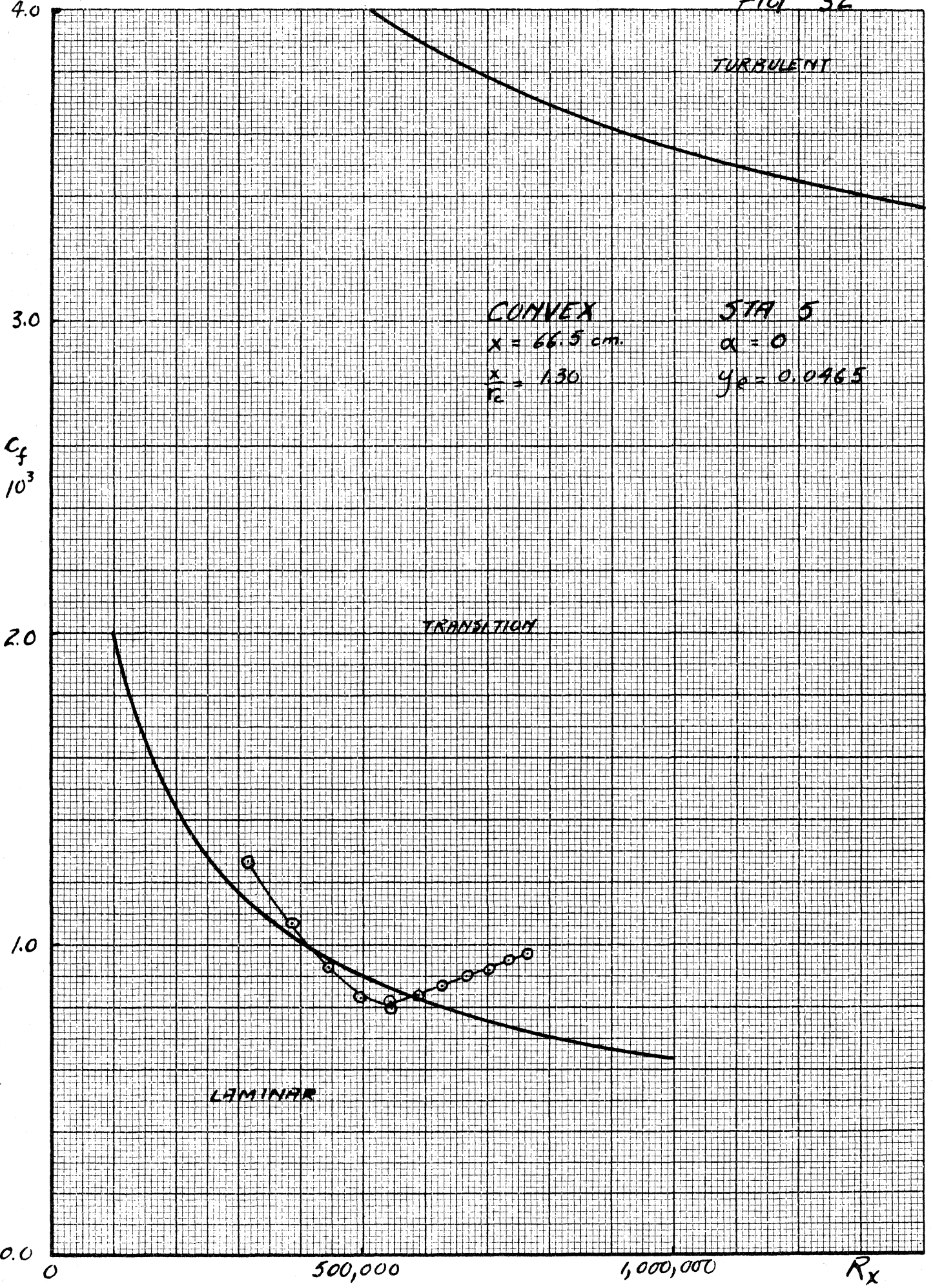
4.0
3.0
2.0
1.0
0.0
$C_f \times 10^3$
TURBULENT
CONVEX
$x = 66.5$ cm.
$\frac{x}{r_2} = 1.30$
STA 5
$\alpha = 0$
$y_e = 0.0465$
TRANSITION
LAMINAR
0
500,000
1,000,000
R_x

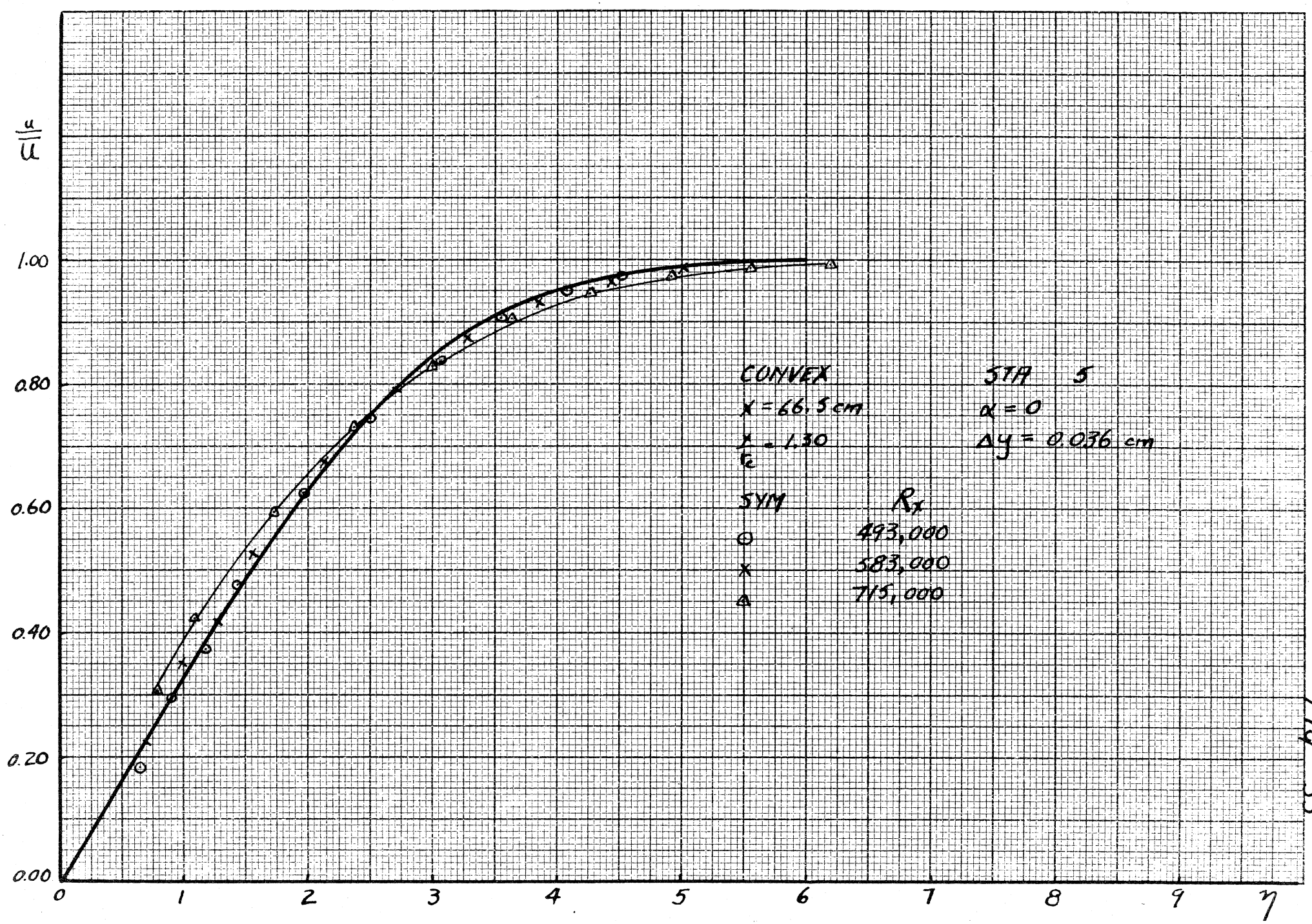
u/U
1.00
0.80
0.60
0.40
0.20
0.00
0
1
2
3
4
5
6
7
8
9
η
CONVEX
x = 66.5 cm
x/c = 1.30
SYM
R_x
493,000
583,000
715,000
STA 5
α = 0
Δy = 0.036 cm

Fig. 33

FIG 34

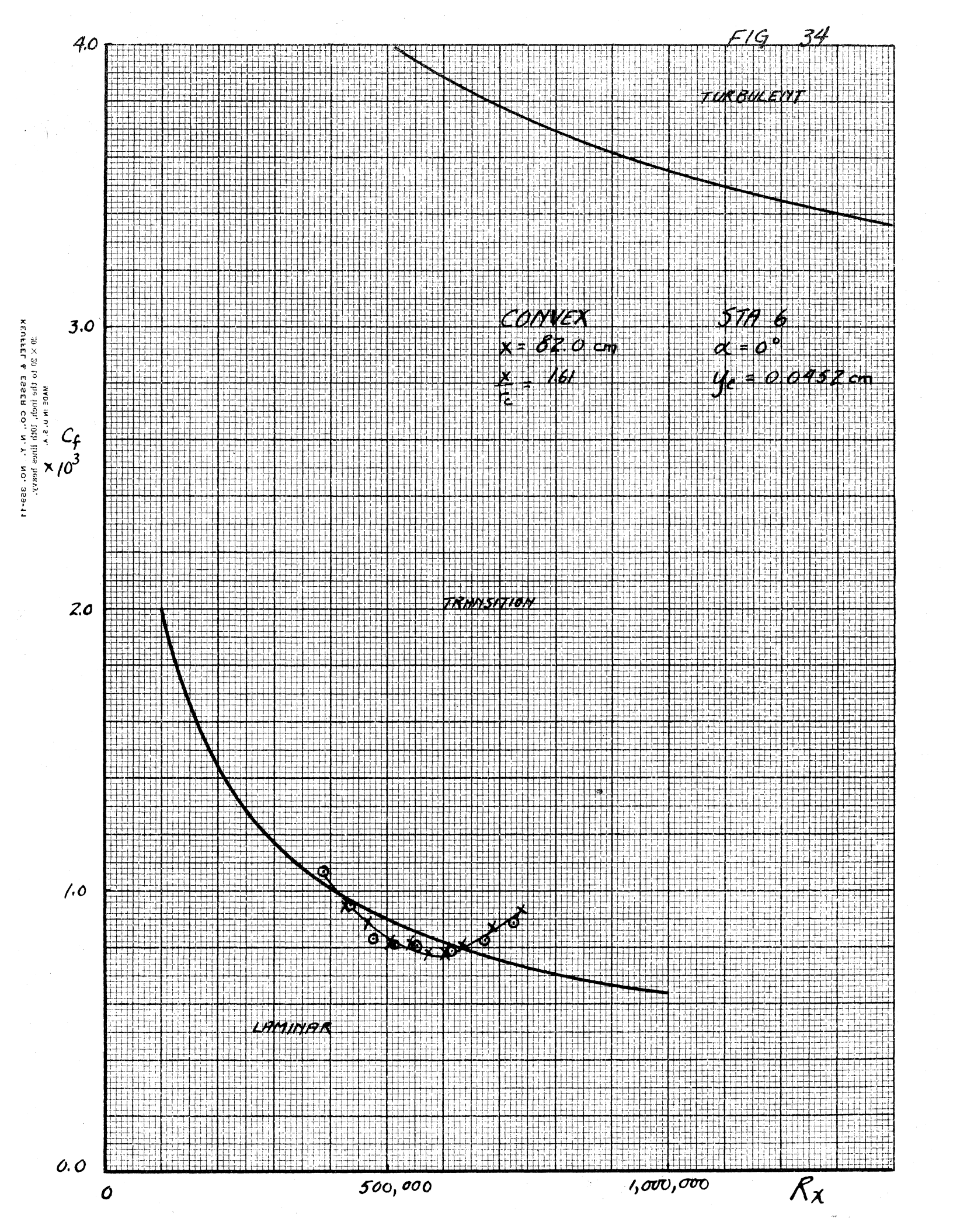

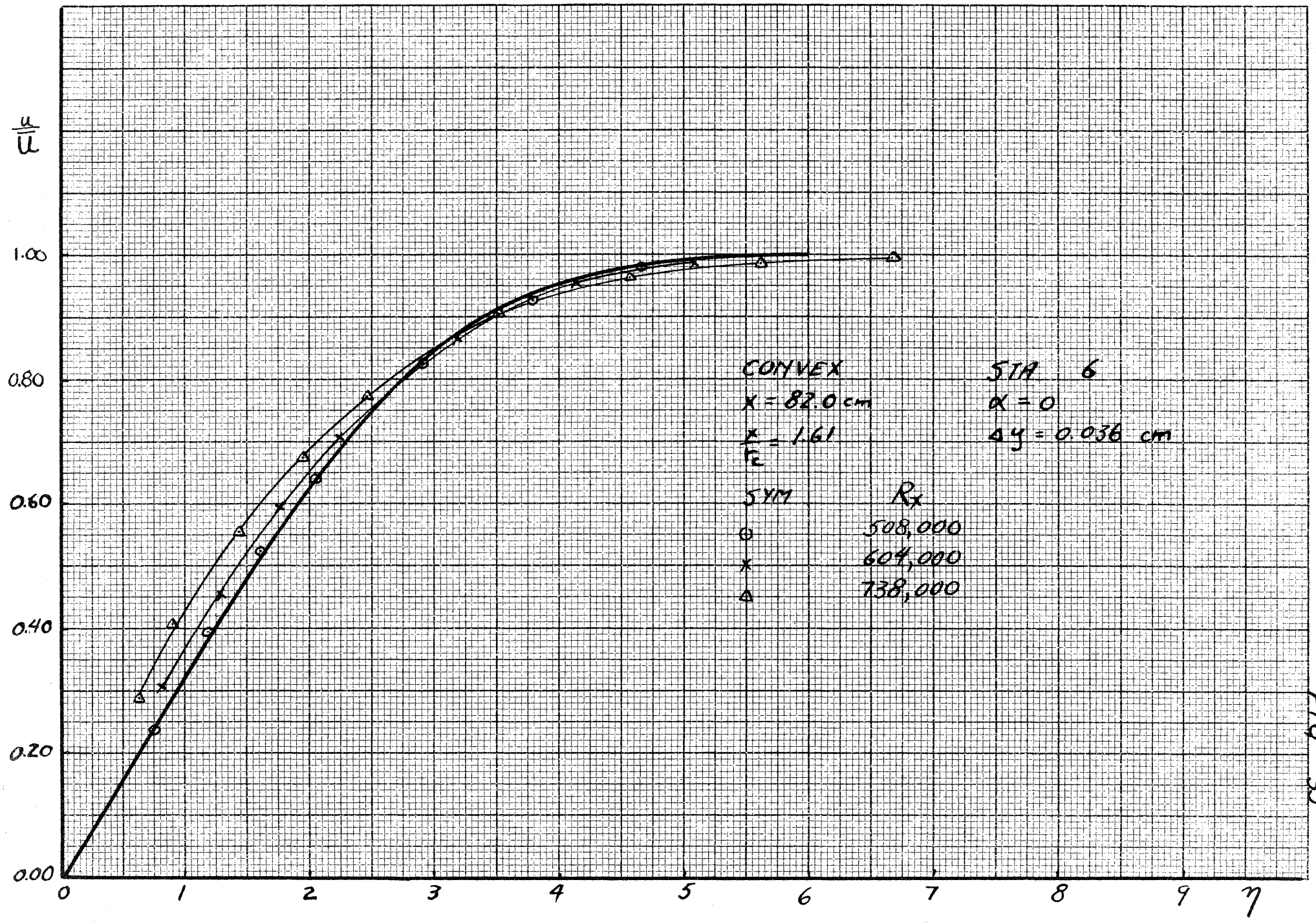
u/U
1.00
0.80
0.60
0.40
0.20
0.00
0
1
2
3
4
5
6
7
8
9
η
CONVEX
x = 82.0 cm
x/c = 1.61
STA 6
α = 0
Δy = 0.036 cm
SYM
Rx
508,000
604,000
738,000

FIG 35

FIG 36

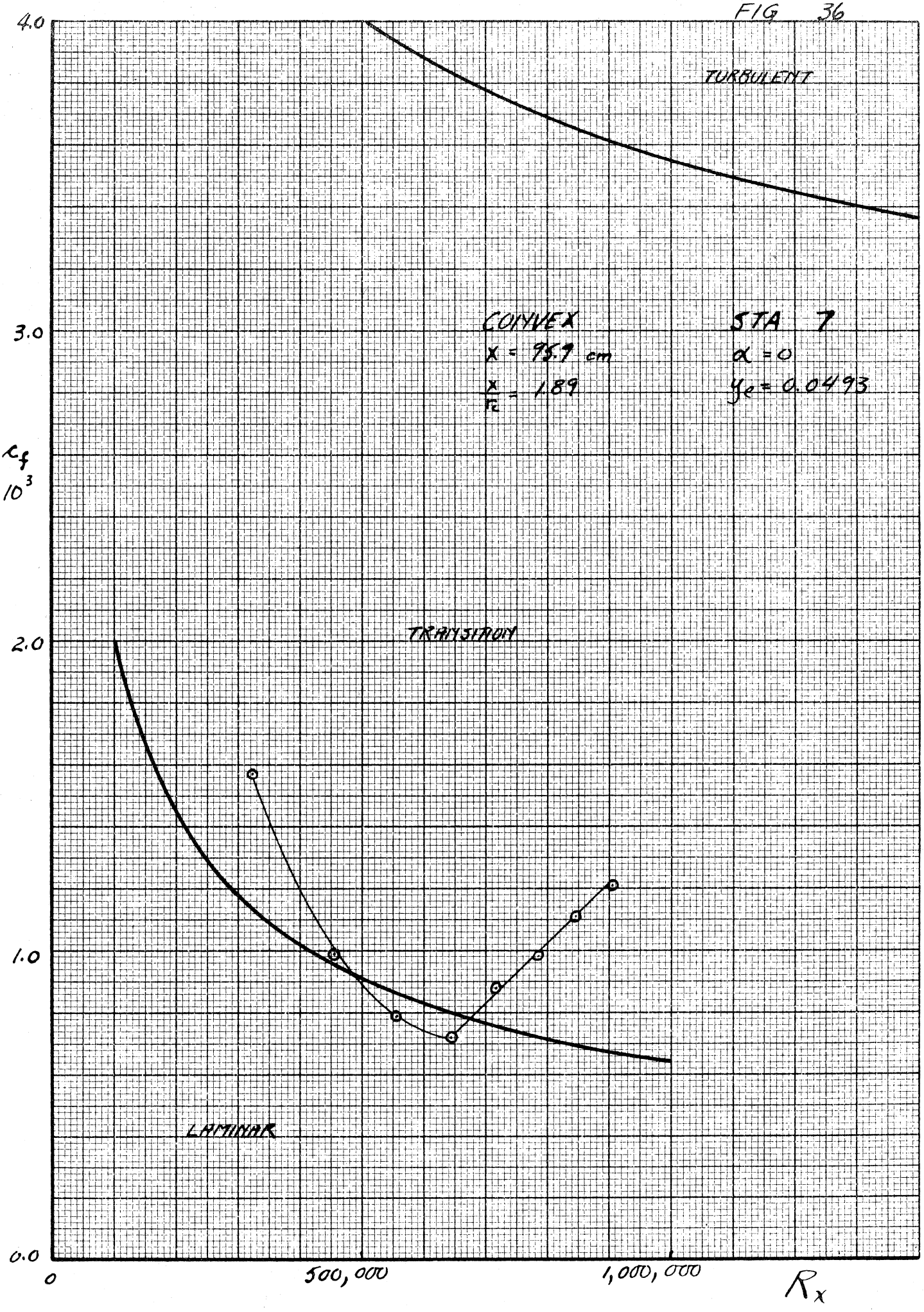
4.0
3.0
2.0
1.0
0.0
$c_f \times 10^3$
TURBULENT
CONVEX
X = 95.7 cm
$\frac{X}{R_L}$ = 1.89
STA 7
α = 0
y_e = 0.0493
TRANSITION
LAMINAR
0
500,000
1,000,000
R_x

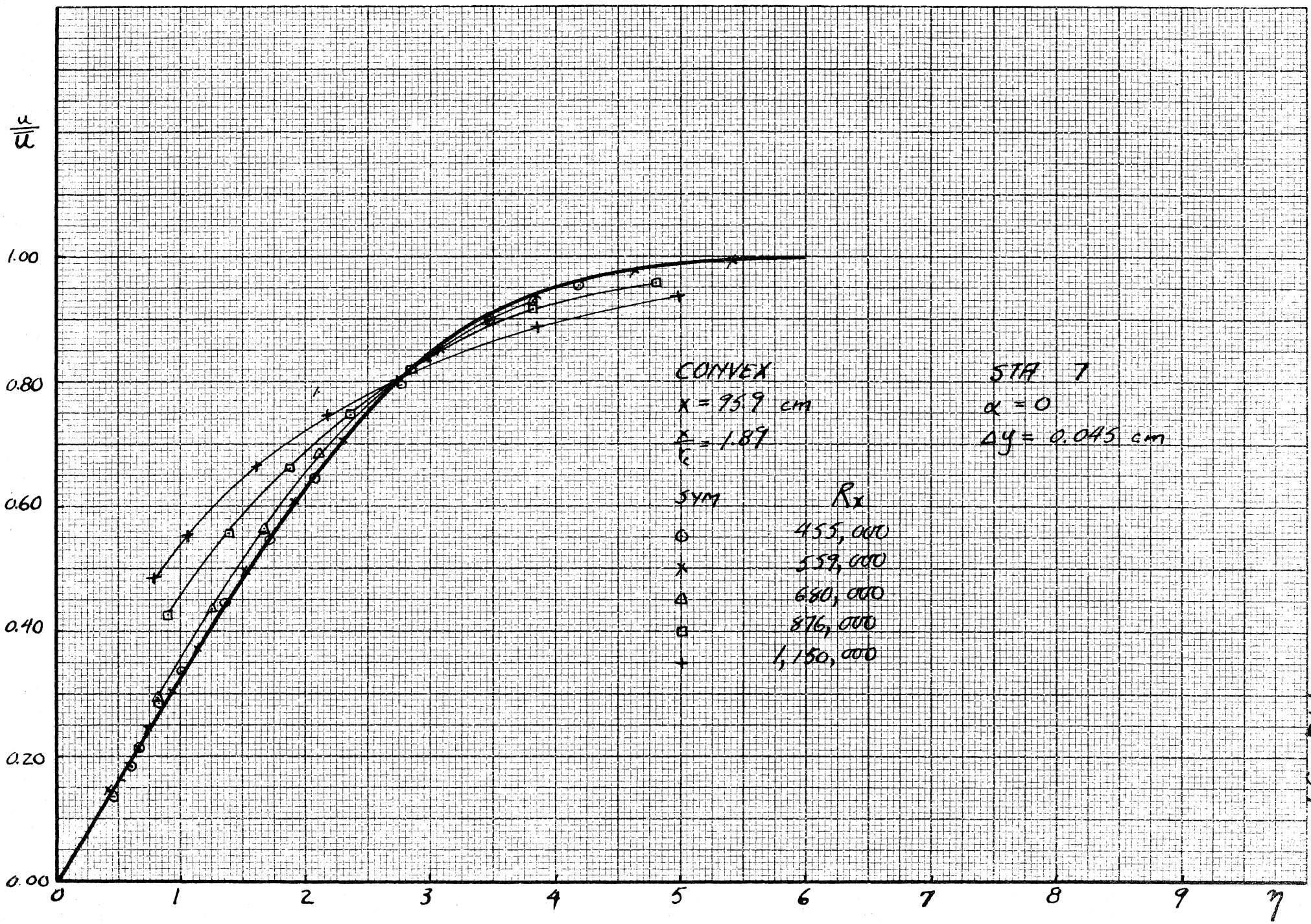
u/U
1.00
0.80
0.60
0.40
0.20
0.00
0
1
2
3
4
5
6
7
8
9
η
CONVEX
x = 95.9 cm
x/c = 1.87
STA 7
α = 0
Δy = 0.045 cm
SYM
Rx
455,000
559,000
680,000
876,000
1,150,000

FIG. 37

FIG 38

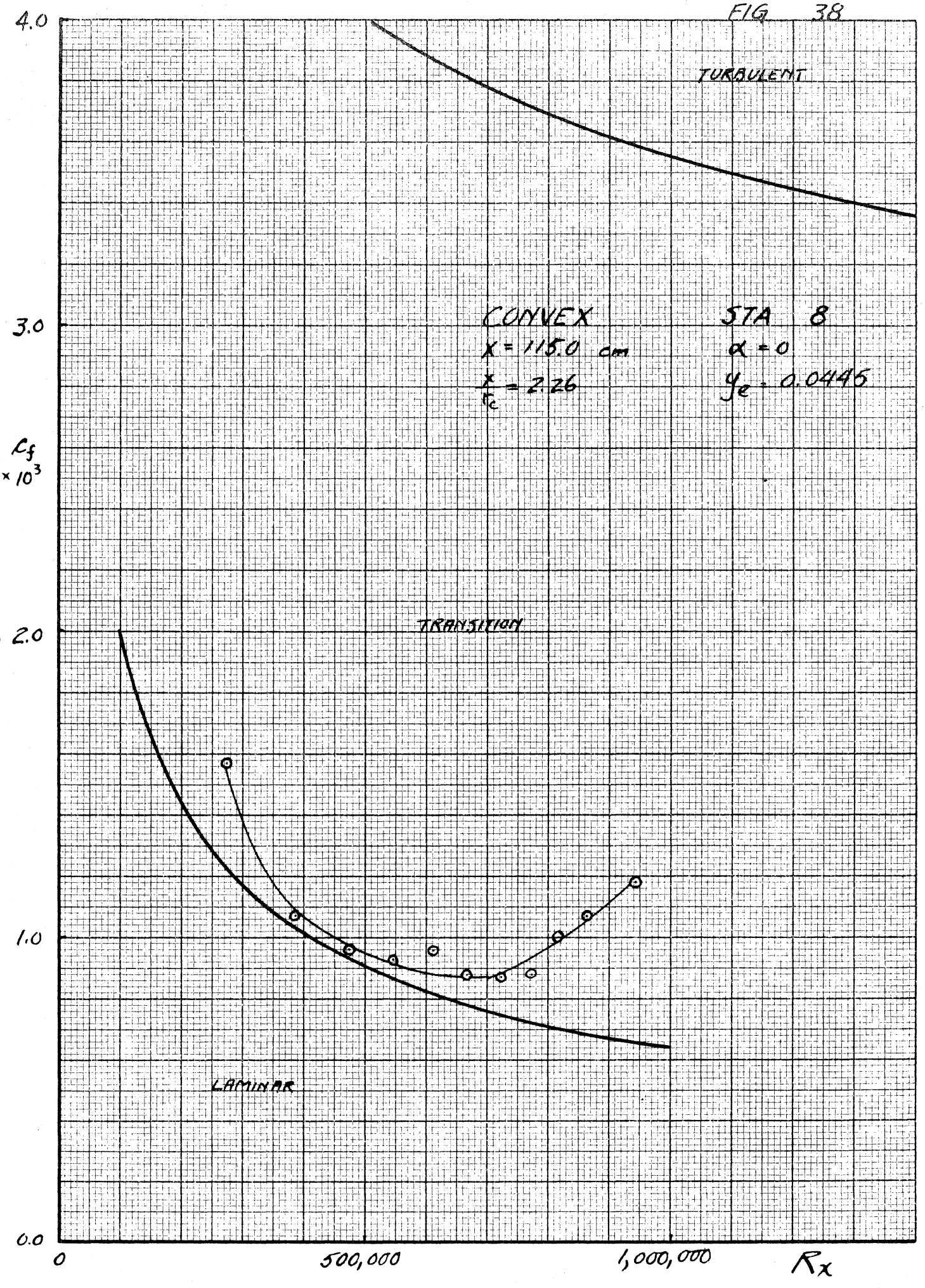
4.0
3.0
2.0
1.0
0.0
$C_f \times 10^3$
TURBULENT
CONVEX
STA 8
$X = 115.0$ cm
$\frac{X}{t_c} = 2.26$
$\alpha = 0$
$y_e = 0.0445$
TRANSITION
LAMINAR
0
500,000
1,000,000
R_x

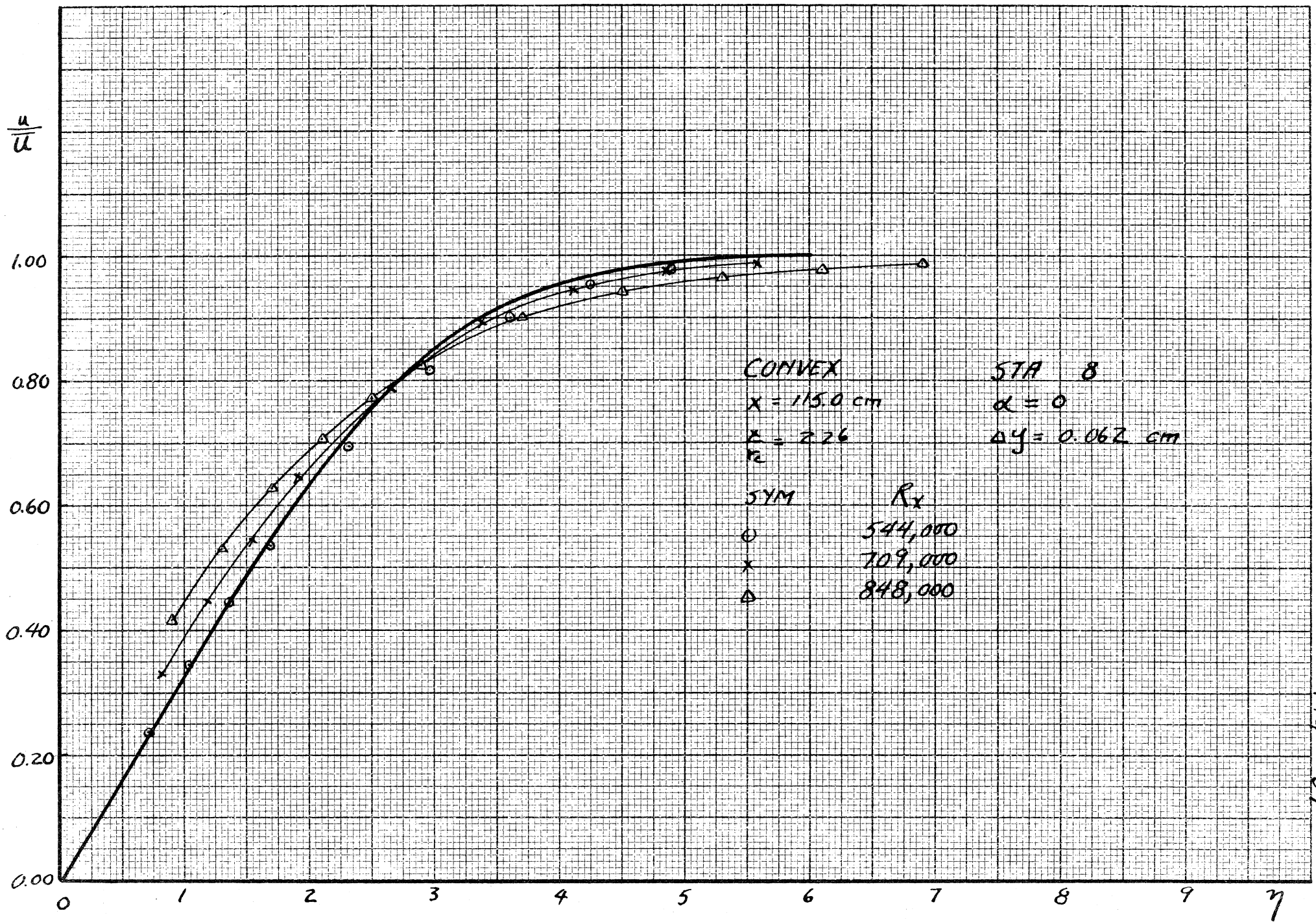
u/U
1.00
0.80
0.60
0.40
0.20
0.00
0
1
2
3
4
5
6
7
8
9
η
CONVEX
x = 115.0 cm
x/R = 2.26
STA 8
α = 0
Δy = 0.062 cm
SYM
Rx
544,000
709,000
848,000

FIG 39

FIG 40

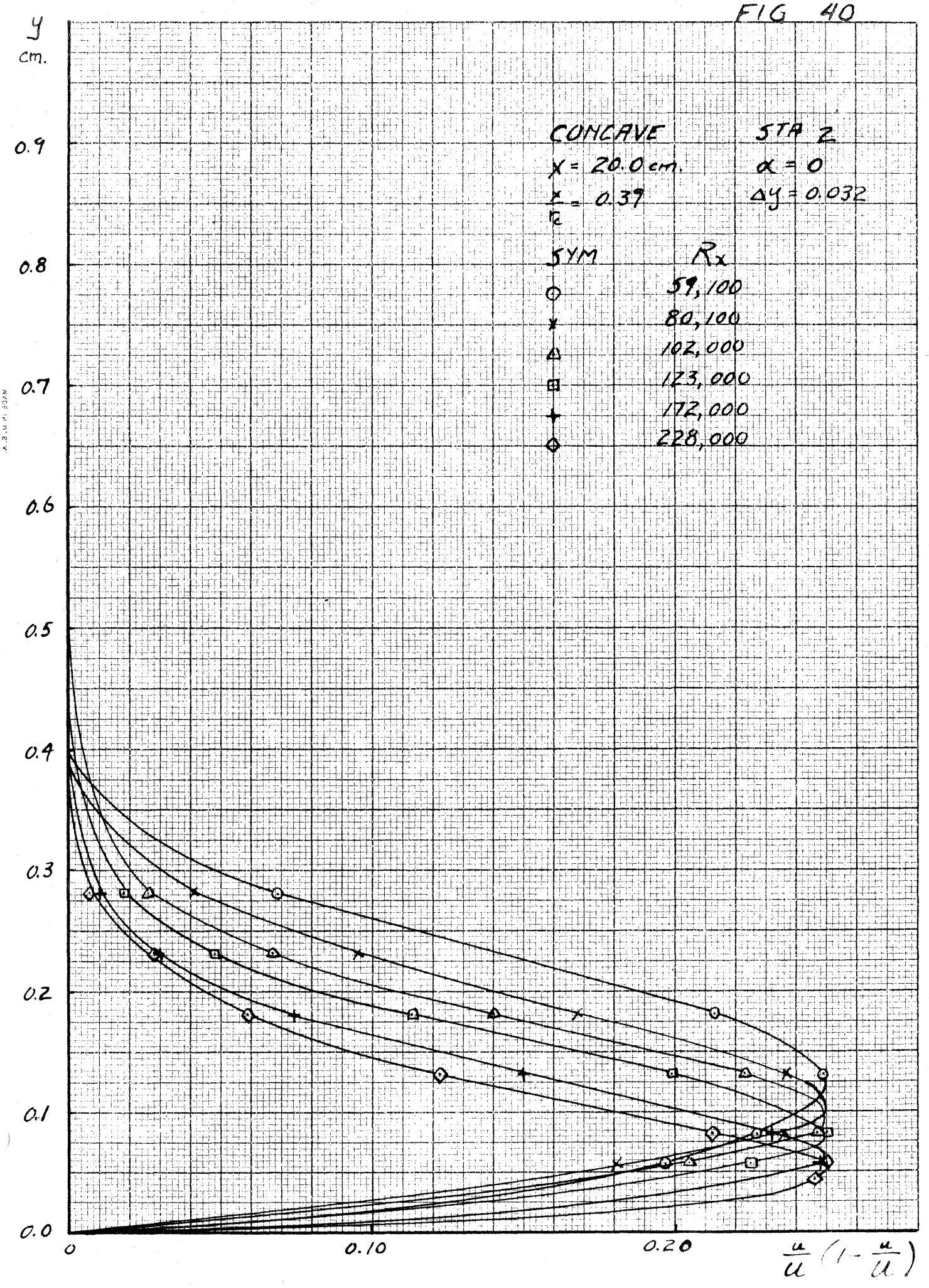
y
cm.
0.9
0.8
0.7
0.6
0.5
0.4
0.3
0.2
0.1
0.0
0
0.10
0.20
$\frac{u}{U}\left(1-\frac{u}{U}\right)$
CONCAVE
STA 2
X = 20.0 cm.
α = 0
$\frac{x}{r_2}$ = 0.37
Δy = 0.032
SYM
R_x
59,100
80,100
102,000
123,000
172,000
228,000

FIG 41

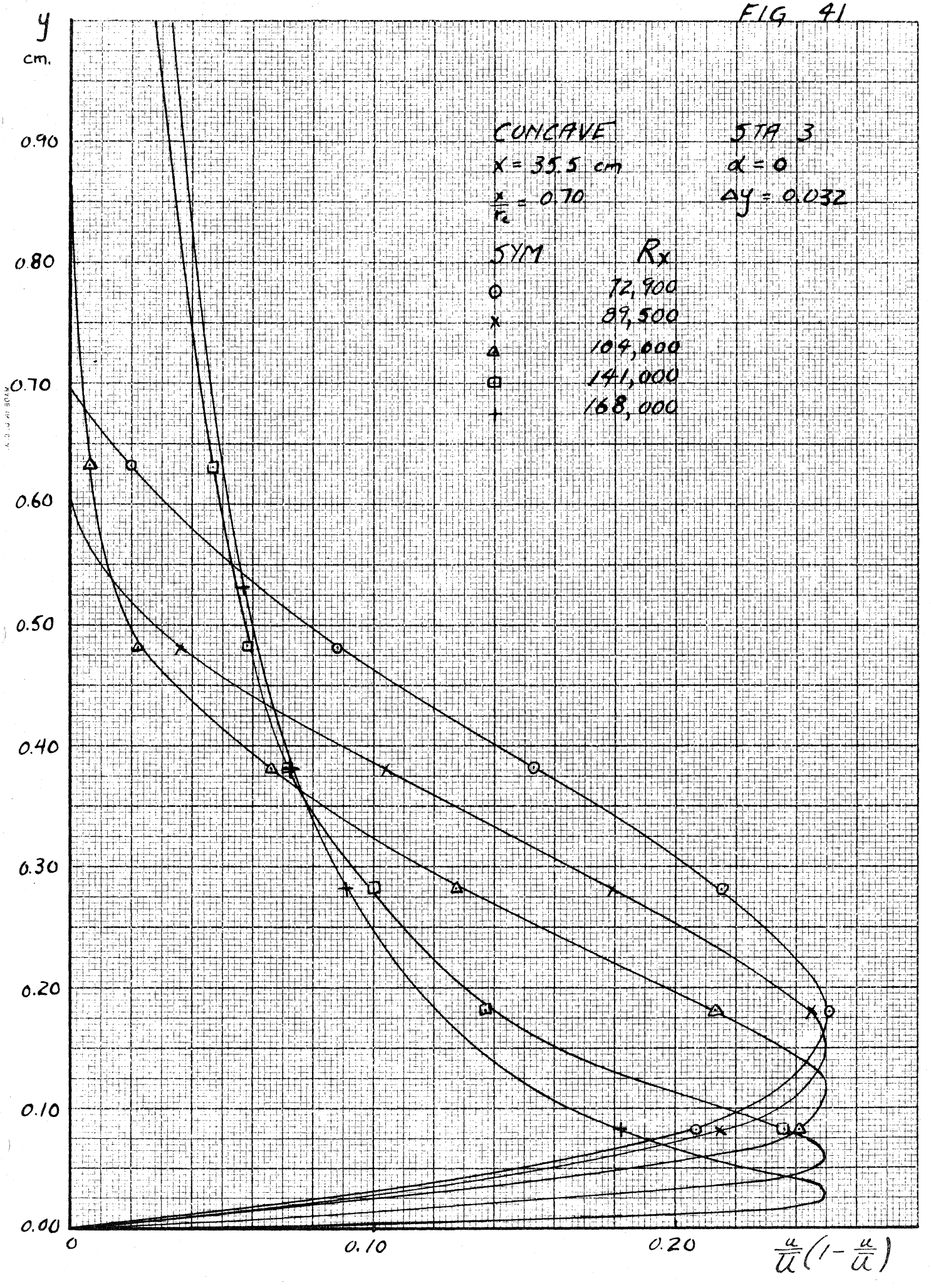
y
cm.
0.90
0.80
0.70
0.60
0.50
0.40
0.30
0.20
0.10
0.00
0
0.10
0.20
$\frac{u}{\bar{u}}(1-\frac{u}{\bar{u}})$
CONCAVE
x = 35.5 cm
$\frac{x}{r_c}$ = 0.70
STA 3
α = 0
Δy = 0.032
SYM
Rx
72,900
89,500
104,000
141,000
168,000

FIG 42

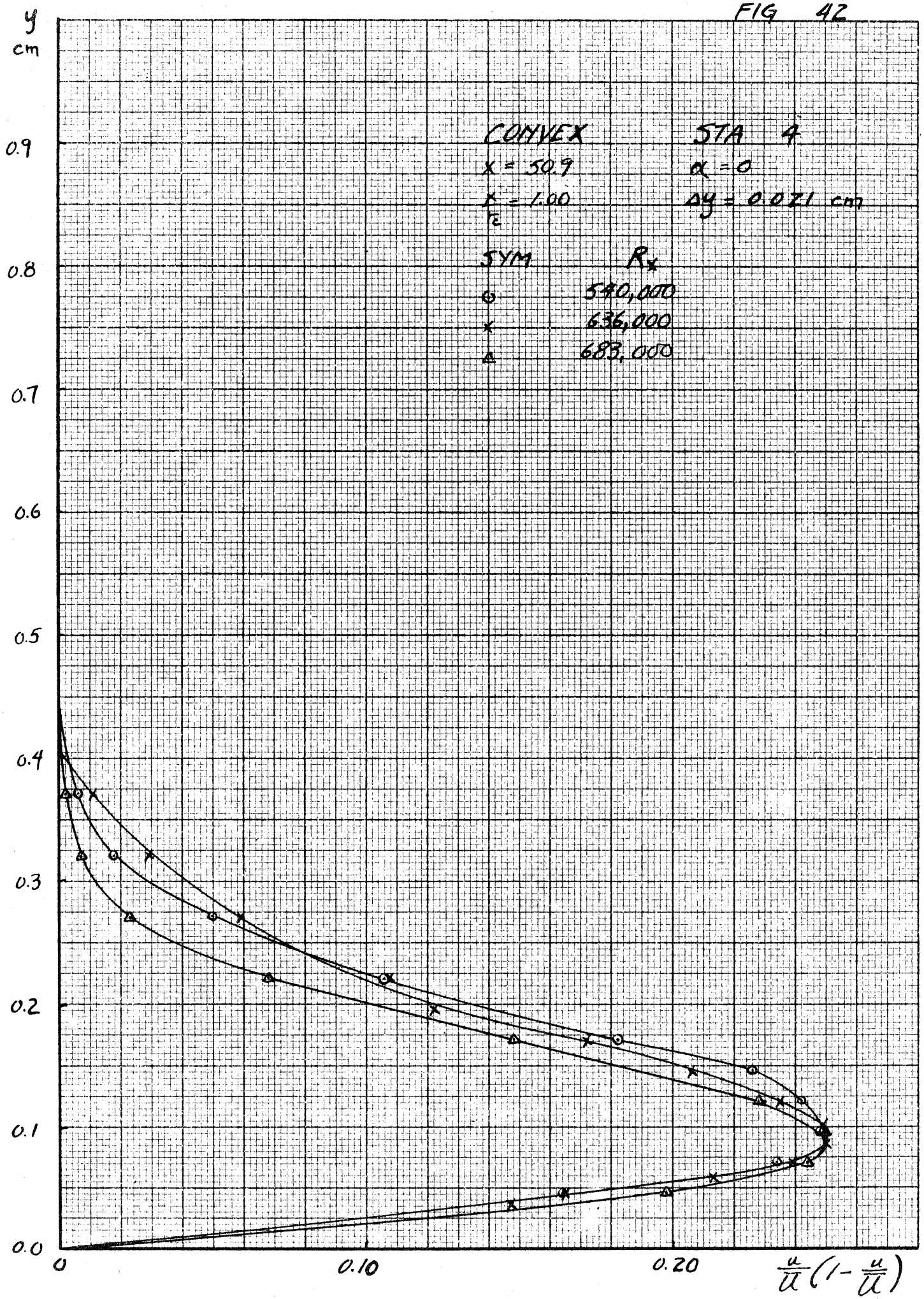

FIG 43

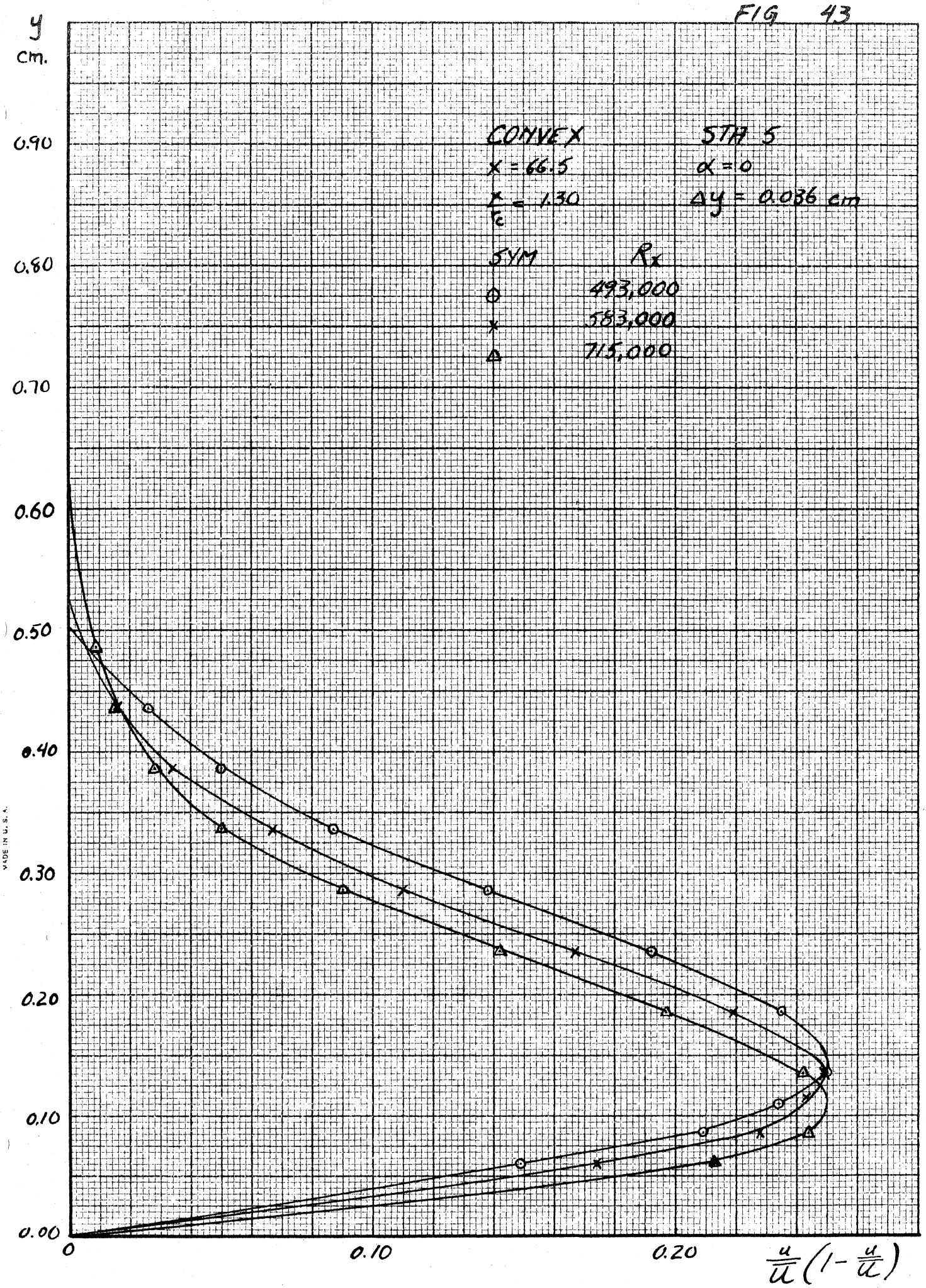

FIG 44

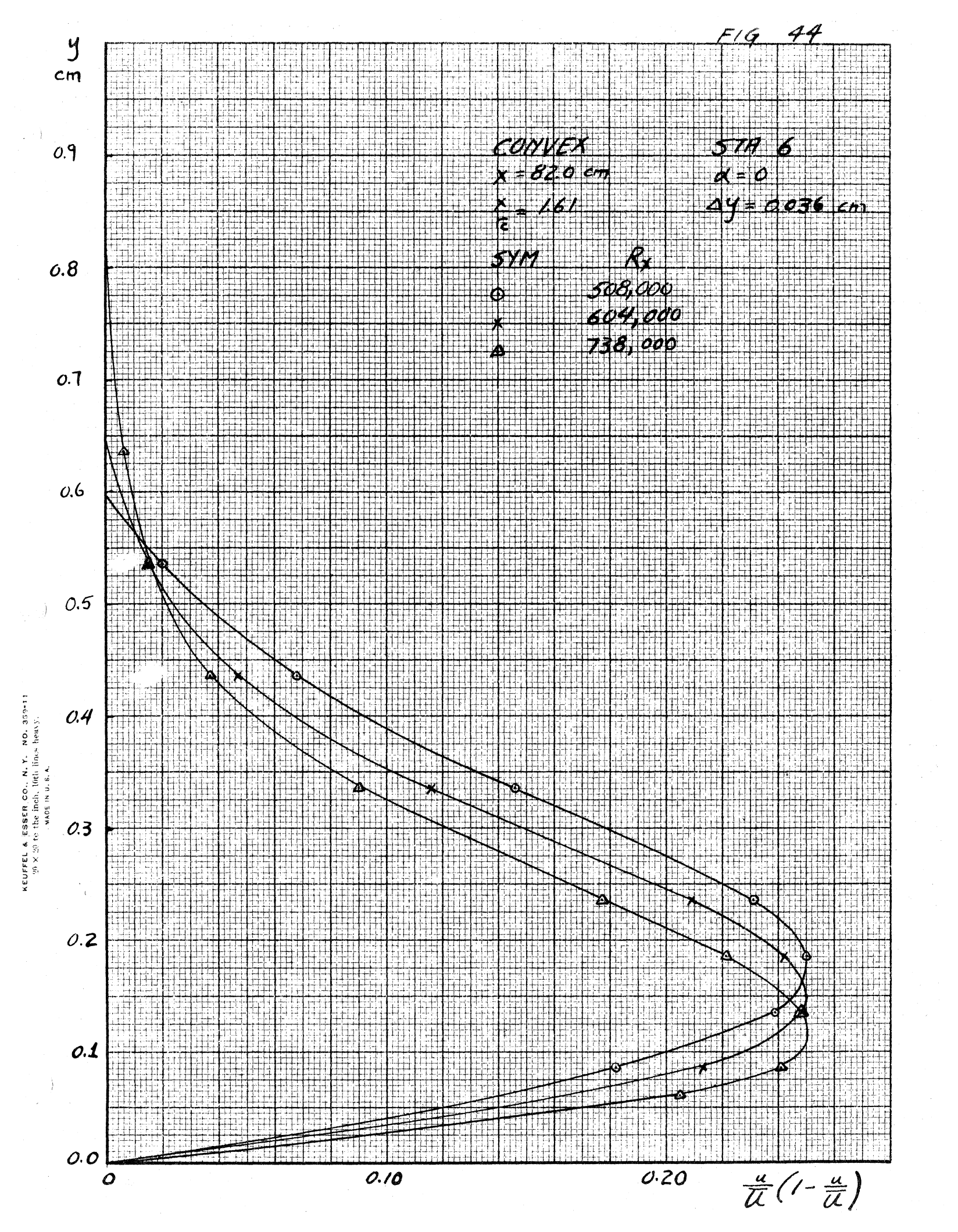

FIG 45

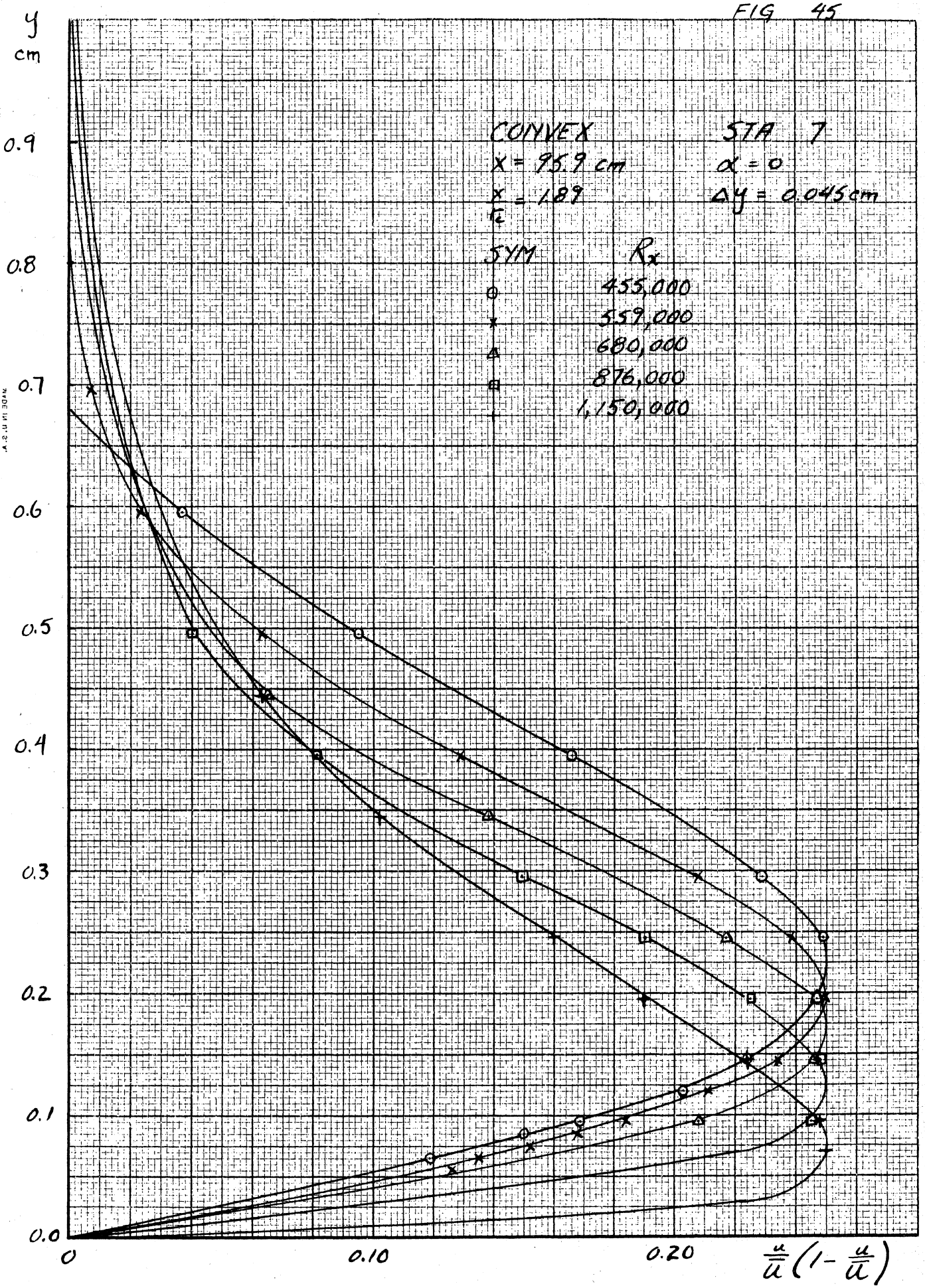
y
cm
0.9
0.8
0.7
0.6
0.5
0.4
0.3
0.2
0.1
0.0
0
0.10
0.20
$\frac{u}{u}\left(1-\frac{u}{u}\right)$
CONVEX
STA 7
x = 95.9 cm
α = 0
x/c = 1.89
Δy = 0.045 cm
SYM
R_x
455,000
559,000
680,000
876,000
1,150,000

FIG 46

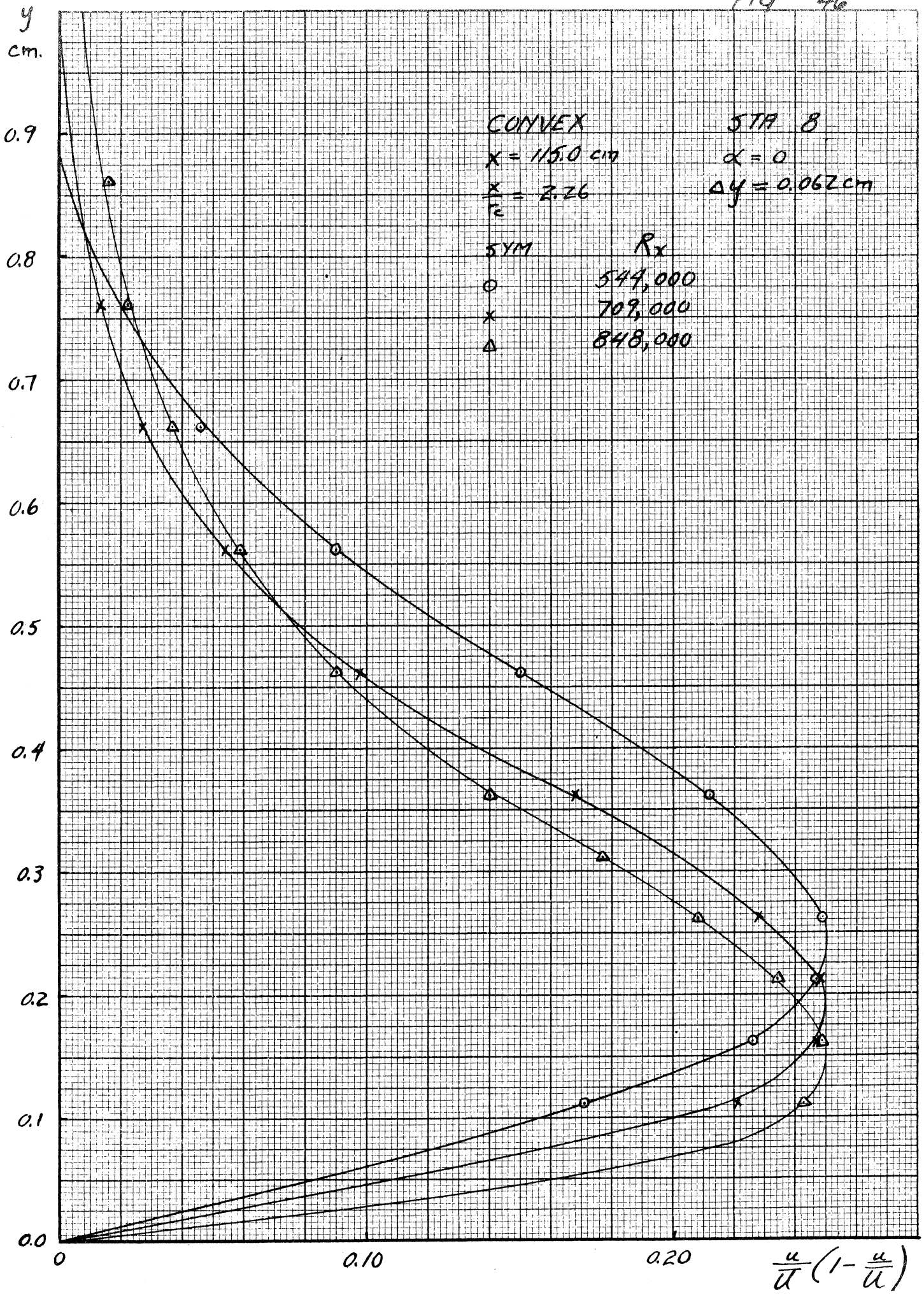

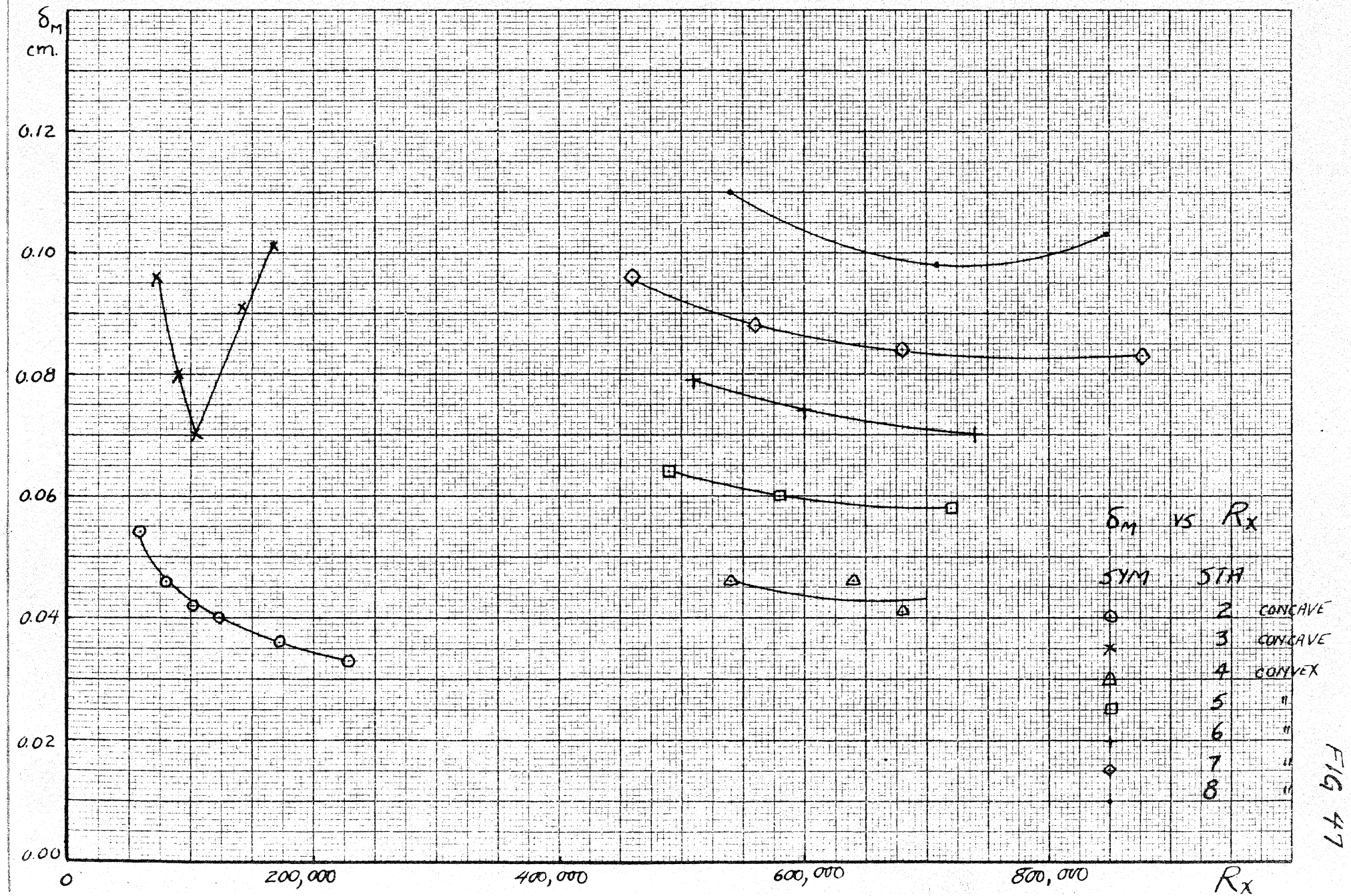
δ_M cm.
0.12
0.10
0.08
0.06
0.04
0.02
0.00
0
200,000
400,000
600,000
800,000
R_X
δ_M vs R_X
SYM
STH
2 CONCAVE
3 CONCAVE
4 CONVEX
5 "
6 "
7 "
8 "

Fig 47

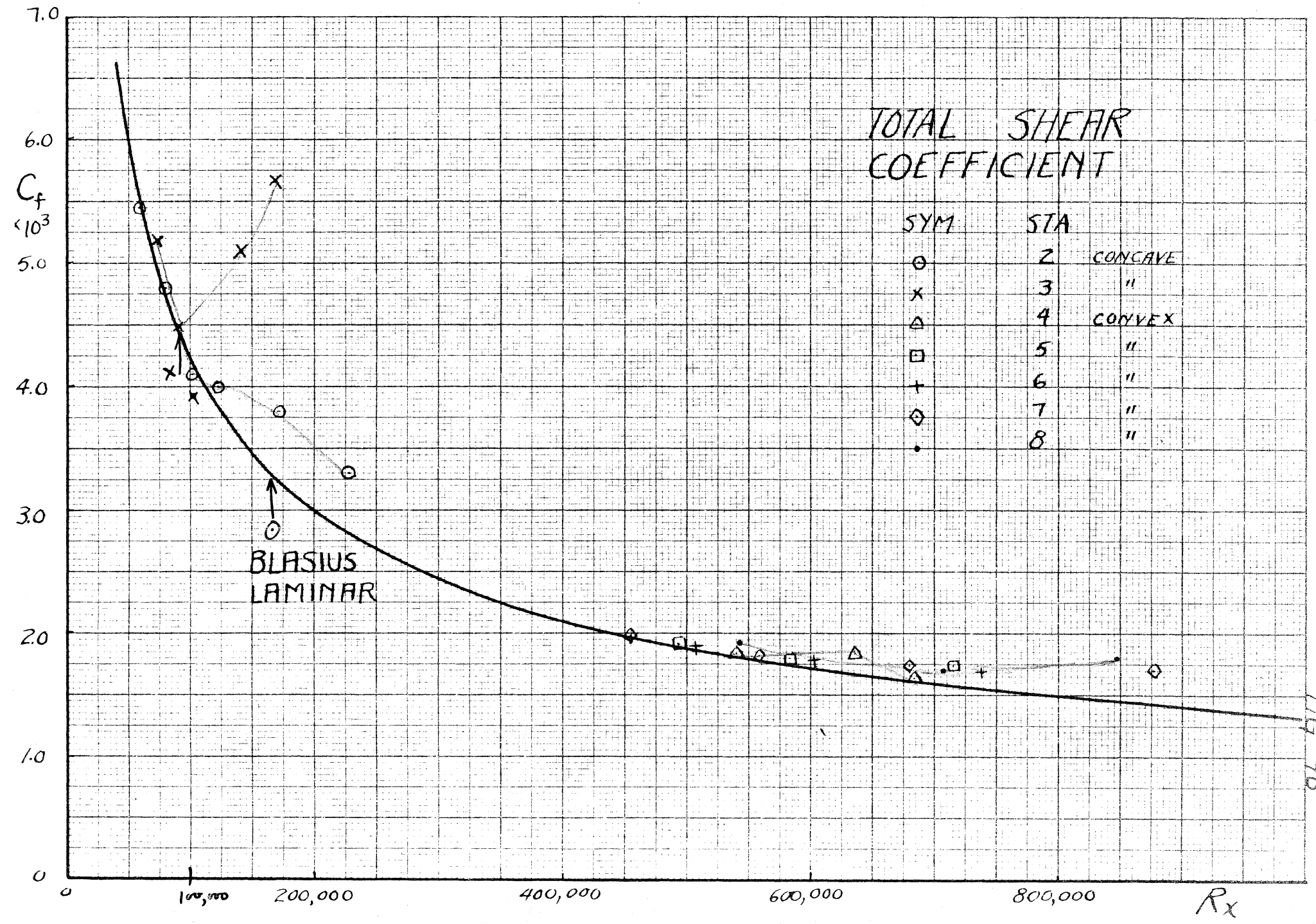
TOTAL SHEAR COEFFICIENT
SYM STA
2 CONCAVE
3 "
4 CONVEX
5 "
6 "
7 "
8 "
BLASIUS LAMINAR
$C_f \times 10^3$
7.0
6.0
5.0
4.0
3.0
2.0
1.0
0
0
100,000
200,000
400,000
600,000
800,000
R_x

FIG 48

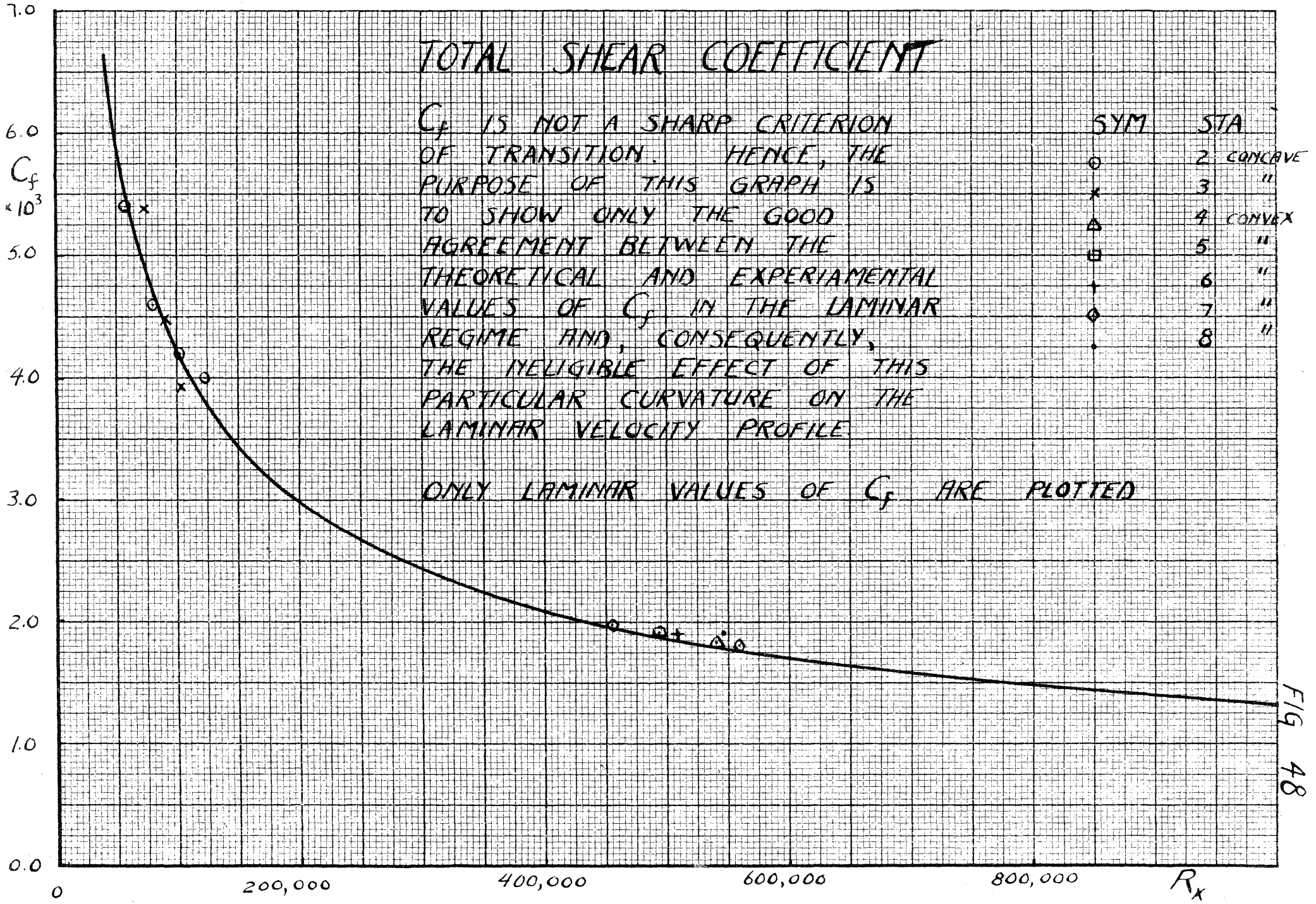

FIG 48

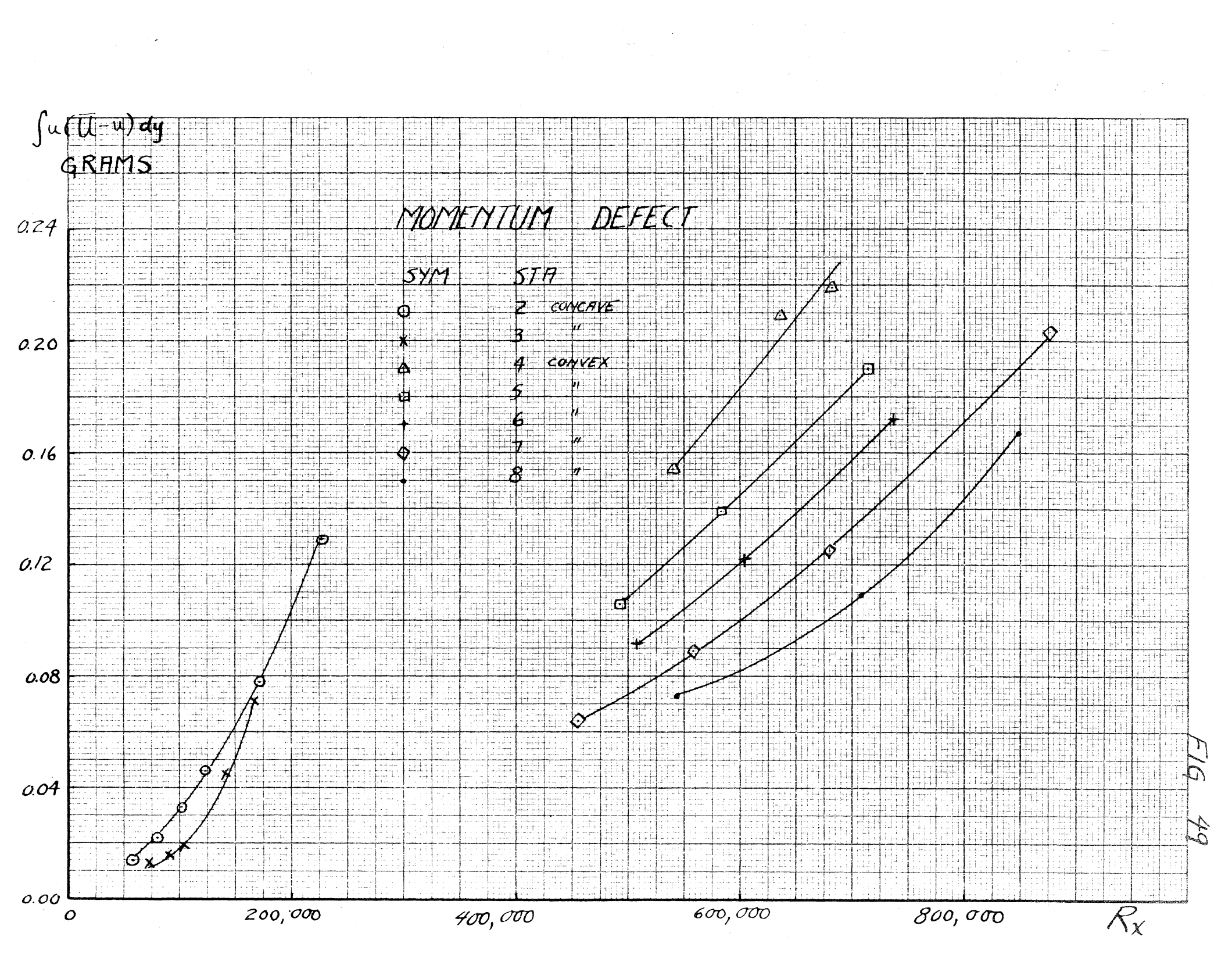
$\int u(\bar{U}-u)\,dy$
GRAMS
MOMENTUM DEFECT
SYM STA
2 CONCAVE
3 "
4 CONVEX
5 "
6 "
7 "
8 "
0.24
0.20
0.16
0.12
0.08
0.04
0.00
0
200,000
400,000
600,000
800,000
R_x

FIG 79

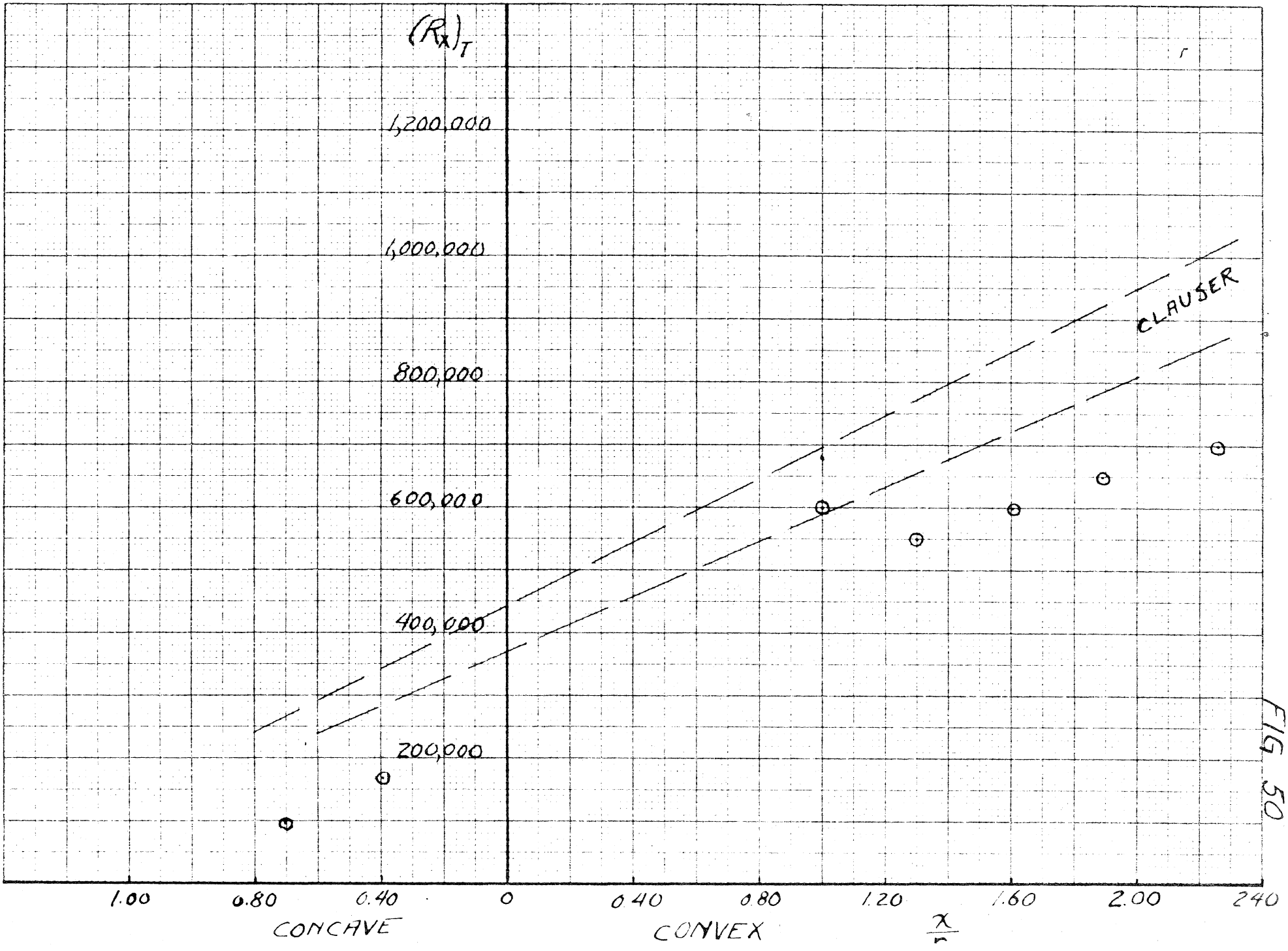
$(R_x)_T$
1,200,000
1,000,000
800,000
600,000
400,000
200,000
CLAUSER
1.00
0.80
0.40
0
0.40
0.80
1.20
1.60
2.00
2.40
CONCAVE
CONVEX
$\frac{x}{r}$

FIG 50

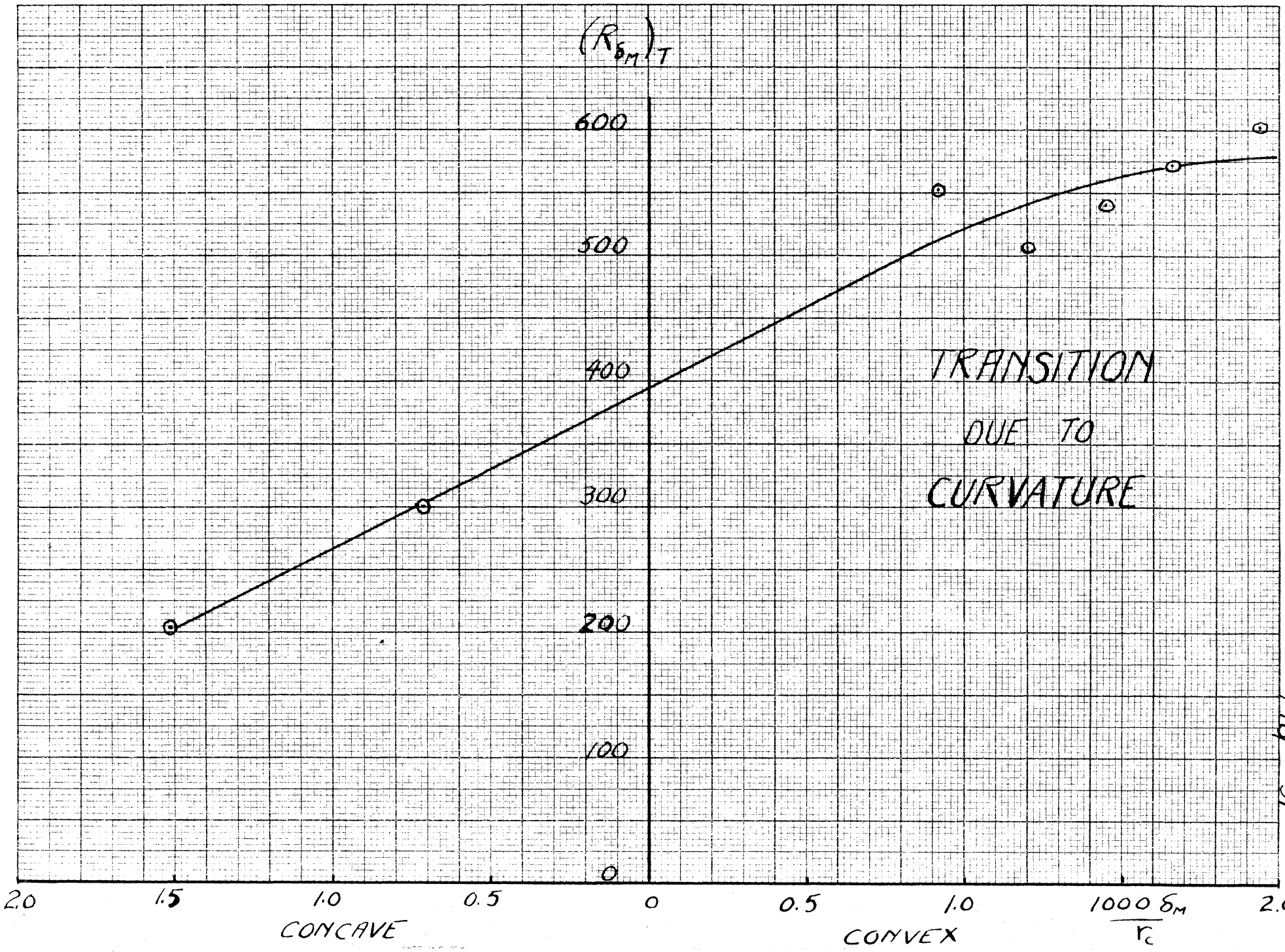
$(R_{\delta_M})_T$
600
500
400
300
200
100
0
TRANSITION
DUE TO
CURVATURE
2.0
1.5
1.0
0.5
0
0.5
1.0
2.0
CONCAVE
CONVEX
$\frac{1000\,\delta_M}{r_c}$

FIG 51

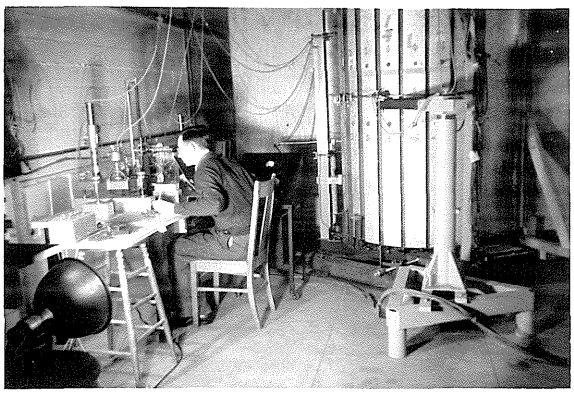

ASSEMBLY SHOWING WORKING SECTION AND INSTRUMENTS DURING EXPERIMENTAL TESTING.

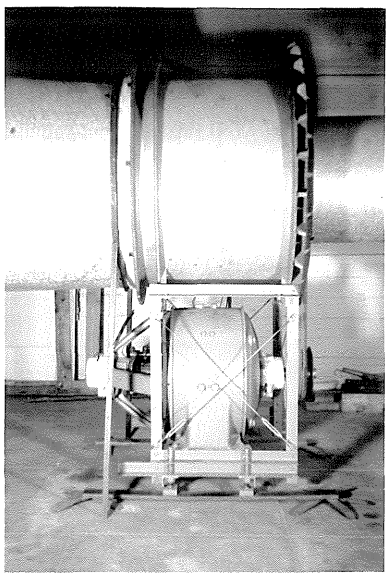

MOTOR-PROPELLER UNIT SHOWING FLEXIBLE CLOTH COUPLING WITH DIFFUSER AND IMPROVED SPRING SUSPENSION.

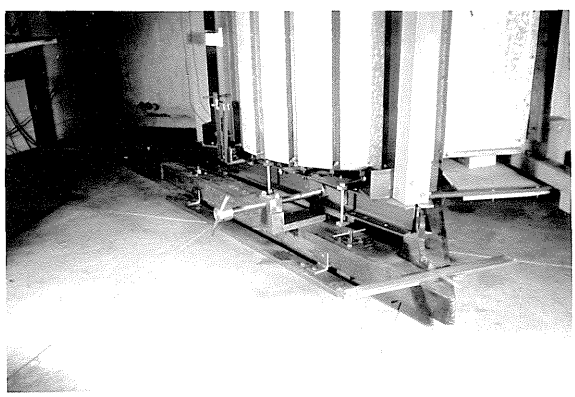

DETAIL OF INCIDENCE CHANGING MECHANISM SHOWING PUSH-PULL BLOCKS AND ANGLE INDICATOR.

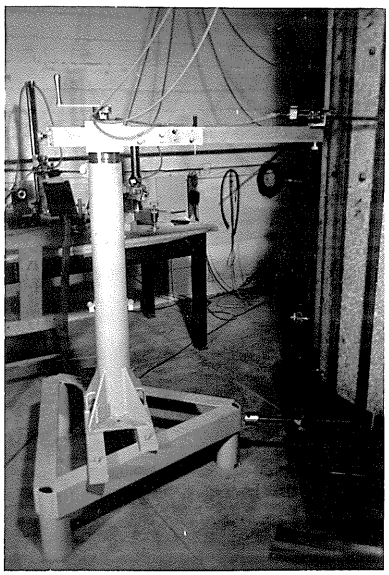

DETAIL OF STANDARD IN POSITION: NOTE TANDEM MICROMETER HEAD CARRIAGE CARRYING TOTAL-STATIC TUBE.

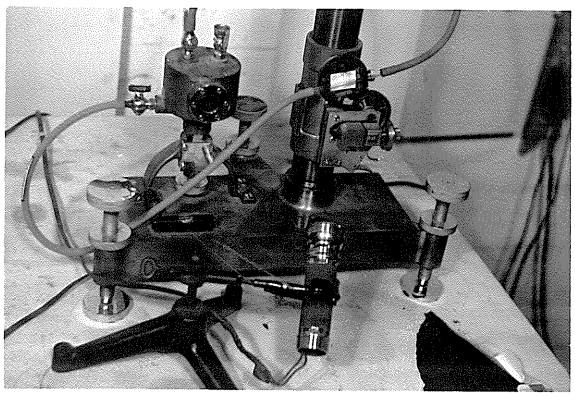

DETAIL OF BASE, RESERVOIR, CARRIAGE, AND BOTTOM OF VERTICAL COLUMN OF STANDARD LABORATORY MANOMETER.

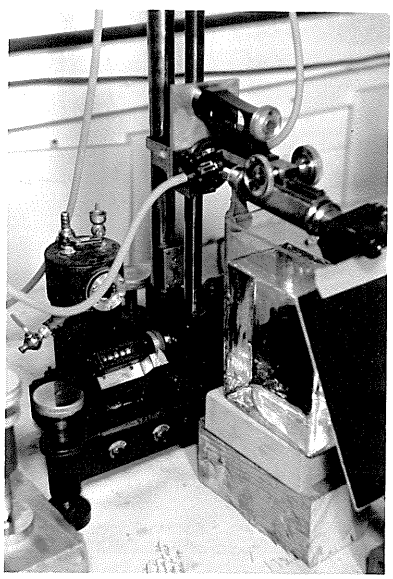

DETAIL SHOWING INSTALLATION OF MICROSCOPE ON CARRIAGE OF STAND. LABORATORY MANOMETER.

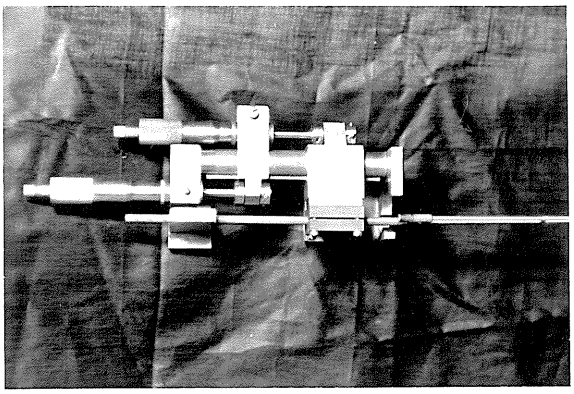

DETAIL OF TANDEM MICROMETER HEAD CARRIAGE NOTE MANNER IN WHICH MEASURING INSTRUMENT IS HELD.

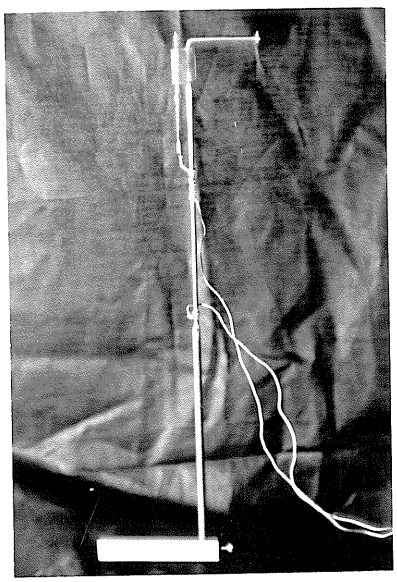

DETAIL OF CONTACT RECTILINEAR INDICATOR. NOTE CONTACTS AT TOP OF PICTURE.

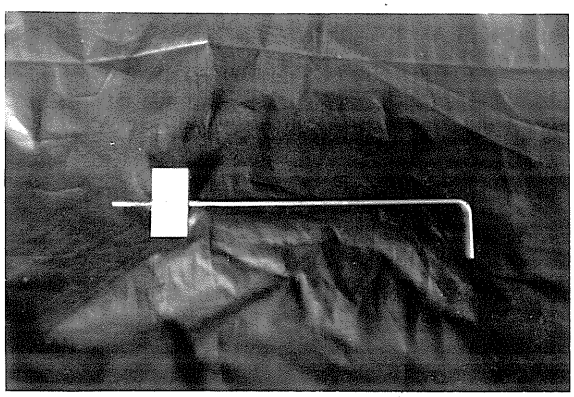

DETAIL OF SMALL STATIC PRESSURE TUBE.

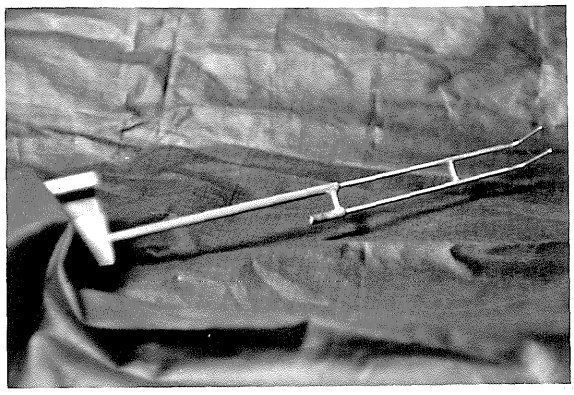

DETAIL OF TOTAL-STATIC TUBE: TOP TUBE IN STATIC TUBE: BOTTOM TUBE IS TOTAL HEAD TUBE.

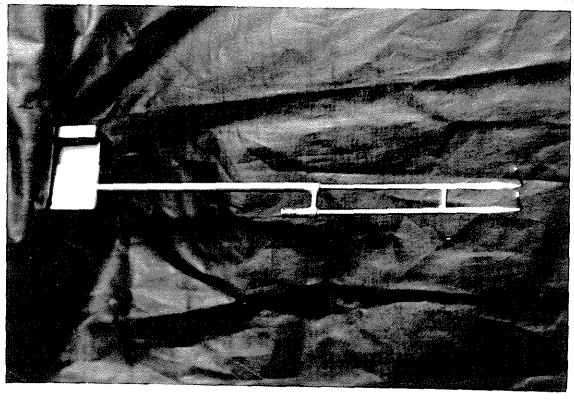

DETAIL OF TOTAL-STATIC TUBE.

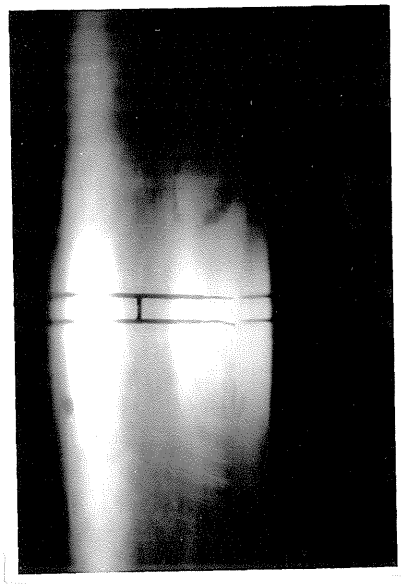

DETAIL SHOWING TOTAL-STATIC TUBE CLOSE TO CENTRAL SHEET (BRIGHTLY ILLUMINATED) NOTE REFLECTION OF TUBE IN SHEET AND SHARP SHADOW LOCATING THE SHEET'S LEADING EDGE.

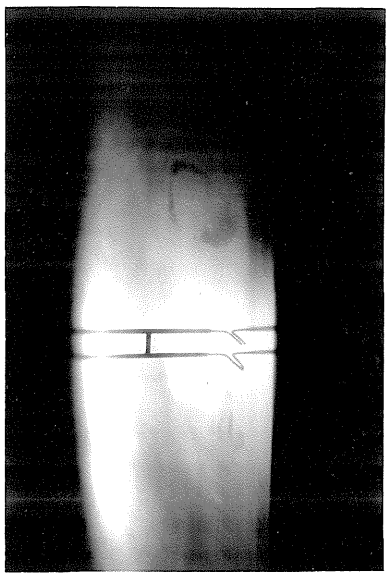

DETAIL SHOWING TOTAL-STATIC TUBE IN CONTACT WITH CENTRAL SHEET: NOTE REFLECTION OF TUBE IN SHEET.

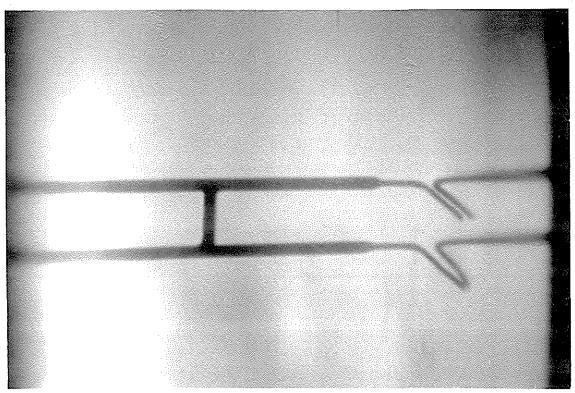

ENLARGEMENT OF ABOVE DETAIL: NOTE THAT WHERE AS THE TOTAL HEAD TUBE MAKES A CLEAN CONTACT WITH THE CENTRAL SHEET, THE STATIC IS ABOUT ONE MILLIMETER AWAY.